UNIVERSITY OF NOVA GORICA
GRADUATE SCHOOL

STRUCTURE OPTIMISATION OF BIOPIGMENT PRODIGIOSIN FROM *SERRATIA MARCESCENS* ATCC 27117 AND ANTIMICROBIAL AND ANTICANCER PROPERTIES OF NOVEL HALOGENATED DERIVATIVES

DISSERTATION

Jelena Lazić

Mentor: Jasmina Nikodinović-Runić, PhD

Nova Gorica, 2022

UNIVERZA V NOVI GORICI
FAKULTETA ZA POSTDIPLOMSKI ŠTUDIJ

STRUKTURNA OPTIMIZACIJA BIOPIGMENTA PRODIGIOZIN IZ BAKTERIJE *SERRATIA MARCESCENS* ATCC 27117 TER ANTIMIKROBNE IN ANTITUMORSKE LASTNOSTI NOVIH HALOGENIRANIH DERIVATOV

DISERTACIJA

Jelena Lazić

Mentor: Jasmina Nikodinović-Runić, PhD

Nova Gorica, 2022. let

UNIVERSITY OF NOVA GORICA
GRADUATE SCHOOL

Jelena Lazić, *Structure optimisation of biopigment prodigiosin from Serratia marcescens ATCC 27117 and antimicrobial and anticancer properties of novel halogenated derivatives*, Dissertation, (2022)

Copyright and moral rights for this work are retained by the author.

A copy can be downloaded for personal non-commercial research or study, without prior permission or charge.

This work cannot be reproduced or quoted extensively from without first obtaining permission in writing from the author.

The content must not be changed in any way or sold commercially in any format or medium without the formal permission of the author.

When referring to this work, full bibliographic details including the author, title, awarding institution and date of the thesis must be given.

Acknowledgements / Захвалнице

Experimental work for this doctoral dissertation was done at the Institute of Molecular Genetics and Genetic Engineering (IMGGE), University of Belgrade, Serbia, under the supervision of Dr Jasmina Nikodinović-Runić, Principal Research Fellow.

I would like to thank the rector of the University of Nova Gorica (UNG), Prof. Danilo Zavrtanik, for approving my PhD transfer to Slovenia. I also want to thank the director of the Molecular Genetics and Biotechnology Graduate Study Programme (Third Level), Ass. Prof. Martina Bergant Marušič, for her excellent guidance, continuous involvement, and prompt support.

I have special thanks to address to the evaluation committee members: Prof. Tanja Gulder (University of Leipzig, Germany), Ass. Prof. Milica Popović (University of Belgrade, Serbia), and Ass. Prof. Lorena Butinar (University of Nova Gorica, Slovenia) for taking part as evaluators and for providing excellent suggestions, which improved the quality of this doctoral dissertation. I also want to address my appreciation to Prof. Tanja Gulder for being my DAAD scholarship host in 2018/2019.

I especially want to thank my mentor Jasmina from the bottom of my heart, for constantly changing my scientific life for better, ever since 2014, when our paths crossed for the first time. She was an always-optimistic, never-sleeping, I-got-your-back support throughout my master studies and my first doctoral studies, and helped me stir my decisions towards the UNG, this Programme, and finally, this achievement – my PhD thesis. Now, I can start working on telling you “ti” instead of “Vi”, hoping that our cooperation, experience exchange, and friendship will continue for many years to come.

I also sincerely want to thank my colleagues from IMGGE in Belgrade, our LAB 05 – Group for Eco-Biotechnology and Drug Development. To Dr Sandra Vojnović, Dr Tatjana Ilić-Tomić, Dr Sanja Jeremić, Dr Jelena Milovanović, Dr Dušan Milivojević, Milena Stevanović, Marija Nenadović, Vukašin Janković, Brana Pantelić and Lena Pantelić: you are the most cooperative, pleasant, and simply the best team I have ever worked with.

I owe special thanks to Dr Ivana Aleksić and Dr Marija Mojićević, who remain my dear friends and with whom I have enjoyed spending time outside the laboratory and working hours. My special thanks go to Dr Sanja Škaro Bogojević, who has been an incredible teammate and friend, as well as a helping pair of hands – I could not wish for a better colleague for all the challenges we have tackled together.

And finally, I want to thank my family, and I will write this part in Serbian, to make sure they understand it perfectly well.

Хвала мојим дивним родитељима, Олги и Малиши, на подршци, на доброти, на стрпљењу, на томе што су ми омогућили да доносим сопствене одлуке у сопствено време; што су ме подржали када сам одлучила да одустанем, а што су ме подржали и када сам одлучила да ипак не одустајем. Хвала им што су увек били ту да ме саслушају о свему; макар и не разумели научну терминологију – увек су разумели мене... Заиста сте најбољи на свету и не бих ја била баш оваква ја да није било вас! ♥

Тешко је било шта написати мојој сестри Милени што би стало у пар реченица, али хајде да пробам. Без тебе ништа не би имало смисла и немогуће је замислити бољу сестру. Мислим да нико (добро, можда мама :) није био толико поносан на мене свих ових (скоро 12) година током којих сам била у статусу студента природних наука. Надам се да ћу наставити да те чиним поносном и бескрајно ти хвала што си одувек веровала у мене! ^(ʻoʻ)^

Последњи, али не најмање важан, јесте Марко, моја срећна звезда у сваком смислу. Од када се он појавио у мом животу, све се покренуло и сви моји дугогодишњи планови су почели да се реализују, укључујући и израду, писање и одбрану овог доктората. Ти си ме у свему подржавао од самог почетка и мени је са тобом све било лепше, опуштеније и боље. Неизмерно ти хвала што си био са мном на сваком кораку овог пута! А толико путева је тек пред нама... :)

I dedicate this thesis to my mom, my dad, and my sister.

Ову тезу посвећујем мојој мами, мом тати и мојој сестри.

Abstract

Prodigiosins (PGs) are a class of bacterial secondary metabolites with remarkable biological activities and colour. In this study, optimised fermentative production of prodigiosin (PG) using waste processed meat as a substrate has been achieved to levels of 83.1 ± 3.0 mg/L from a commercially available *Serratia marcescens* ATCC 27117 strain within 12 h. Methods were established for the reliable PG extraction from both the bacterial cell pellet and the culture supernatant, while gravitation column chromatography was used to obtain pure bacterial PG.

The structure of the isolated PG was optimised by environmentally acceptable oxidative bromination reactions, obtaining mono- and dibrominated derivatives (PG-Br and PG-Br_2). Chemical structures were confirmed by structural characterisation using nuclear magnetic resonance (NMR) spectroscopy and mass spectrometry (MS), showing that PG-Br is a mixture of two monobrominated isomers in approximately equal ratios, while PG-Br_2 was afforded as a pure derivative.

PG and its brominated derivatives (Br-derivatives) showed anticancer potential with half-maximal inhibitory concentration (IC_{50}) values ranging from 0.62 to 17.00 µg/mL on four tested cancer cell lines (A549 lung, A375 skin, MDA-MB-231 breast, HCT116 colon) and an induction of early apoptosis, but low selectivity against healthy cell lines (MRC-5 lung fibroblasts and HaCaT skin keratinocytes). All three PG, PG-Br and PG-Br_2 compounds did not affect roundworms (*Caenorhabditis elegans*) at concentrations up to 50 µg/mL. However, an improved toxicity profile of Br-derivatives in comparison to the parent PG was observed *in vivo* using zebrafish (*Danio rerio*) model system, when 10 µg/mL applied at 6 h post fertilisation caused death rate of 100, 30 and 0% by PG, PG-Br and PG-Br_2, respectively, which is a significant finding for further structural optimisations of bacterial PGs.

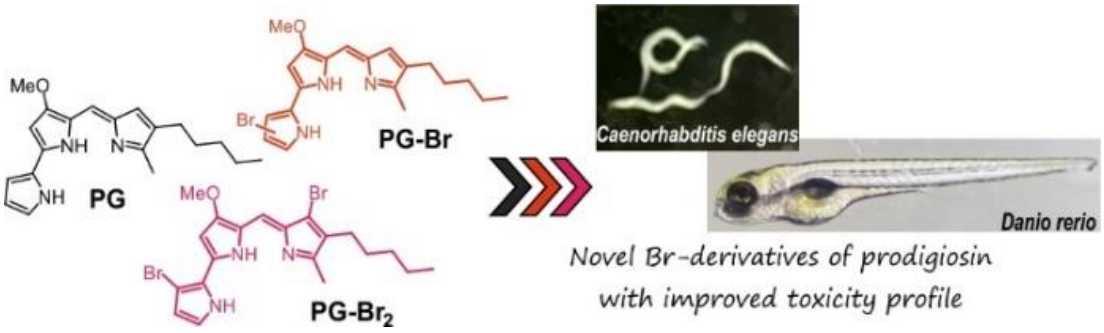

Keywords: prodigiosin, *Serratia marcescens*, meat waste, halogenation, novel derivatives, anticancer activity, apoptosis, zebrafish embryotoxicity

Povzetek

Prodigiozini (PG) so razred obarvanih sekundarnih bakterijskih metabolitov z izjemno biološko aktivnostjo. V doktorski raziskovalni nalogi smo za proizvodnjo prodigiozina uporabili komercialni sev bakterije *Serratia marcescens* ATCC 27117, kot substrat za fermentacijo pa odpadne produkte procesiranja mesa. Na ta način smo pridobili do 83.1 ± 3.0 prodigiozina v 12-ih urah fermentacije. V nadaljevanju smo vzpostavili metode za ekstrakcijo PS tako iz peleta bakterijskih celic kot tudi iz supernatanta bakterijske kulture. Za pridobitev čistega bakterijskega PG smo uporabili gravitacijsko kolonsko kromatografijo.

Strukturo izoliranega PG smo optimizirali z okolju prijazno metodo oksidativnega bromiranja, pri čemer smo dobili mono- in di-bromirane derivate (PG-Br in PG-Br_2). Strukturna karakterizacija bromiranih spojin s pomočjo jedrske magnetne resonance (NMR) in masne spektrometrije (MS) je pokazala, da je PG-Br zmes dveh mono-bromiranih izomer v približno enakih razmerjih, medtem ko je bil PG-Br_2 pridobljen kot čisti derivat.

PG in njegove bromirane derivate smo testirali na štirih rakavih celičnih linijah (A549 – pljučne celice, A375 – kožne celice, MDA-MB-231 – celice raka na prsih in HCT116 – črevesne celice). Potrdili smo antitumorske lastnosti PG in njegovih bromiranih derivatov s polovičnimi maksimalnimi inhibitornimi koncentracijami (IC_{50}) v razponu od 0,62 do 17,00 µg/mL ter indukcijo zgodnje apoptoze, vendar hkrati tudi nizko selektivnost proti zdravim celičnim linijam (MRC-5 - pljučni fibroblasti in HaCaT - kožni keratinociti). Nobena od testiranih PG, PG-Br in PG-Br_2 spojin ni imela opaznega vpliva na gliste *Caenorhabditis elegans* pri koncentracijah do 50 µg/mL. Ugotovili pa smo manjšo toksičnost bromiranih derivatov PG v primerjavi z matičnim PG v modelnem sistemu rib cebric (*Danio rerio*) *in vivo*. Pri cebricah, ki so bile 6 ur po oploditvi izpostavljene 10 µg/mL PG, PG-Br oziroma PG-Br_2, smo ugotovili 100%, 30% in 0% smrtnost, kar je pomembna ugotovitev za nadaljnjo strukturno optimizacijo bakterijskih PG.

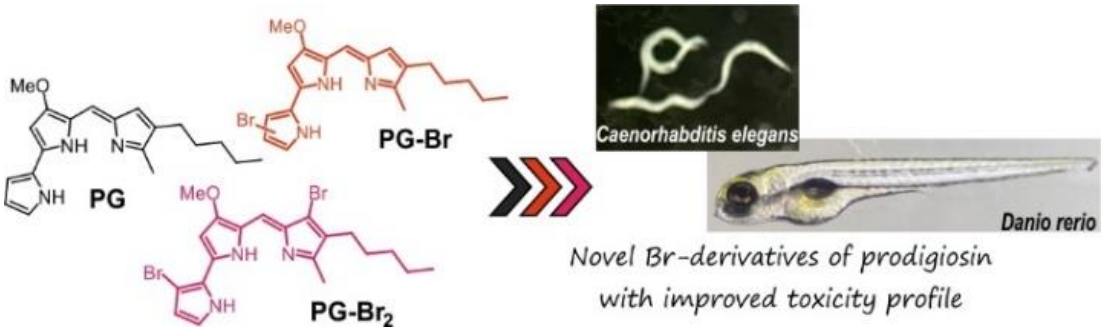

Ključne besede: prodigiozin, *Serratia marcescens*, mesni odpadki, halogeniranje, novi derivati, antitumorsko delovanje, apoptoza, embriotoksičnost cebric

Table of contents

List of abbreviations

ACP	acyl-carrier protein
Arg	arginine
ATP	adenosine triphosphate
CDW	cell dry weight
cfu	colony forming units
CoA	coenzyme A
DCM	dichloromethane (CH_2Cl_2)
DMSO	dimethyl sulfoxide, C_2H_6OS
DNA	deoxyribonucleic acid
EC_{50}	the half maximal effective concentration; the concentration of a drug effective in producing 50% of the maximal response
Et_2O	diethyl ether, $C_4H_{10}O$
EtOAc	ethyl acetate, $C_4H_8O_2$
EtOH	ethanol, C_2H_5OH
FAD	flavin adenine dinucleotide
FB	Fermentation Broth
FBS	foetal bovine serum
FMN	flavin mononucleotide
hpf	hours post fertilisation
HPLC–MS	high performance liquid chromatography mass spectrometry
HR–LC–ESI–MS	high resolution liquid chromatography electrospray ionization mass spectrometry
IC_{50}	the half maximal inhibitory concentration; the concentration of a tested compound where the response (or binding) is reduced by 50%
kb	kilobase, a thousand base pairs of DNA
LB	Luria Bertani medium
LC_{50}	the half maximal lethal concentration; the concentration of a substance that will lead to the deaths of 50% of the treated population
Lys	lysine
λ (lambda)	wavelength
MBC	minimum bactericidal concentration
ME	second-grade canned meat waste
MeCN	acetonitrile
MeOH	methanol
MES	2-(N-morpholino)ethanesulfonic acid, $C_6H_{13}NO_4S$
MIC	minimum inhibitory concentration

MS	mass spectrometry
MTT	3-(4,5-dimethylthiazol-2-yl)-2,5-diphenyltetrazolium bromide, $C_{18}H_{16}BrN_5S$
MW	molecular weight
$NADP^+$	nicotinamide adenine dinucleotide phosphate
NB	Nutrient Broth
NGM	Nematode Growth Medium
NMR	nuclear magnetic resonance
OECD	Organisation for Economic Co-operation and Development
PCP	peptidyl carrier protein
PDB	protein data bank
PG	prodigiosin
PG-Br	monobrominated prodigiosin
$PG\text{-}Br_2$	dibrominated prodigiosin
pH	potential of hydrogen (H); it describes the concentration of H^+-ions in a solution and is the indicator of acidity or alkalinity of the solution
PI	propidium iodide
PLP	pyridoxal 5′-phosphate
PPTase	4′-phosphopantetheinyltransferase
PUR-FC	polyurethane foam cubes
rcf	relative centrifugal force (g-force)
rpm	revolutions per minute
RT	retention time
SCF	Seed Culture Fluid
SD	standard deviation
Ser	serine
TLC	thin layer chromatography
TPP	thiamine pyrophosphate
TSB	Tryptic Soy Broth
UV-Vis	ultraviolet and visible spectroscopy
v/v	volume per volume
VHPO	vanadium-dependant haloperoxidase
w/v	weight per volume
wt	wild-type enzyme

List of figures

List of tables

List of schemes

1. Introduction

1.1. Natural products as sources with great therapeutic potential

Natural products have had a principal role in the treatment of various human conditions throughout the history of humankind.[1] Exceptional efforts have been made to isolate novel natural products (secondary metabolites), from microbes, plants, insects and other living organisms.[2] Isolation of numerous secondary metabolites of great diversity and structural complexity has improved the quality of life, starting from traditional remedies, to contemporary therapeutic formulations, most notably in the areas of infectious diseases and anticancer therapies.[3] While relatively few of the isolated natural products reach clinical application with an unchanged structure, these unique molecules often serve as models for the preparation of more efficacious natural product analogues.

In a review on natural products in drug discovery and development published in 1997, a total of 520 newly approved drugs reported between 1983 and 1994 was analysed based on their source and divided into 5 categories according to their origin: B (biologic), N (natural product), ND (natural product derived), S (synthetic), S* (synthetic, but inspired by natural product) (Fig. 1a, see Table 1 for detailed category clarifications).[4] The same authors have published several similar comprehensive reviews[5-8], the most recent one in 2020[9] and revealed that the total of newly approved drugs reported between 01/1981 and 09/2019 was 1881, while classifying them into now expanded 9 categories based on their source: B, N, ND, S, S*, S/NM S*/NM, V, NB (Fig. 1b, see Table 1 for details on categories and subcategories).

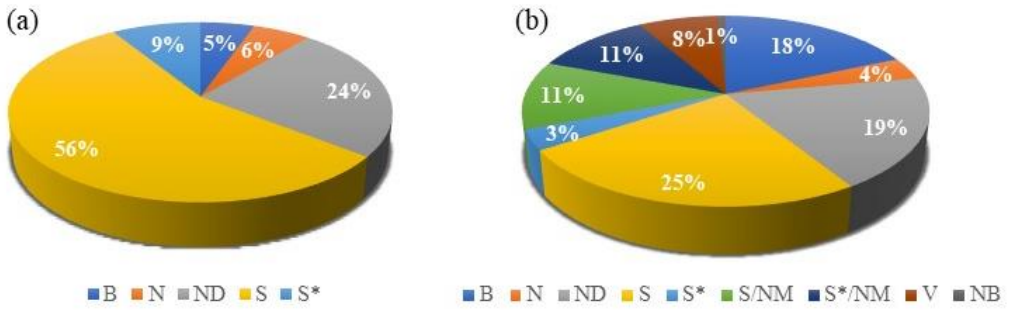

Figure 1. Origins of newly approved drugs: (a) from 1983-1994 (11 years)[4]; (b) from 1981-2019 (38 years)[9]. (See Table 1 for detailed category clarifications).

Table 1. Classification of newly approved drugs based on their origin.[4-9]

	Definition of the category from:	
Category	**1997 (first review)[4]**	**2020 (most recent review)[9]**
B	Biologics (vaccines, monoclonals, *etc*. derived from mammalian sources).	Biological macromolecule; usually a large (> 50 residues) peptide or protein either isolated from an organism/cell line or produced by biotechnological means in a surrogate host.
N	Derived from an unmodified natural product source.	Natural product.
ND	Derived from a natural product source (*e.g.*, semi-synthetics).	Derived from a natural product and is usually a semi-synthetic modification.
S	Exclusively from a synthetic source.	Totally synthetic drug, often found by random screening or modification of an existing agent.
S*	From a synthetic source, but originally modelled on a natural product parent.	Made by total synthesis, but the pharmacophore is from a natural product.
S/NM	/	Natural product mimic: isosteric groups (equivalents of naturally occurring functional groups) are used and they are metabolised *in vivo* to afford active agents.
S*/NM	/	Natural product mimic: modelled by natural substrates (agonists, antagonists), thus causing a direct displacement of the natural substrate.
V	/	Vaccine.
NB	/	Natural product "Botanical" (in general, these have been recently approved).

In the first review from 1997, in the area of novel *antibacterial agents* (n = 64, n = the total number of newly approved drugs), drugs of natural origin (N and ND) predominated with 78%, while the remaining 22% were synthetic drugs (S).[4] In the latest report from 2020, in the same area, just over 55.5% of antibacterial drugs were of natural origin (N, ND or S*/NM categories), followed by 22% of synthetic drugs (S), 20% of vaccines (V) and 2.5% biologics (B) (n = 162).[9] This decreasing trend of the number of antibacterial drugs from natural sources exhibits the need for novel natural product leads, especially having in mind the upsurge of antibiotic resistance.

On the other hand, the *anticancer drugs* reported in 1997 (n = 37) were mostly of natural origin (N and ND) with 41%, 11% were modelled on natural product pharmacophores (S*), with biologics (B) taking up 16% and synthetic drugs (S) at 32%.[4] As for the most recent anticancer drugs reported in the 2020 review (n = 247), they originated from all 9 categories represented in Table 1, where 25% were from natural sources (N, ND and NB), 23% were modelled on natural products (S* and S*/NM), 15% are isosteric mimics of natural products (S/NM), 21% are biological macromolecules (B), 12% are synthetic drugs (S) and 4% are vaccines (V).[9] It is interesting to notice the decrease in the number of purely synthetic anticancer drugs, from 32% to 12%, showing that random screening and modifications of existing agents are most likely not fruitful strategies in this research area.

Natural products still represent an inexhaustible source of bioactive compounds and drug leads in synthetic chemistry and biology, necessary for the discovery of effective agents against a variety of human health conditions and diseases. While relatively few of the isolated natural products reach clinical application with an unchanged structure (Fig. 1, “N” category), these unique molecules often serve as models for the preparation of more efficacious natural product analogues through the methods of semi-synthesis.

1.2. Prodigiosins (prodiginines): history and structures

Prodigiosins (PGs) are biologically active pyrrolylpyrromethene alkaloids, with the first records of their notion and appearance dating back to the VI century BC.[10] PGs derive their name from the miraculous (prodigious) events associated with their occurrence (Fig. 2), and the identification of a producing strain happened for the first time in 1819 in the city of Padua by a Venetian pharmacist Bartolomeo Bizio, attributing the organism to an episode of blood-red discoloration of polenta.[11]

Figure 2. *Serratia marcescens* can grow and produce PG on altar bread wafers[a], making "blood spots".

PGs have a common tripyrrolic structure with a conjugated system of double bonds responsible for their intensive red to purple colour and minor chemical differences represented in their linear (Fig. 3a, prodigiosin, undecylprodigiosin) or cyclic (Fig. 3b, cycloprodigiosin, streptorubin B, streptorubin A) alkyl substituents.[12] Enzymatic cyclisation of *n*-alkylated PGs (Fig. 3a) was described to proceed by *Rieske* non-haem iron oxygenases, but their underlying enzymatic mechanisms still remains elusive.[13] For instance, cycloprodigiosin (cPG, Fig. 3b) is formed by enzymatic oxidation of prodigiosin, and Streptorubin A and B (Fig. 3b) are generated by enzymatic oxidations from undecylprodigiosin (UP).

[a] Figure taken from: https://www.pinterest.com/pin/72690981469568100/?mt=login

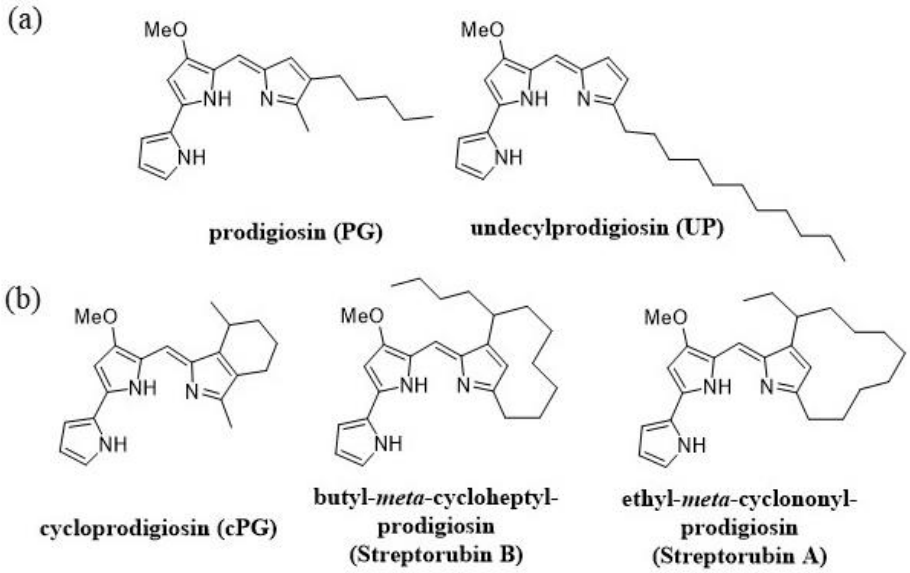

Figure 3. Molecular structures of various prodigiosins (PGs).

This family of compounds can be produced by both Gram-negative bacteria, *e.g., Serratia* spp. and Gram-positive bacteria, *e.g., Streptomyces* spp.[14] They are formed by the producer strain's secondary metabolism in the late exponential and stationary stages of bacterial growth.[11]

1.2.1. Biopigment prodigiosin

The first discovered pigment belonging to the family of PGs was prodigiosin, $C_{20}H_{25}N_3O$ (PG, Fig. 3a) in 1902 and it was investigated for 60 years until the exact structure of PG isolated from *S. marcescens* was finally confirmed in 1962 by total synthesis.[10, 15]

PG consists of three pyrrole rings (A, B and C, Fig. 4a), where A and B rings are bridged in a bipyrrole unit and B and C rings are attached in a dipyrrin moiety, which makes the monopyrrole moiety (C ring) connected to the methoxy bipyrrole moiety (A and B rings) by a methylene bridge. The plated culture of the PG-producing commercially available bacterial strain *Serratia marcescens* ATCC 27117 has a characteristic red colour due to the production and the presence of PG (Fig. 4b).

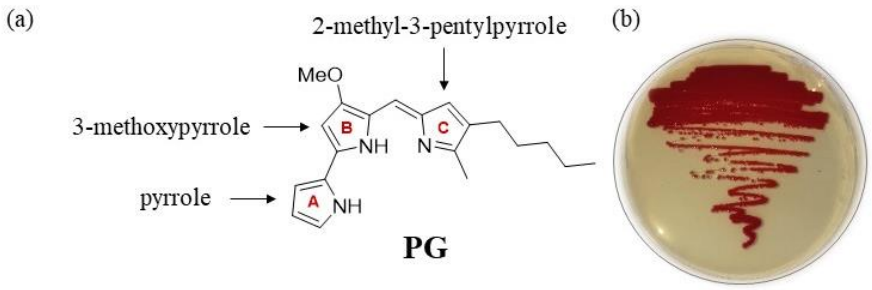

Figure 4. (a) Prodigiosin molecular structure (A, B and C rings); (b) Red colour of the prodigiosin-producing strain *S. marcescens* ATCC 27117 on a nutrient agar plate.

The common tripyrrole structure of all PGs, including PG, can take two different conformations (Fig. 5) and the ratio of the different rotamers is dependent on the pH of the solution.[16] At a neutral and alkaline pH, the *trans* (β) rotamer is preferred, while at an acidic pH, the *cis* (α) rotamer is favoured. However, the measured conformational energy difference between these rotamers is very low, creating a possibility that equilibrium may occur in favour of either of the rotamers, and the preferred one may depend on the intracellular environment of the biological target.[17]

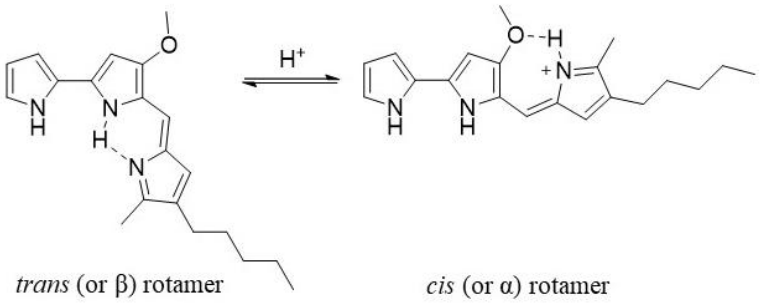

Figure 5. Possible conformations of the pyrrolylpyrromethene skeleton of PG; intramolecular hydrogen bonds are presented as dashed lines (- - -).

1.3. Prodigiosin production in *Serratia* spp.

Serratia spp. are ubiquitous, motile, rod-shaped, Gram-negative, facultative (aerobic and anaerobic) bacteria belonging to the Enterobacteriaceae family.[18-20]

Serratia spp. have been isolated from water, sewage, soil, air, plants, insects, food, as well as animals (rabbits, horses, deer, buffalos).[19, 20] The nonpigmented *Serratia* spp. seem to be restricted to hospitalised patients, whereas pigmented ones are ubiquitous.[11]

Despite being broad host range pathogens capable of opportunistic infections to humans, they secrete a variety of bioactive molecules (PGs, carbapenems, antifungals, volatile organic compounds…)[21] and can potentially be used in agriculture for biocontrol purposes. In addition to secondary metabolites like PG, they secrete extracellular enzymes (chitinases, nucleases, lipases, proteases), as well as produce a wetting agent or surfactant called serrawettin, which helps in the colonisation of surfaces.[20]

Out of the 18 classified *Serratia* species so far, only four have been described and characterised by their ability to produce the red biopigment PG: *S. marcescens* (Fig. 3b), *S. nematodiphila*, *S. plymuthica* and *S. rubidaea*[21], however, they are rarely deposited in the accessible culture collections.

In addition to *Serratia* spp., bacterial species which readily produce PG are numerous, including *Vibrio* spp., *Zooshikella* spp., *Pseudoalteromonas* spp., marine bacteria *Hahella chejuensis*, *Pseudomonas magnesiorubra* and other.[10, 22, 23]

1.3.1. Prodigiosin biosynthetic pathways in *Serratia* spp.

Early research has shown that the PG biosynthesis in *Serratia* spp. is a result of bifurcated biosynthetic pathways[24], finally giving the A, B and C rings of the pyrrolylpyrromethene skeleton (Fig. 3a). In one of these pathways, starting from 2-octenal, 2-methyl-3-pentyl-pyrrole is formed (MPP, Sch. 1).[10]

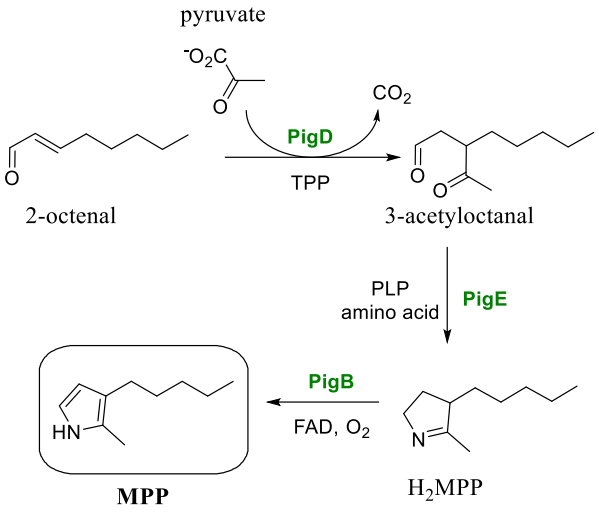

Scheme 1. Biosynthesis of 2-methyl-3-pentyl-pyrrole (MPP) in *Serratia* spp. (**PigD**, **PigE**, **PigB** enzymes).

The precursor for the biosynthesis of MPP, 2-octenal, may be generated by fatty acid biosynthesis enzymes or derived by autooxidation of unsaturated fatty acids.[10] In the presence of thiamine pyrophosphate (TPP), two carbon atoms from the pyruvate are transferred to 2-octenal by the **PigD** enzyme, forming 3-acetyloctanal. In the presence of pyridoxal 5′-phosphate (PLP) as the cofactor and an amino acid, the **PigE** transaminates the aldehyde group of 3-acetyloctanal, resulting in an aminoketone, which spontaneously cyclises to form H_2MPP. The final step in the biosynthesis of MPP is a 2-electron oxidation of H_2MPP using the **PigB** enzyme and flavin adenine dinucleotide (FAD) as the cofactor, to yield the MPP. [10, 25-27]

In the other biosynthetic pathways, 4-methoxy-2,2'-bipyrrole-5-carbaldehyde (MBC) is formed from L-proline (Sch. 2).[10, 25]

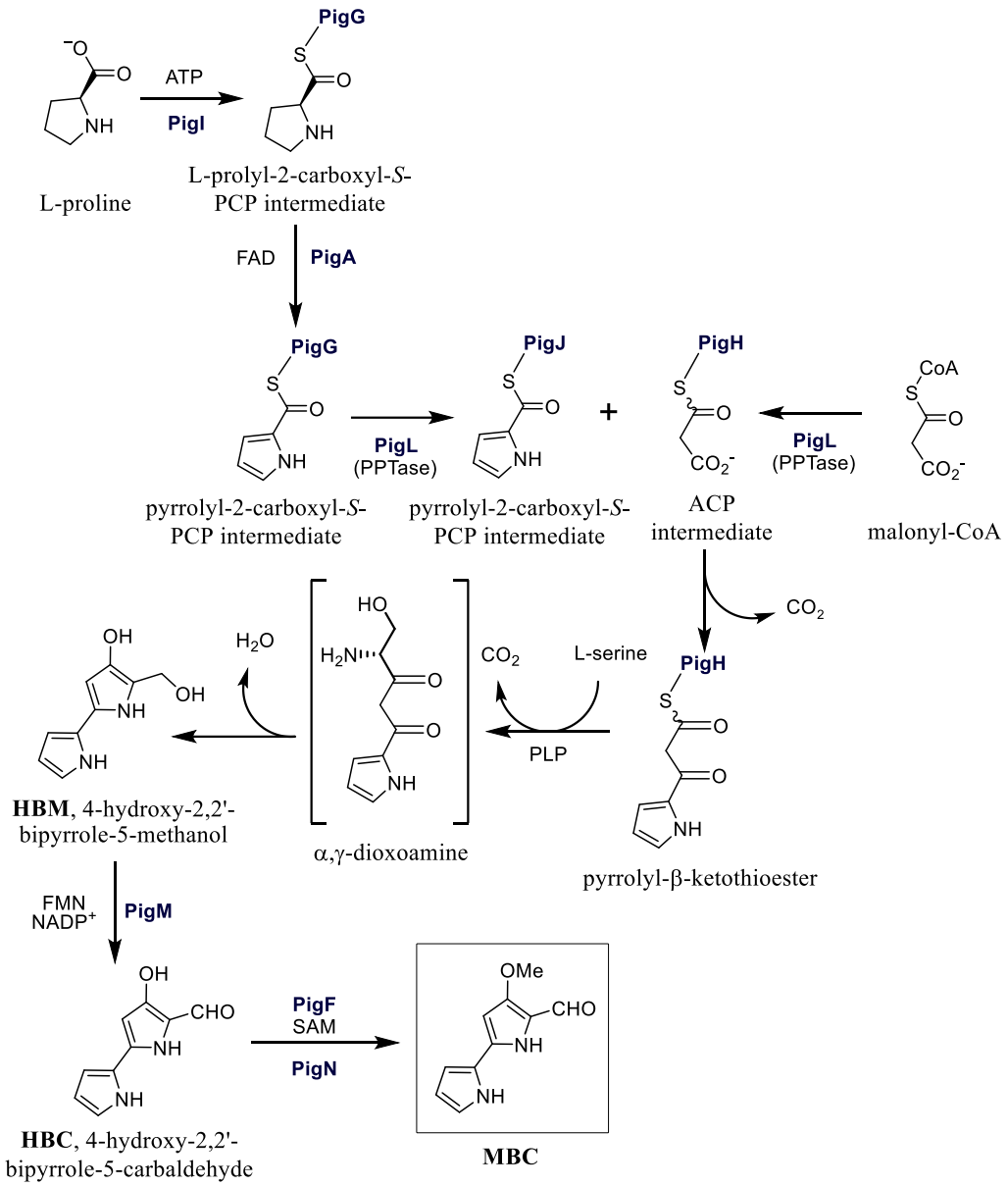

Scheme 2. Biosynthesis of 4-methoxy-2,2'-bipyrrole-5-carbaldehyde (MBC) in *Serratia* spp. (**PigI**, **PigG**, **PigA**, **PigL**, **PigJ**, **PigH**, **PigM**, **PigF**, **PigN** enzymes; no role is assigned yet to **PigK**).

The biosynthesis starts with the enzyme **PigI**, which activates L-proline using adenosine triphosphate (ATP), then transfers the prolyl group to the thiol group of the phosphopantetheine moiety of the **PigG**, which is a peptidyl carrier protein (PCP), and

finally forms an L-prolyl-2-carboxyl-*S*-PCP intermediate. **PigA** then oxidises the L-prolyl-*S*-PCP to pyrrolyl-2-carboxyl-*S*-PCP in the presence of FAD. The 4′-phosphopantetheinyl transferase (PPTase) **PigL** then catalyses the addition of a 4′-phosphopantetheinyl moiety to the conserved serine residue of **PigG**, converting the enzyme from its inactive (apo) form to its active (holo) form in a post-translational phosphopantetheinylation. Next, the pyrrole-2-carboxyl group is transferred from the **PigG** to the cysteine active site (ketosynthase-like domain) of **PigJ** by transthioesterificaton, generating another pyrrole-2-carboxyl thioester. The aforementioned enzyme (**PigL**) also phosphopantetheinylates the acyl carrier protein (ACP) domain of **PigH**, converting the enzyme to its active form, thus enabling a malonyl-CoA (coenzyme A) incorporation into the **PigH** to form an ACP intermediate. In this stage, the biosynthetic pathway introduces a polyketide-type chain extension of the pyrrolyl-2-carboxyl-*S*-PCP intermediate. The bound malonyl then undergoes decarboxylation, resulting in a subsequent condensation with the pyrrole-2-carboxyl thioester attached to **PigJ** and forms pyrrolyl-β-ketothioester attached to the **PigH**. The **PigH** catalyses a decarboxylative condensation of L-serine and pyrrolyl-β-ketothioester, to form α,γ-dioxoamine, which likely undergoes spontaneous cyclisation, dehydration and tautomerisation to generate 4-hydroxy-2,2'-bipyrrole-5-methanol (HBM) in the presence of PLP as the cofactor for transamination. Up to this stage, all of the intermediated are protein-bound. The alcohol group of HBM is oxidised by **PigM** in the presence of flavin mononucleotide (FMN) and nicotinamide adenine dinucleotide phosphate ($NADP^+$) to make 4-hydroxy-2,2'-bipyrrole-5-carbaldehyde (HBC). The final step of MBC biosynthesis involves the methylation of the HBC hydroxyl group by the *S*-adenosylmethionine (SAM)-dependent methyltransferase **PigF** and the oxidoreductase **PigN**.[10, 25-27] No role in the biosynthesis of MBC has been yet assigned to the **PigK**, but it has been speculated that it may have a role as a molecular chaperone assisting the folding of one or more of the Pig enzymes in the later stages of the MBC biosynthesis.[28]

The last step in the biosynthesis is the condensation of MPP and MBC catalysed by **PigC**, an enzyme with relaxed specificity, also being able to incorporate analogues of MPP, after which the tripyrrolic skeleton of PG is formed (Sch. 3).[10] The MBC biosynthesis pathway is highly conserved in all PGs producing species, including the same early precursors, such as proline, acetate, serine and *S*-adenosylmethionine (SAM), which are incorporated into the bipyrrole, however, the biosynthesis pattern for the monopyrrole intermediates (such as the MPP) differs in terms of the 3-pyrrole substituents on the C ring, which suggests that monopyrroles are responsible for the natural diversity of bacterial PGs (Fig. 3).[29]

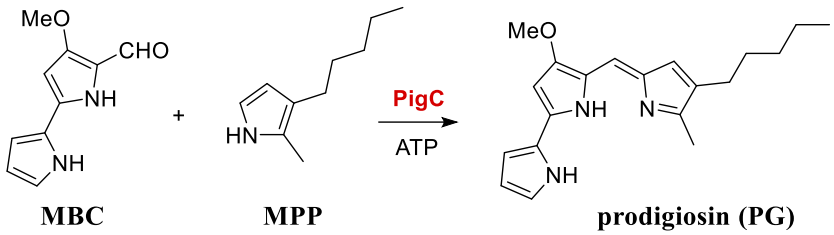

Scheme 3. Biosynthesis of prodigiosin (PG) from 4-methoxy-2,2'-bipyrrole-5-carbaldehyde (MBC) and 2-methyl-3-pentyl-pyrrole (MPP) in *Serratia* spp. (**PigC** enzyme).

In the presented biosynthetic pathways, several proteins play important roles and they are similar to other natural products' synthesising enzymes: peptidyl carrier proteins (PCP), acyl-carrier proteins (ACP), 4′-phosphopantetheinyl transferases (PPTases), domains of the nonribosomal peptide synthetases (NRPS) and ketosynthase domains of the polyketide synthases (PKS).[10] These proteins are present in many bacterial cells that produce secondary metabolites and not only in the ones synthesising PGs.

1.3.2. Gene clusters for prodigiosin biosynthesis and their regulation

Gene clusters for prodigiosin biosynthesis (*pig* genes, 21.0 kilobases) are one directional (Fig. 6) and they have been successfully cloned and expressed in various heterologous hosts, such as GRAS-certified (generally recognised as safe) strain *Pseudomonas putida* KT2440.[29]

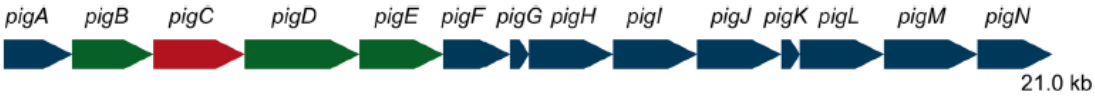

Figure 6. Prodigiosin *pig* gene cluster of *S. marcescens*: **blue** – genes for 4-methoxy-2,2'-bipyrrole-5-carbaldehyde (MBC) biosynthesis; **green** – genes for 2-methyl-3-pentyl-pyrrole (MPP) biosynthesis; **red** – genes for the final condensation step.[29]

The conserved biosynthetic clusters that encode Pig enzymes, which are capable of generating chemical diversity, can allow evolution under environmental pressures.[10] Regulation of biosynthesis of PGs is multifaceted and can be caused by both physiological and environmental changes, which are summarised below.

Physiological changes (biotic factors)[10]

- Signalling inside the cell – synthesis of small signal molecules which can activate/inactivate enzymes responsible for PG biosynthesis.
- Signalling outside the cell (*quorum sensing*, QS) – a mechanism of coordination of separate cells based on the total population density. Cells can produce signal molecules (autoinducers) that accumulate until they reach a limit concentration, after which they cause changes in the expression of specific genes that play a role in the PG synthesis.
- Transcriptional regulators – regulatory proteins that can control transcription or translation of DNA, such as PigP or Rap (regulator of antibiotic and pigment). In the tertiary structure of PigP, there is a specific helix-turn-helix (HTH) domain which modulates the expression of six other important prodigiosin regulators (*pigQ*,

pigR, pigS, pigV, pigX and *rap*), as well as *pigA-pigO* transcription. Rap contains a winged-helix (WH) HTH DNA-binding motif and also activates the transcription of *pigA-pigO* and therefore the PG biosynthesis. Regulatory proteins are like "nodes" through which many signals can be channelled, thus affecting the secondary metabolism in general.

Environmental changes (abiotic factors)[10]

- Signal transduction and two-component system – transforming external cell stimuli into the internal PG biosynthesis through the so called 'phosphorelay'. Enzymes change from their inactive (apo) form into their active (holo) form and *vice versa*. This process is common in Gram-negative bacteria like *Serratia* spp., but it is even more present in the eucaryotic organisms.

- Ecological signalling – as for many other secondary metabolites, the biosynthesis of PG is dependent on the bacterial growth phase, and it is at its highest level under stressful conditions of nutrient deprivation that occurs once the culture is about to reach the stationary phase. These stressors can be a temperature change, oxygen concentration, pH, the amount of light, or the ionic force of the environment. Also, the amount of C (carbon) and N (nitrogen) sources in the medium can vary and cause changes in the biosynthesis of PG, as well as the concentration of inorganic phosphates (P_i), salts, detergents, various cations, anions and amino acids. It is evident that numerous physiological inputs can be "sensed" in the cell and complex genetic networks are used to integrate these signals into the biosynthesis of bioactive secondary metabolites, such as PG.

- Horizontal gene transfer – *pig* gene cluster in *Serratia* spp. is always located between two genes coding the copper-transporting ATPase efflux pumps, *cueR* and *copA*, which maintain cell homeostasis of Cu (copper), which might be indicative of the *pig* cluster being incorporated in the *cueR*/*copA* locus by horizontal gene transfer in some *Serratia* strains. This possibility has been confirmed in an experiment where the whole *pig* cluster has been horizontally transferred into the clinical strain *S. marcescens* 12 (*Sma* 12) which was not a natural PG producer but acquired the pigment biosynthesis ability upon the horizontal gene transfer and expression.

1.4. Biological activities of prodigiosin

PG seems to be living up to its name, as a host of numerous biological activities.[26] Extensive research has been done so far regarding the biological activities of PG and numerous pharmacological properties were established[25, 30]. However, there are no ongoing clinical trials involving PG at the moment.[b]

The antiprotozoal/antimalarial IC_{50} activity of PG was 8 nM against *Plasmodium falciparum*, while the clinically used drug Chloroquine (CQ, $C_{18}H_{26}ClN_3$) has shown IC_{50} of 11 nM.[31]

When the antiparasitic activity of PG was tested against epimastigotes of *Trypanosoma cruzi*, the IC_{50} value was 0.46 ± 0.03 μM for synthetic PG and 0.54 ± 0.25 μM for natural PG, showing a significantly better activity than benznidazole ($C_{12}H_{12}N_4O_3$) at 18.96 ± 7.07 μM, which is the drug currently used for the treatment of the Chagas disease.[32]

The immunosuppressive activity has also been established and PG can act as T cell-specific immunosuppressant, inhibiting primarily IL-2Rα (interleukin-2 receptor α-chain) expression in the IL-2/IL-2R signalling and delaying the progression of autoimmune diabetes.[33] Namely, nonobese diabetic (NOD) mice with the onset of insulitis were treated with 10 mg/kg PG on alternate days from 14 to 20 weeks of age. Blood glucose levels of the NOD mice were measured on the last day and were 750 ± 140 mg/L, with 93% of intact pancreatic islets. On the other hand, untreated NOD mice treated with 0.4% Tween-80 ($C_{64}H_{124}O_{26}$, which was used to dissolve PG) had blood glucose levels of 5060 ± 250 mg/L on the last day, with only 14% of intact pancreatic islets.

PG also has antioxidative properties and can act as a free radical scavenger.[34] The free radical scavenging of 2,2-diphenyl-1-picrylhydrazyl (DPPH, $C_{18}H_{12}N_5O_6$), which has an absorption maximum (λ_{max}) at 515 nm, was increased with the increase in the concentration of PG, and at a concentration of 10 μg/mL PG, the antioxidant capacity was astonishing at 99%, measured as a decrease in absorption at 515 nm.

[b] For more information, please visit: www.clinicaltrials.gov

Research was conducted to assess the UV protective activity in an experiment where cultures were exposed to germicidal UV lamp irradiation (324 J/m^2) during a cultivation over 24 hours.[35] In the case of non-pigmented mutant cells of *Vibrio* sp. DSM 14379, the Malthusian fitness[c] was −13.4 ± 0.5. However, for *Vibrio* sp. DSM 14379 strain which produces PG, the Malthusian fitness was −10.1 ± 0.6, showing a 1000-fold more successful survival. These results suggest an eco-physiological role of PG.

1.4.1. Antimicrobial activity of prodigiosin

Microbial ecology dominance over competitor species is further reflected in the antimicrobial activity of bacterial PG against a panel of Gram-positive and Gram-negative bacteria[34, 36, 37], which was interpreted as a physiological response to microbial competition in the natural soil and surface water environments.[36] Also, antifungal activity of PG was noticed against plant pathogenic fungus *Phoma lingam* at 8.09 µg/mL, whereas a half-lower concentration of 4.04 µg/mL had no effect on its hyphal growth, while the pathogenic fungus *Sclerotinia sclerotiorum* was less sensitive to PG, which had no effect on its hyphal growth even at 16.17 µg/mL.[38] In addition to these environmental plant pathogens, synergistic antifungal activity of chitinolytic enzymes (endochitinase and chitobiase) and PG from *S. marcescens* B2 was proved effective against *Botrytis cinerea* (grey mould pathogen) spore germination at 100 µg/mL of PG.[39] Antimicrobial activity of PG was attributed to plasma-membrane damage of some human pathogens, including *Candida albicans*, *Escherichia coli* and *Staphylococcus aureus*, by causing leakage of intracellular metabolites, such as K^+-ions, sugars, amino acids and proteins.[37]

Antibacterial activity of PG was assessed against 5 food pathogens in a disc-diffusion assay[34] (*Escherichia coli* MTCC 2939, *Bacillus cereus* MTCC 8372, *Clostridium botulinum* ATCC 27022, *Vibrio vulnificus* ATCC 27562, *Salmonella enterica* ATCC 29630) and was compared with the chemical food preservative sodium nitrite ($NaNO_2$) as a positive control. PG showed a statistically insignificant improved

[c] The Malthusian fitness was calculated based on CFU counts as a natural logarithm of the ratio between the final and the initial cell number.

antimicrobial activity on the discs in comparison with $NaNO_2$, with the lowest activity of 0.2 cm inhibition zone at 500 µg/mL of PG against *V. vulnificus* ATCC 27562. However, when the meat extract powder (MEP) was preserved with PG (MEP@PG) or $NaNO_2$ (MEP@$NaNO_2$) and compared to the non-preserved control (MEP@C), the colony counting method showed 20×10^8 CFU/g of bacterial population contamination for MEP@C, 32×10^6 CFU/g for MEP@$NaNO_2$ and only 6×10^1 CFU/g for MEP@PG, showing the potential of PG to be used as an alternative additive for the disinfection of pathogens in the food industry, which could extend the shelf life of products.[34]

In a more recent study aimed at PG being used for food packaging[40], composite materials based on oxidised-bacterial cellulose (BC) and poly(vinyl alcohol)-chitosan (PVA-CH) nanofibers were produced by needleless electrospinning and functionalised with the bacterial pigment PG. Two different double-layered PG-containing antimicrobial materials were produced for different food packaging applications: against interior foodborne pathogens, with PG incorporated into the inner layer (BC/PVA-CH_PG composite) and against external contamination, with PG added to the outer layer of BC (BC_PG/PVA-CH composite). The materials were assessed against *Staphylococcus aureus* ATTC 6538 and *Pseudomonas aeruginosa* PA25, which are among the most common foodborne bacteria. The incorporation of PG into the inner layer (PVA-CH_PG) exhibited significant bacterial reductions, with 97.38 ± 0.57% growth inhibition for *S. aureus* ATTC 6538 and 98.62 ± 0.37% for *P. aeruginosa* PA25, while the incorporation of PG into the outer layer (BC_PG) revealed evident growth inhibition of 97.65 ± 2.04% for *S. aureus* ATTC 6538 and 97.09 ± 1.54% for *P. aeruginosa* PA25. The minimum inhibitory concentration (MIC) of PG itself was 240 µg/mL against *S. aureus* ATTC 6538 and 1250 µg/mL against *P. aeruginosa* PA25, so the results were more than justified, since the concentration of PG in the materials (15% weight) was significantly higher than the established MICs against both pathogenic strains.[40]

1.4.2. Anticancer activity of prodigiosin

PG has been researched the most as an anticancer agent and has exhibited anticancer activities against numerous cell lines, including lung[41], ovarian and gastric[42], breast cancer[43] and many others.[12] Anticancer potential of PG has been demonstrated in several studies, on various types of cancer and through diversified modes of action (Table 2), with a high potential of PG for the induction of apoptosis (programmed cell death) in different cell types, even in combined therapy.[44] Interestingly, the same mechanism of action (induction of apoptosis) was noticed for undecylprodigiosin and some other PGs, too.[14]

Table 2. Antiproliferative activity of PG (IC_{50}, μM) after different exposure time treatments of various cancer cell lines.

Cancer type (in humans)	Cell line	Expo-sure(h)	IC_{50} (μM)	Mode(s) of action	Reference
Brain malignant glioma	U87MG	24	12.29	autophagic cell death, apoptosis	Cheng *et al*. 2018[45]
Lung cancer	GLC4	24	0.105	apoptosis	Llagostera *et al*. 2005[46]
Breast cancer	MDA-MB-468	48	0.261	Wnt/β-catenin signaling antagonist	Wang *et al*. 2016[43]
B-cell chronic lymphocytic leukemia	B-CLL	48	0.116	apoptosis	Campas *et al*. 2003[47]
Hepatocellular carcinoma	Hep G2	72	0.224	apoptosis	Yenkejah *et al*. 2017[48]
Colon adenocarcinoma	HT-29	72	0.40	apoptosis	Dalili *et al*. 2011[49]

The apoptotic mechanism of PG was studied in detail, and the intracellular target of PG was investigated in melanoma cells, suggesting that PG could interact

with the BH3 domain of the BCL-2 family of anti-apoptotic regulatory proteins (BLC-2, BCL-X_L and MCL-1).[50] In survival conditions, the aforementioned anti-apoptotic proteins normally sequester the pro-apoptotic proteins BAX and BAK which regulate the mitochondrial outer membrane permeabilisation. In stressful conditions, BH3-mimetic molecules such as PG can bind to the BH3 domain of anti-apoptotic BCL-2 proteins, displacing and releasing BAX and BAK which cause the cell membrane to discharge cytochrome C into the cytosol, thus activating procaspase-9 and leading to apoptosis.[50]

PG was potently cytotoxic in both estrogen receptor positive (MCF-7) and negative (MDA-MB-231) breast cancer cell lines.[51] Moderately increased levels of cytochrome C in the cytosol were detectable in MCF-7 cells as early as 30 min after PG treatment, and a marked increase was observed at 12 h, indicating that PG-mediated apoptosis occurs using primarily mitochondria to transduce its death inducing message. PG also induced the activation of the main proteases that executes apoptosis, such as the initiator caspases-9 and -8 and also the effector caspase-7, as well as cleavage of the caspase substrate PARP, poly (ADP-ribose) polymerase, again suggesting that PG acts using the mitochondrial pathway to cause apoptosis.[51]

PG could reactivate p53 family-dependent transcriptional activity and restore p53 signalling in p53-deficient human colon cancer cells and this activation induced cell-cycle arrest and apoptosis through its transcriptional regulation of specific target genes (*e.g. p21, bax…*).[52]

However, the interaction between PG and intracellular target proteins needs more precise evaluation, as targets still seem diversified.[53]

Although the anticancer potential of PG and other PGs has been demonstrated through the induction of apoptosis and other modes of action (Table 2), *in vivo* toxicity studies of PG are not readily available in the literature. The nematode *Caenorhabditis elegans* is a model system with well-known developmental stages[54], which can be utilised in anticancer drug discovery for toxicity, immunity, as well as pharmacogenetics studies, among others[55], so it represents a fitting model system for PG safety research. In addition, biomedical research model zebrafish (*Danio rerio*) are commonly used in anticancer drug screens for toxicity assessment, as the transparency

of embryos for up to 5 days post fertilisation facilitates the visualisation of potential toxicities (cardiotoxicity, hepatotoxicity…).[56, 57]

The anticancer activity of PG was tested in 2005 *in vivo* on mice that were inoculated i.v. (intravenously) with mouse melanoma B16BL6 cells[d].[41] In this animal experiment, i.p. (intraperitoneal) administration of 5 mg/kg of PG for 2 weeks after inoculation decreased the number of metastatic nodules by 53% (from 72 to 34) and elevated the survival rate of mice from 43% (negative control) to 86% (treated experimental animals). It is interesting to mention that a year later, the first synthetic prodigiosin derivative GX15-070 (Obatoclax) reached phase I/II clinical studies in oncology (solid tumour and haematological malignancies) in single-compound and dual-agent trials and that PG itself entered pre-clinical trials in 2007 for the treatment of pancreatic cancer (AIDA Pharmaceuticals Inc., China)[10, 12, 58] but did not reach the market. Antitumor antibiotics like PG are amongst the most important cancer chemotherapeutic agents[1], so PG is also commercially available for biotesting purposes, but extremely expensive to purchase, with the cost of 1 mg ranging from 390 € to the astonishing 4,490 € in the form of its hydrochloric salt (Table 3).

Table 3. Prices and purities of 1 mg of PG from different manufacturers as on 26th September 2022.

PG price (per 1 mg)	**Manufacturer**	**Producing strain**	**Purity**	**Source**
390 EUR	abcam	*Proteobacterium* strain (Gamma)	> 95%	Link
702 EUR	Santa Cruz Biotechnology	*Serratia marcescens*	> 95%	Link
745 EUR	Merck	*Serratia marcescens*	≥ 95%	Link
1,150 USD	Adooq Bioscience	/	> 98%	Link
1,190 USD	MyBioSource	*Serratia marcescens* MST-AS5330	~ 95%	Link
4,490 EUR†	Merck	*Serratia marcescens*	≥ 98%	Link

† $C_{20}H_{25}N_3O \cdot HCl$

[d] Pulmonary metastasis of mouse melanoma is an acknowledged animal model about metastasis.

In general, the remarkably high prices of bacterial natural products could have multiple explanations. On the one hand side, commonly used and readily available nutrient for *S. marcescens* growth, such as peptone (obtained by proteolytic digestion of casein from bovine milk) comes expensive when large-scale fermentations are envisioned, which raises the overall cost of the PG production process and the cost of the final natural product. On the other hand side, microbes generate and accumulate many alkaloids, sometimes structurally quite similar, which makes efficient purification difficult and expensive.[29]

In comparison to peptone and other costly nutritional media components, waste stream products are low-priced and recycling them adds to sustainable development, thus addressing some of the major societal issues. For example, part of the environmental pollution is caused by the amount of generated organic waste and by-products, which arguably represent useful sources of carbohydrates, proteins, lipids and minerals.[59] This is why the spotlight is now on recycling of organic wastes for the cost-effective processes in biotechnology, which can afford valuable biologically active molecules.[60, 61]

1.5. Halogenation of natural products

Halogen atoms (X = F, Cl, Br, I), as substituents with biological activity, are widely present in pharmacology and pharmaceutically relevant compounds; around 50% of molecules in high-throughput screening (HTS) are halogenated, as are around 40% of drugs currently on the market or in clinical trials (data from 2016).[62] Furthermore, an estimated 25% of medicinal chemistry papers, as well as patents, include the addition of halogen atoms at a late stage of the synthesis (late-stage functionalisation).[62] This method is an efficient way to generate natural product derivatives for drug discovery and chemical biology.

Halogens form a halogen bond (X–bond, D–$X\cdots A$, D = donor, A = acceptor), analogous to the hydrogen bond (H–bond, D–H$\cdots A$) with a proximal halogen-bond acceptor (A = O, N, S) and even the aromatic rings (halogen–π interactions).[63] These intermolecular interactions are weak, non-covalent, highly directional, specific and have attracted great attention in pharmacology, because they can improve ligand

affinities without disrupting other important interactions of pharmacophores[e] and they allow investigation of steric effects on the biological activity. Also, the incorporation of halogen entities in lead compounds has been predominantly performed to introduce higher target affinity, to increase lipophilicity and bioavailability, as well as to alter metabolic stability/pharmacokinetics and to lessen adverse effects.[64]

The presence of halogen substituents (–Cl, –Br, –I) increases the bulkiness of the molecule, adding to the membrane permeability and the absorption profile of the compound, while the presence of highly electronegative halogens (–F, –Cl, –Br) adds to the polarisation of the structure.[63] In particular, bromination is expected to affect hydrophobicity of molecules, as well as facilitate transport across membranes and binding to hydrophobic pockets, especially since bromine substituents were proven more hydrophobic than methoxy-moieties *in vitro* and *in silico*.[65]

1.5.1. Halogenated natural products and their biological activity

Notable examples of halogenated bioactive compounds are natural products isolated from various living organisms. Often, these natural products contain more than one halogen atom (these halogens are usually bromine and chlorine). Their plethora of biological activities are generally assigned to their halogen substituents (Fig. 7).

[e] Pharmacophore is defined as a spatial arrangement of chemical groups or features in a molecule responsible for a particular pharmacological interaction.

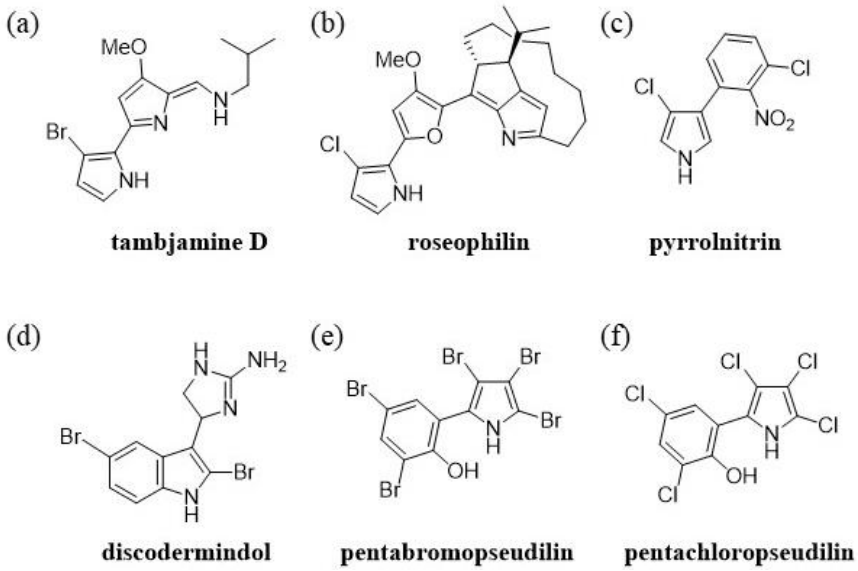

Figure 7. Molecular structures of halogenated heterocyclic natural products produced by bacteria.

Tambjamin D (Fig. 7a), a close relative of PG with an enamine in the place of the C ring, has been isolated from bryozoan marine sources. Although it is less potent than PG, this and other tambjamines (A-J) have exhibited cytotoxicity and nuclease activity in the presence of Cu^{2+}.[66] A halogenated natural product roseophilin (Fig. 7b) isolated from *Streptomyces griseoviridis*, which is a relative of PG with a methoxyfuran ring in the place of methoxypyrrol, shows *in vitro* anticancer properties against leukaemia and other cancer cell lines.[66] Pyrrolnitrin (Fig. 7c) was isolated from *Pseudomonas pyrrocinia* as an antibiotic showing activity against fungi, yeast and Gram-positive bacteria.[67] Another example of a halogenated natural product is discodermindol (Fig. 7d), a brominated aminoimidazolinylindole isolated from the sponge *Discodermia polydiscus,* which shows activity against P-388 (murine leukaemia), A549 (human lung), and HT-29 (human colon) cancer cell lines.[68] The first ever reported marine bacterial metabolite was pentabromopseudiline (Fig. 7e) isolated from *Pseudomonas bromoutilis*, a compound made up of more than 70% bromine by weight showing antibiotic properties against Gram-positive bacteria.[68] Structurally similar to pentabromopseudiline is pentachloropseudilin, another phenylpyrrole alkaloid (Fig. 7f) produced by *Actinoplanes* sp. ATCC 33002.[67] The producer strain of pentabromopseudiline is not able to produce pentachloropseudilin

and *vice versa*, which signifies that the enzymes involved are highly specific concerning their halide substrate.[68]

As an additional example of halogen importance in a biologically active molecule, the antibiotic potential of vancomycin against *Bacillus subtilis* decreased 30-50% when chlorine atoms (one or both) were removed from the structure, exhibiting the importance of halogen substituents, regardless of the fact that chlorine atoms make only 4.9 mass% of the entire vancomycin molecule, $C_{66}H_{75}Cl_2N_9O_{24}$.[63]

Because of the unique bioactivities associated with natural halogenated compounds, they continue to serve as powerful lead structures in drug design and development. Despite the existence of halogenated tambjamine D and roseophilin (Fig. 7a and 7b, respectively), obtaining halogenated derivatives of PG has not been investigated so far, especially not in the context of late-stage functionalisation of this natural product. By means of different halogenations reactions, derivatives of PG with introduced *X*-atom(s) may be generated and new *X*–bond(s) could be formed with the target macromolecules, which might improve the existing biological properties of PG.

Selective halogenation of natural products is becoming a popular research area due to the important pharmacological properties of organo-halide molecules.[69] Introducing *X*-atom(s) into natural products such as PG can be assessed by using two halogenation approaches for late-stage modifications: enzymatic and chemical halogenations.

1.6. Enzymatic halogenations

Nature has evolved different strategies to create carbon-halogen (C–*X*) bonds in a highly effective and specific manner, as evidenced by approximately 4000 halogenated natural products isolated to date, many of which are reportedly produced by marine organisms.[70] Various structures of many halogenated secondary metabolites (Fig. 7) suggest that there are naturally occurring halogenating enzymes that have a high degree of substrate specificity and are capable of regioselective halogen incorporation.[71]

Halogenating enzymes can be grouped into two classes based on their mechanism: haloperoxidases and halogenases, both dependent on specific cofactors.[63] Haloperoxidases (HPOs) are less specific, and they can be metal-dependent (haem iron-dependent or vanadium-dependent haloperoxidases), and metal-free (perhydrolases, no coenzyme needed); their enzymatic electrophilic halogenation is mainly achieved using oxidative mechanisms triggered by both metal-containing and organocatalytic proteins.[72] Haloperoxidases have traditionally been classified on the basis of the halide that is oxidised.[73] Halogenases are highly substrate-specific and require oxygen for enzymatic activity: flavin($FADH_2$)-dependent halogenases, enzymes responsible for the synthesis of pyrrolnitrin (Fig. 7c), pentabromopseudilin (Fig. 7e) and pentachloropseudilin (Fig. 7f), α-ketoglutarate-dependent halogenases (non-haem iron-α-ketoglutarate-dependent/O_2) for radical halogenation reactions, and *S*-adenosylmethionine (SAM)-dependant halogenases for nucleophilic halogenation reactions.

The detection of the first haem iron-dependent haloperoxidase, chloroperoxidase (CPO), from the fungus *Caldariomyces fumago* in 1959 was the starting point for studies on biological halogenation and for about 35 years, haloperoxidases were the only halogenating enzymes known to oxidise halides.[74] However, a new class of halogenating enzymes was discovered in 1993 from fungus *Curvularia inaequalis*, and in 1995 the first vanadium-dependant haloperoxidase (VHPO) was crystallised.[63] Indeed, the pace of discovery of new haloperoxidases and halogenases has been increasing exponentially over the years with the use of genomic and bioinformatic approaches.[73]

Haloperoxidase enzymes generate an electrophilic, oxidised halogen as the reactive reagent, most likely in form of a hypohalite "O*X*—", using stoichiometric amounts of the corresponding halide and an oxidant such as hydrogen peroxide (H_2O_2) or oxygen (O_2). The electrophilic halogen species (X^+) is then released from the active site, providing a freely circulated strong oxidant which then reacts with electron-rich organic substrates.[63] Among these biocatalysts, the vanadium-dependent haloperoxidases (VHPOs) exhibit remarkable features not addressable with today's synthetic halogenation methods and halogenation of even remote sites is particularly significant in this context.

The VHPOs contain vanadate ion (VO_4^{3-}) as a prosthetic group and catalyse the oxidation of halides (Cl^- or Br^-) in the presence of hydrogen peroxide as the oxidant (Sch. 4).

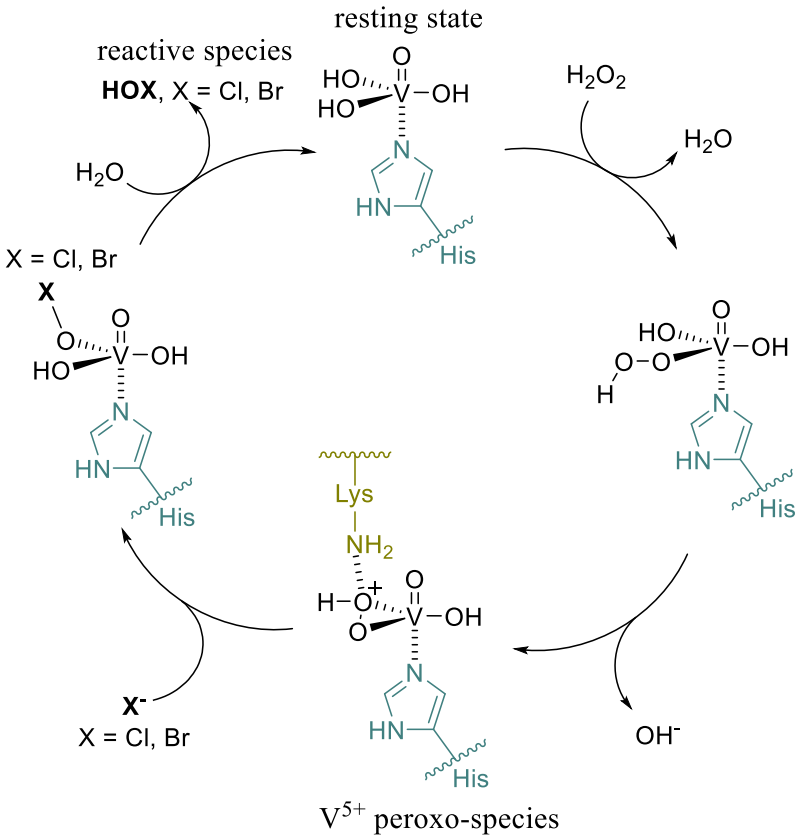

Scheme 4. Mechanism of oxidative halogenations by the vanadium-dependant haloperoxidase (VHPO) *via* peroxo intermediate of the vanadate (6 o'clock).[63]

In the resting state of the VHPOs, vanadium contains four oxygen ligands, while the free coordination site is occupied by a catalytic histidine (His) residue, resulting in a coordinate-covalent bond and in trigonal bipyramidal coordination geometry of vanadium (Sch. 4, 12 o'clock). In the presence of hydrogen peroxide, a hydroxyl group is substituted by peroxide (Sch. 4, 3 o'clock). Upon elimination of the hydroxide ion (OH^-), a cycloperoxo-species is generated, which is stabilised by a catalytic lysine (Lys) residue (Sch. 4, 6 o'clock) and this is probably an essential feature of the catalytic reaction, as it increases the potential of the oxoperoxo-V^{5+} center for halide oxidation. This cyclic intermediate is opened by the addition of a halide (Sch. 4, 9 o'clock). The vanadium-bound hypohalite can then be hydrolysed by water, leading to the release of hypohalous acid, the oxidised halogen form that can

proceed to electrophilic oxidation. During catalysis, vanadium does not change its oxidation state (V^{5+}). These VHPO enzymes have attracted the attention of researchers because of their biocatalytic properties, including an unusual stability in organic solvents and tolerance to heat and high concentrations of H_2O_2.[75]

1.7. Chemical halogenations

PG is a complex heteroaromatic natural product with several reactive positions on A, B and C rings (Fig. 3a). The descriptions of chemical reactions, that introduce carbon–halogen (C–*X*) bonds into the molecule, are not available in the literature. This is assumably because regioselective and chemoselective halogenations are, in general, not easily accomplished under extreme conditions necessary for a "classical" halogenation reaction.[76, 77] These extreme conditions are often energy-demanding, and imply using toxic, corrosive and hazardous molecular halogens, such as chlorine gas or elemental bromine, as well as modified reagents such as *N*-bromo- and *N*-chlorosuccinimide (NBS and NCS, respectively) which are synthesised from molecular halogens or hypohalous acids.[63, 76, 77] Due to the sensitivity of PG to light[78], its sensitivity to some solvents and its instability at high temperatures[79], mild, late-stage functionalisation is preferable.

Considering a continued need for generating halogenated organic compounds, the research focus is also on the development of more environmentally friendly and sustainable synthetic methods for generating C–*X* bonds that mimic enzymatic halogenation reaction conditions.[80, 81] Methodologies for halogenation have been developed to be milder, environmentally acceptable and to allow for some control of the reaction outcome.[80-84] These halogenation reaction conditions should exhibit high functional group tolerance and be applicable on a variety of electron-rich compounds, including PG.

Natural sources of halide atoms are inorganic salts and acids, but they require an oxidant to generate a source of the electrophilic "X^+" *in situ* and to enable electrophilic aromatic substitution (EAS).[81] Hydrogen peroxide (H_2O_2) is a suitable choice, as it works for both bromination and iodination. It is stable with a variety of functional groups, it does not easily oxidise heteroaromatic rings and its waste

by-product is water.[80] As an atom-economical halide source, hydrohalic acids (H*X*, *X* = Cl for hydrochloric, *X* = Br for hydrobromic) can be used. When hydrobromic acid is oxidised in a two-step process, first the elemental bromine is formed (Sch. 5a), which is then immediately disproportionated in water, generating HOBr (Sch. 5b), the reactive Br^+ species.[80] Oxidative halogenation of this type offers interesting perspectives, as there are no reagent residues (apart from water) and the reaction occurs with 100% halogen atom economy.[81]

(a) **$2\ HBr + H_2O_2 \rightarrow Br_2 + 2\ H_2O$**
(bromide oxidation to bromine)

(b) **$Br_2 + H_2O \rightarrow HBr + HOBr$**
(bromine disproportion generates HOBr, which acts as the Br^+ source)

Scheme 5. Proposed mechanism of halogenations with H_2O_2/HBr.[80]

Other oxidising agents, such as dimethyl sulfoxide (DMSO), can be used to generate electrophilic "X^+ species" from X_2, as the slow generation of X_2 *in situ* is crucial.[83] According to literature (Sch. 6), HBr can be oxidised by DMSO to generate Br_2 or DMS·Br_2. The reaction of Br_2 or DMS·Br_2 with arenes affords the aryl halides with the formation of HBr, which is again oxidised by DMSO for the next oxidative cycle. Thus, stoichiometric quantities of DMSO and HBr are sufficient for full and efficient halogenation reaction under mild oxidative conditions.

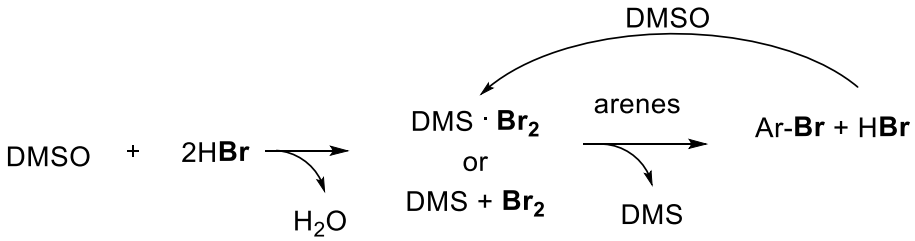

Scheme 6. Proposed mechanism of halogenations with DMSO/HBr.[83]

1.7.1. Synthetic halogenated heterocycles

Synthetic pharmaceuticals, which have a halogenated heterocyclic skeleton, are classified into various therapeutic groups such as antineoplastics, antibacterial and antifungal agents, antipsychotics, benzodiazepine tranquilizers, tricyclic antidepressants, antimalarials, antiallergics, thiazide diuretics and others (Fig. 8).[64]

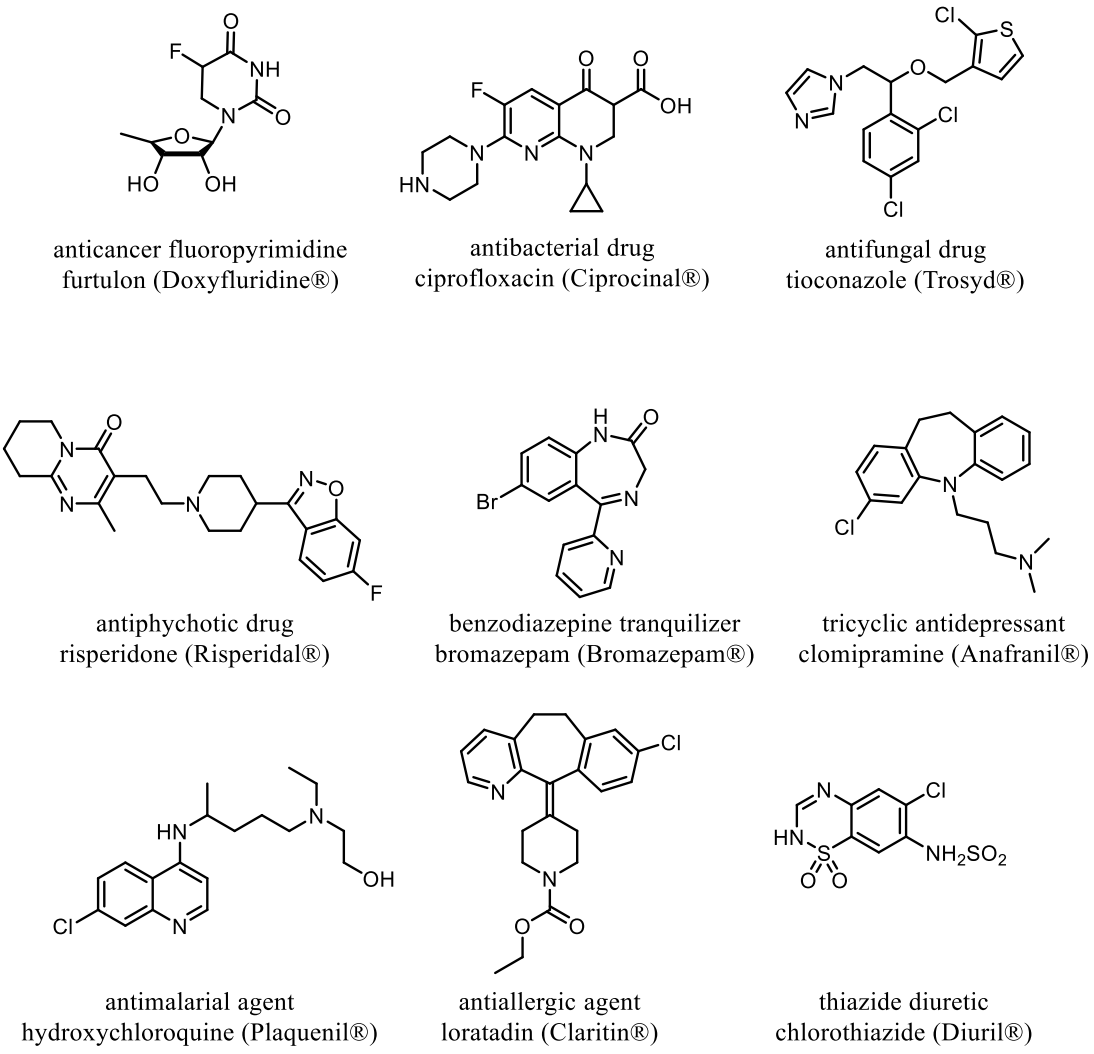

Figure 8. Halogenated heterocycles used in clinical practice (trade name given in parentheses).[64]

The most prominent halogen introduced into active agents is fluorine with 57%, followed by chlorine with 38%. Brominated compounds are rarely found in drugs, making up only 4% and iodine is the rarest halogen used in halogenated drugs with only 1%. Apart from pharmacological activity, halogenated heterocycles find their use in different fields, such as biopharmaceutic building blocks for palladium catalysed cross-coupling methodologies for C–C and C–*Y* (*Y* = N, O, S) bond formations in arenes and heterocycles, as well as novel imaging technologies, in which radioactive isotopes ^{18}F- and ^{124}I-labelled probes are utilised as tracers in positron emission tomography (PET) for *in vivo* studies of protein function and enzyme catalysis.[63]

2. Aims of the research work

Many studies have been performed using PG isolated from wild-type *Serratia* spp. found in natural environments, such as animal fleshing[34] or soil[79], in patients having a wound infection[18], or upon genetic mutations of these PG-producing strains[85], but the optimisation of PG production together with a biological activity assessment have rarely been reported for commercially available PG producers.

The overall aim of this study was to develop an efficient and economical protocol for PG production from a commercially available bacterial strain, to isolate and structurally optimise the natural biopigment PG through generation of novel halogenated derivatives, and to assess the bioactivity of PG and its novel derivatives. The aim was divided and realised through specific objectives:

1) To use commercially available strain *Serratia marcescens* ATCC 27117 to obtain bacterial PG *via* optimisation of the biotechnological production process, in particular by using waste stream from food industry as a source of carbon and nitrogen.

2) To find a suitable and sustainable method for the extraction of the biopigment ensuring a high yield, and to achieve maximum purity of the target natural product PG.

3) To obtain novel halogenated derivatives of this natural product (PG-X_n) using mild late-stage functionalisation through different methodological approaches (enzymatic and chemical), and to confirm the PG and PG-X_n structures by complete structural characterisation.

4) To evaluate biological activity properties of PG and its novel halogenated derivatives as antimicrobial and anticancer compounds *in vitro*, to investigate if the potential for the induction of apoptosis is retained in the novel halogenated derivatives, and to assess their toxicity and safety on *in vivo* model systems of roundworms (*Caenorhabditis elegans*) and zebrafish (*Danio rerio*).

3. Materials and methods

3.1. Reagents

3.1.1. Bacteriological media components

Constituents of bacteriological media were molecular biology reagent-grade. Tryptone, peptone and Tryptic Soy Broth (TSB) were purchased from Torlak, Serbia. Yeast extract and agar were purchased from Biolife, Italy. The beef extract was purchased from Becton Dickinson, US.

3.1.2. Chemicals

All chemicals were of reagent-grade quality or higher and used without further purification. Hydrogen peroxide (H_2O_2), HBr, cholesterol, 3-(4,5-dimethylthiazol-2-yl)-2,5-diphenyltetrazolium bromide (MTT), tricaine, $NaHCO_3$, KH_2PO_4, Na_2HPO_4, $(NH_4)_2SO_4$, 2-(N-morpholino)ethanesulfonic acid (MES), $CaCl_2 \cdot 2H_2O$, $KMnO_4$ and NaOH were purchased from Sigma Aldrich, Germany. Glycerol, Tween-80, Na_3VO_4, imidazole, Na_2SO_4, RPMI 1640 medium, foetal bovine serum (FBS), penicillin and streptomycin were purchased from Thermo Fisher Scientific, UK. KBr and tris(hydroxymethyl)aminomethane hydrochloride (Tris-HCl) were purchased from Carl Roth GMBH, Germany. NaCl was purchased from Biolife, Italy. HCl was purchased from Avantor, Poland. $MgSO_4 \cdot 7H_2O$ was purchased from Acros Organics, Belgium. KCl was purchased from Becton Dickinson, US. Instant Ocean® Salt was purchased from Instant Ocean, US.

3.1.3. Solvents

Solvents were used as received. Ethyl-acetate (EtOAc) and dimethyl sulfoxide (DMSO) were purchased from Sigma Aldrich, Germany. Methanol (MeOH), methylene-chloride (CH_2Cl_2 *i.e.*, DCM), acetonitrile (MeCN) and acetone were

purchased from Thermo Fisher Scientific, UK. Ethanol (EtOH) was purchased from Zorka, Serbia. Diethyl-ether (Et_2O) was purchased from Avantor, Poland. Hexane was purchased from J. T. Baker, The Netherlands. Chloroform ($CHCl_3$) was purchased from Lach:ner, Czech Republic. Deuterated methanol (MeOD, methanol-d_4) was purchased from Carl Roth GMBH, Germany. Deuterated chloroform ($CDCl_3$) was purchased from Acros Organics, Belgium.

3.2. Instrumentation

All cultivation media were prepared using distilled water and sterilised in a vertical Autoclave ST-G series (Lab Companion from Jeio Tech, US) at 121 °C temperature, 0.12 MPa pressure for 15 min.

Erlenmeyer flask cultivations were performed on Innova 2100 platform shakers from New Brunswick Scientific (Eppendorf UK Limited, UK) placed in a room with a constant temperature.

Bacterial batch fermentations were done in a bioreactor with 4.5 L working volume Bio4, EDF-5.4_1 (Biotehniskais centrs AS, Latvia).

Blending of processed meat waste for media preparation was done using a Nutribullet cooking extractor (Delimano, Serbia).

The elemental analysis (C, H, N and S) was performed by using Elemental Analyzer Vario EL III (Elementar, Germany).

Centrifugations were done based on the volume: up to 2 mL in Eppendorf 5418 bench top centrifuge (Eppendorf, Germany), from 2–50 mL in Eppendorf 5804R bench top centrifuge (Eppendorf, Germany) and more than 50 mL in DuPont Instruments Sorvall RC-5B Refrigerated Superspeed Centrifuge (LabX Media Group, Canada).

Vortexing was done on IKA® Vortex Genius 3 Orbital S2 (IKA-Werke GmbH & Co.KG, Germany).

Ultraviolet and visible spectra (UV-Vis) and specific absorbances were recorded on the spectrophotometer Ultrospec 3300pro (Amersham Biosciences, US).

Drying under reduced pressure was done on BÜCHI Rotavapor® R-200 (BÜCHI Labortechnik AG, Switzerland).

^{1}H- and ^{13}C-NMR (nuclear magnetic resonance) spectroscopy was recorded with the Bruker Avance III™ spectrometer 500 and 126 MHz (Bruker Biospin AG, Germany), respectively, at room temperature. The samples were dissolved in methanol-d_4 or $CDCl_3$ and transferred into a 5 mm NMR tube. Chemical shifts (δ) are expressed in ppm and coupling constants (J) are given in Hz.

Enzymatic reactions were performed in an ALEMADR-MS Thermo Shaker Incubator (COLO Lab Experts, Slovenia).

Enzymatic and test chemical reactions were monitored by high performance liquid chromatography – mass spectrometry, HPLC–MS (Thermo Fisher LCQ fleet coupled with a Dionex UltiMate 3000 HPLC system, UK).

Mass spectra were determined by high resolution – liquid chromatography – electrospray ionization – mass spectrometry, HR–LC–ESI–MS (Thermo Fisher LTQ FT Ultra coupled with a Dionex UltiMate 3000 HPLC system, UK) in a positive ion polarity mode.

Flat-bottomed microtiter plates (6-, 24- and 96-well; Sarstedt, Germany) were used for *in vitro* assays. Plates were read using the Tecan Infinite 200 Pro multiplate reader (Tecan Group Ltd., Switzerland).

Microscopy of MRC-5 and HCT116 cells was performed using DM IL LED Inverted Microscope (Leica Microsystems, Germany) at 20× magnification.

The eBioscience™ Annexin V Apoptosis Detection Kit APC (Invitrogen by Thermo Fisher Scientific, UK) was used for the assessment of cellular integrity and the externalisation of phosphatidylserine. Flow cytometry analysis was done on a CyFlow Space Partec flow cytometer, with Partec FloMax software (Partec GmbH, Germany).

Nematodes were visualised and counted using a Carl Zeiss™ Stemi 508 Stereomicroscope (Zeiss Group, Germany) at 40× magnification.

Zebrafish were examined using a Stereomicroscope SMZ-143-N2GG (Motic, Germany) at 3.5× magnification.

3.3. Microorganisms, enzymes, cell lines and model system organisms

Two bacterial strains were purchased from ATCC (American Type Culture Collection, US): *Serratia marcescens* 27117 (PG-producing strain) and *Staphylococcus aureus* 25923 and three bacterial strains were purchased from NCTC (National Collection of Type Cultures, UK): *Listeria monocytogenes* 11994, *Pseudomonas aeruginosa* PAO1 10332, *Escherichia coli* 9001.

Selected fungal strains were obtained from ATCC, US: *Candida albicans* 10231, *Candida glabrata* 2001, *Candida krusei* 6258, *Candida parapsilosis* 22019.

Wild-type vanadium-dependant haloperoxidase enzyme from *Acaryochloris marina* MBIC 11017 (*Am*VHPO I wt) and its two mutants (Arg425Ser and Arg425Lys) were kindly provided by Prof. Tanja Gulder (Institute of Organic Chemistry, Leipzig University, Germany).

Selected cell lines were obtained from ATCC, US: MRC-5 (lung fibroblasts), HaCaT (skin keratinocytes), A549 (lung cancer), A375 (melanoma, skin cancer), MDA-MB-231 (breast cancer), HCT116 (colon cancer).

Nematode roundworms (*Caenorhabditis elegans* AU37) were obtained from the Caenorhabditis Genetics Center (CGC), University of Minnesota (Minneapolis, Minnesota, US).

Wild-type zebrafish (*Danio rerio*) strain was obtained from a commercial supplier (Pet Center, Belgrade, Serbia).

3.4. Prodigiosin production

3.4.1. Bacterial strain cultivation

S. marcescens ATCC 27117 was kept in 20% glycerol at –80 °C. The producing strain was revived on LA plates (Luria Bertani with 1.5% agar) at 30 °C overnight and grown at 180 rpm (revolutions per minute) at 30 °C for 18 h in Luria Bertani (LB, Table 4) medium for optimisation experiments.

3.4.2. Liquid media optimisation

Five media were assessed for PG production by *S. marcescens* ATCC 27117 (Table 4): LB (Luria Bertani), NB (Nutrient Broth), TSB (Tryptic Soy Broth), SCF (Seed Culture Fluid) and FB (Fermentation Broth) for 5 days at 180 rpm at 30 °C. Cultivation conditions were evaluated in NB in Erlenmeyer flasks (1:5, culture to volume ratio) for 3 days: pH 4.0, 5.0, 6.0, 7.0, 8.0, 9.0, 10.0; temperatures: 18, 25, 30, 37 °C; agitation rates: 100, 125, 150, 180, 200 rpm.

Table 4. Microbiological media composition evaluated for *S. marcescens* ATCC 27117 cultivation and PG production.

Medium	Composition
LB	10.0 g/L tryptone, 5.0 g/L yeast extract, 10.0 g/L NaCl
NB	5.0 g/L peptone, 1.0 g/L beef extract, 2.0 g/l yeast extract, 5.0 g/L NaCl
TSB	30.0 g/L Tryptic Soy Broth
SCF	10.0 g/L peptone, 5.0 g/L yeast extract, 3.0 g/L NaCl, 2.0 g/L KCl
FB	15.0 g/L peptone, 0.3% (v/v) glycerol, 3.0 g/L NaCl, 2.0 g/L KCl, 2.0 g/L $MgSO_4$

3.4.3. Waste stream-based substrate

The second-grade canned meat waste, ME (Takovo d.o.o., Serbia) represents a canned product with a passed expiration date. ME was mixed with water in a 1/1 (w/v) ratio, blended using Nutribullet at maximum power setting for 1 min and sterilised prior to use.

Elemental analysis of ME was performed (C, H, N and S). Briefly, ME sample was dried in a dryer at 50 °C for 5 days and then at 50 °C for 2 h under reduced pressure (1 mmHg), which was enough to achieve a constant weight.

Seven ME-based media (Table 5) were assessed for PG production by *S. marcescens* ATCC 27117 for 48 h at 180 rpm at 30 °C. FB (Table 4) was selected as a model for ME-based media composition, and the peptone component of FB was

partially or fully replaced with ME (Table 5), as were the salts in the cultivation medium. FB was used as a control medium.

Table 5. Waste stream-based substrate media composition for the optimisation of PG production in *S. marcescens* ATCC 27117 cultivation.

Medium	Composition
ME-1	18 g/L ME
ME-2	15 g/L ME, 0.3% (v/v) glycerol
ME-3	18 g/L ME, 3.0 g/L NaCl, 2.0 g/L KCl, 2.0 g/L $MgSO_4$
ME-4	15 g/L ME, 0.3% (v/v) glycerol, 3.0 g/L NaCl, 2.0 g/L KCl, 2.0 g/L $MgSO_4$
ME-5	3.6 g/L ME, 12 g/L peptone, 0.24% (v/v) glycerol, 3.0 g/L NaCl, 2.0 g/L KCl, 2.0 g/L $MgSO_4$
ME-6	9.0 g/L ME, 7.5 g/L peptone, 0.15% (v/v) glycerol, 3.0 g/L NaCl, 2.0 g/L KCl, 2.0 g/L $MgSO_4$
ME-7	12 g/L ME, 3.0 g/L peptone, 0.3% (v/v) glycerol, 3.0 g/L NaCl, 2.0 g/L KCl, 2.0 g/L $MgSO_4$

3.4.4. Prodigiosin adsorption on a solid carrier

Propagation of *S. marcescens* ATCC 27117 was done in SCF using 1% (v/v) of inoculum from LB and cultivated at 180 rpm at 30 °C for 24 h.[86] PG production was done in FB with or without 1.8% (v/v) Tween-80, using 4% (v/v) inoculum from SCF. In addition, polyurethane foam cubes (PUR-FC) that serve as solid hydrophobic carriers for PG adsorption were added to the FB/Tween-80 medium.[87] Solvent- and temperature-resistant (–40 °C to +120 °C) PUR foam sponge roll 18–40 kg/m^3 was purchased from SSA Pana Foamtec d.o.o., Serbia and manually cut into 1 cm^3 cubes (Fig. 9). The ratio used was 1 g of PUR-FC on 200 mL of the medium before the sterilisation.

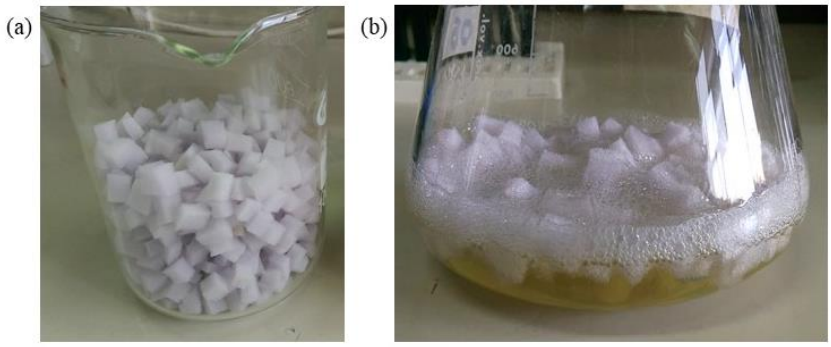

Figure 9. (a) Cut polyurethane foam cubes (PUR-FC);
(b) PUR-FC in the FB (Fermentation Broth) production medium.

3.4.5. Bioreactor design and experimental setup

For the starter culture (used for the inoculation of the fermentation medium), *S. marcescens* ATCC 27117 was cultivated in LB at 180 rpm at 30 °C for 24 h. Batch cultivations were performed in the bioreactor in 3 L of the fermentation medium, using different inoculations of the starter culture (Table 6) at 28.0 ± 2.0 °C, pH 7.0 ± 1.0 and a maximum 500 rpm agitation rate to secure a minimum 40 ± 20% of aeration level during the fermentation process. The pH was maintained at 7.0 using 10 M NaOH solution and 20% HCl. Aliquots of the fermentation culture were taken at regular intervals to monitor bacterial growth and PG production.

Table 6. Fermentations details for *S. marcescens* ATCC 27117 cultivations in NB, FB and ME-1.

Fermentation medium	Starter culture inoculum (%)	Fermentation time (h)	Regular aliquoting (h)
NB	2	24	1
FB	4	48	6
ME-1	4	14	1

Bacterial growth was tracked spectrophotometrically with optical density measurements at 600 nm.

To monitor PG production spectrophotometrically, 1 mL of EtOAc containing 1% conc. HCl (v/v) was added to 1 mL of the bacterial culture, followed by the addition of NaCl (*c.a*. 10 mg) to enable phase separation. The phases were shaken vigorously and separated by 2 min centrifugation at 16873 rcf (relative centrifugal force). PG concentration in the organic phase (mg/L) was calculated by using Lambert-Beer law by measuring the absorbance at 535 nm (absorption maximum of PG, A_{max})[88] on the spectrophotometer and by using the extinction coefficient ε_{535} of 0.159 L/(mg×cm).[89]

For biomass monitoring, 2 mL of the culture was centrifuged for 2 min at 16873 rcf, the supernatant was discarded, and the wet cells were dried at 37 °C to a constant cell dry weight (CDW), which was achieved after 24 h.

After stopping the fermentation, 3 L of the cell culture were centrifuged at 6037 rcf for 20 min at 4 °C and bacterial cells were separated from the culture supernatant.

3.4.6. Prodigiosin extraction

3.4.6.1. From the solid carrier

After 72 h cultivation in FB/Tween-80 at 180 rpm at 30 °C, PUR-FC were easily separated from the cultivation medium by decanting through a glass funnel and the collected FCs were rinsed with water before the extraction. Five organic solvents were added over PUR-FC cubes to assess their extraction potential of PG: Et_2O, EtOAc, MeOH, DCM and acetone. Onto 0.20 g of PUR-FC, 10 mL of the selected organic solvent was added, and the extraction was successfully performed by gentle shaking for 10 min. Each solvent was filtered off, dried over anhydrous Na_2SO_4, evaporated to dryness and the mass of the crude extract was weighed.

3.4.6.2. From bacterial cells

Bacterial cells (pellet after centrifugation) were dried at 37–42 °C while on a shaker at 180 rpm for 24 h affording 20 mL of a thick, yet fluid slurry of wet bacterial cells containing some residual medium. PG was extracted from this slurry using 405 mL of $CHCl_3$/MeOH/H_2O (5/1.5/7) and the phases were left to rest and separate at 4 °C overnight. The mixture was centrifuged at 6037 rcf for 20 min at 4 °C, the organic phase was collected, dried over anhydrous Na_2SO_4 and evaporated under reduced pressure to afford the crude cell-extract.

3.4.6.3. From the culture supernatant

The supernatant was treated with EtOAc in 2/1 (v/v) ratio, 0.4% (w/v) of NaCl and 0.1% (v/v) of conc. HCl. The biphasic mixture was shaken at 140 rpm for 1 h. The mixture was centrifuged at 6037 rcf for 20 min at 4 °C, organic phase was collected, washed with water and brine (saturated NaCl solution), dried over anhydrous Na_2SO_4 and evaporated under reduced pressure to afford the crude supernatant-extract.

3.4.7. Prodigiosin purification

Crude bacterial extracts of PG (usually 800 mg in 60 cm column) were purified using gravitation column chromatography performed on 20 g silica gel (SiO_2, particle size 0.040–0.063 mm). Solvent mixtures are reported as volume/volume (v/v). Elution was done with *n*-hexane/Et_2O 2/1 (150 mL), EtOAc (300 mL) and MeOH (100 mL).

3.5. Prodigiosin derivatisation

Two approaches for the halogenation of PG were assessed: enzymatic halogenation reactions and chemical synthesis using mild halogenating reagents.

3.5.1. Enzymatic halogenation reactions

Vanadium-dependent haloperoxidase I wild-type enzyme (PDB ID: 5LPC[f]) was obtained by cloning the appropriate codon-optimised synthetic gene from *Acaryochloris marina* MBIC 11017 into pET28-based *E. coli* expression vector as described previously by sequence and ligation independent cloning (SLIC).[75] Successful insertion of the gene and the absence of undesired mutations were verified by Sanger sequencing (GATC). The obtained pET28-*Am*VHPO expression vector was used to transform *E. coli* BL21 (DE3) cells for protein production.[75]

Mutants of *Am*VHPO I were generated by site-directed mutagenesis (QuikChange site-directed mutagenesis kit, Agilent), whereby Arg at position 425 was substituted either with Ser for bromination (*Am*VHPO I Arg425Ser), or by Lys for bromination and chlorination (*Am*VHPO I Arg425Lys).

Transformed cells were grown in 3–6 L expression cultures at 37 °C while shaking at 150–180 rpm. At an optical density of 0.6, protein production was induced by the addition of IPTG (isopropyl β-D-1-thiogalactopyranoside) to a final concentration of 1 mM and cultures were incubated overnight at 18 °C. Cells were harvested by centrifugation and washed with 50 mM Tris pH 7.0 and 300 mM NaCl. Pellets were stored at 18 °C until further use.[75]

For protein purification, pellets were resuspended in Ni-NTA (nitriloacetic acid) wash buffer (50 mM Tris pH 7.0, 300 mM NaCl and 30 mM imidazole) containing a protease inhibitor. Cells were disrupted by sonication, and soluble and insoluble fractions were separated by centrifugation at 40,000 g for 30 min. The supernatant was heated to 65 °C for 30 min, followed by another centrifugation under the same conditions. The soluble protein fraction was subsequently loaded onto a

[f] https://www.rcsb.org/structure/5LPC

Histrap FF column equilibrated with wash buffer, which was washed with 10-column volumes of the same buffer, prior to elution of the target protein with a 10-column volume gradient from 30 to 500 mM imidazole. Protein peak fractions were analysed by SDS-PAGE (sodium dodecyl sulfate polyacrylamide gel electrophoresis) and those containing the haloperoxidase were pooled for subsequent size-exclusion chromatography. The obtained peak fractions were analyzed by SDS-PAGE prior to pooling and freezing the protein of highest apparent purity in liquid nitrogen and storing it at –80°C until further use.[75]

The enzymes, which were obtained and purified as described above, were used in the biocatalytic reactions of PG:

- for aromatic bromination (wild type *Am*VHPO I wt, *Am*VHPO I Arg425Ser mutant and *Am*VHPO I Arg425Lys mutant)
- for aromatic chlorination (*Am*VHPO I Arg425Ser mutant).

The enzymatic reactions were performed, following the previously described procedure[75] in a MES buffered (pH 6.0, 55.5 mM) mixture of MeCN/water (1/7) in a total volume of 160 µL. The enzyme (30 µL; 2.5 mg/mL; preincubated in 50 mM Tris buffer pH 7.0 with 100 µM Na_3VO_4), either KBr (157.1 µg, 1.32 µmol, 1.1 eq) or KCl (98.4 µg, 1.32 µmol, 1.1 eq) and H_2O_2 (44.9 µg, 1.32 µmol, 1.1 eq) were added to a solution of PG (388.2 µg, 1.2 µmol, 1.0 eq) in MeCN. The reactions were heated to 30 °C and mixed at 300 rpm for 72 h in the dark. The reactions were stopped by the addition of brine (80 µL) and saturated $(NH_4)_2SO_4$ (80 µL) solutions, to separate the precipitated enzyme and to allow phase separation. The mixture was extracted with EtOAc (400 µL), the organic phase was evaporated to dryness and analysed on HPLC-MS.

3.5.2. Chemical halogenation reactions

Chemical reactions of PG were monitored by thin layer chromatography (TLC) carried out on alumina plates with 0.25 mm silica gel layer with F-254 indicator *i.e.*, Silicagel 60 F_{254} (Merck, Germany) using *n*-hexane/EtOAc 1/1 as the eluent, as well as UV light (254/366 nm) and $KMnO_4$ as the visualising agents.

3.5.2.1. Monobromination of prodigiosin

Monobromination of PG was done following a literature procedure.[80] PG (8.0 mg, 0.025 mmol, 1.0 eq) was dissolved in 1.8 mL MeOH, then 48% HBr in H_2O (4.17 µL, 0.025 mmol, 1.0 eq) and 30% H_2O_2 (3.35 µL, 0.027 mmol, 1.1 eq) were added. The reaction was allowed to proceed at room temperature in the dark until full conversion was detected by TLC (24 h). The mixture was evaporated to dryness, water was added, and the product was extracted with EtOAc. The combined organic phases were washed with saturated $NaHCO_3$, brine, dried over anhydrous Na_2SO_4, filtered and the solvent was evaporated under reduced pressure. The mixture was purified by gravitation column chromatography on SiO_2 using *n*-hexane/EtOAc 9/1 to 8/2. Monobrominated prodigiosin, PG-Br, was obtained as an orange-brown oil (8.12 mg, 0.025 mmol, 81%).

3.5.2.2. Dibromination of prodigiosin

Dibromination of PG was done following a literature procedure.[75] PG (9.0 mg, 0.028 mmol) was dissolved in 1.9 mL EtOAc, then 48% HBr in H_2O (10.38 µL, 0.056 mmol, 2.0 eq) and DMSO (4.37 µL, 0,062 mmol, 2.2 eq) were added. The reaction was heated at 60 °C in the dark until full conversion was detected by TLC (2 h). After cooling to room temperature, water was added, and the mixture was extracted with EtOAc. The combined organic phases were washed with saturated $NaHCO_3$, brine, dried over anhydrous Na_2SO_4, filtered and the solvent was evaporated under reduced pressure. The mixture was purified by gravitation column chromatography on SiO_2 using *n*-hexane/EtOAc 9/1. Dibrominated prodigiosin, PG-Br_2, was obtained as a purple film (8.5 mg, 0,018 mmol, 63%).

3.5.3. Structural characterisation of prodigiosin and its Br-derivatives

All compounds were characterised by UV-Vis spectra, ^{1}H- and ^{13}C-NMR spectra and mass spectra (on HR-LC-ESI-MS).

3.6. *In vitro* biological assays with prodigiosin and its Br-derivatives

3.6.1. Antimicrobial assays

Minimum inhibitory concentrations (MICs) were determined according to CLSI broth microdilution guidelines (Clinical and Laboratory Standards Institute 2008, 2012) according to standardised methodology. Standardised methodology used in this study is recommended by the National Committee for Clinical Laboratory Standards (M07-A8) for bacteria and Standards of European Committee on Antimicrobial Susceptibility Testing (v 7.3.1: Method for the determination of broth dilution minimum inhibitory concentrations of antifungal agents for yeasts) for *Candida* spp.[90] All tested compounds were first dissolved in DMSO, at a concentration of 50 mg/mL which allowed a high starting concentration in µg/mL for further dilutions. The highest tested concentration in 96-well flat-bottomed microtiter plates was 200 µg/mL and the serial dilutions were made down to 1.57 µg/mL. Antibacterial MICs were determined in LB and antifungal MICs in RPMI 1640 medium, in triplicate. The inoculums were 5×10^5 colony forming units (CFU/mL) for bacteria and 1×10^5 CFU/mL for fungal species. The MIC value was recorded as the lowest concentration that inhibited the growth after 24 h at 37 °C.

3.6.2. Cell viability and proliferation assay

Antiproliferative activities of PG and its Br-derivatives were measured using the standard colorimetric MTT assay.[91] Briefly, cells were plated in a 96-well flat-bottomed microtiter plate at a concentration of 1×10^4 cells per well, grown in a humidified atmosphere of 95% air with 5% CO_2 at 37 °C and maintained as monolayer cultures in RPMI 1640 medium supplemented with 10% FBS, 100 U/mL penicillin and 100 µg/mL streptomycin. Each tested compound was added to the cells at a concentration of 0.05–100.00 µg/mL and the treatment lasted for 48 h. The MTT assay was performed two times in four replicates and the results were presented as a percentage of the DMSO-treated control that was arbitrarily set to 100%. The extent of MTT reduction was measured spectrophotometrically at 540 nm using the multiplate reader.

To assess the effect of the treatment duration, exposure of MRC-5 and HCT116 cells to PG and its Br-derivatives was observed after 24, 48 and 72 h. The changes in absorbance were measured using the MTT assay, as described above. MRC-5 and HCT-116 cells treated for 24 h were additionally analysed using an inverted microscope.

3.6.3. Flow cytometry analysis

MRC-5 cells were plated in a 6-well plate at a concentration of 2.5×10^5 cells per well, grown for 24 h in a humidified atmosphere of 95% air and 5% CO_2 at 37 °C in RPMI 1640 medium supplemented with 10% FBS, 100 U/mL penicillin and 100 μg/mL streptomycin. Each tested compound was added to the cells at IC_{50} concentration, and the incubation continued for another 24 h under the same conditions. Upon incubation, cells were collected, washed once with Dulbecco's Phosphate-Buffered Saline (Gibco™ by Thermo Fisher Scientific, UK) and stained with Annexin V FITC and Propidium Iodide (PI) under the manufacturer's instructions. Briefly, MRC-5 cells were resuspended in 1×Binding Buffer at $1–5\times10^6$ cells per mL and incubated with 5.00 μL Annexin V FITC for 15 min at room temperature in a final volume of 100 μL. After incubation, cells were washed and resuspended in 200 μL of 1×Binding Buffer, 5.00 μL of PI staining solution was added and incubation at room temperature continued for another 15 min. Immediately after staining, cells were analysed on a flow cytometer.

3.7. *In vivo* biological assays with prodigiosin and its Br-derivatives

3.7.1. Roundworm (*C. elegans*) survival assay

C. elegans AU37 (glp-4; sek-1) were propagated under standard conditions: they were synchronised by hypochlorite bleaching and cultured on Nematode Growth Medium (NGM) containing in 1 L of water 3.0 g/L NaCl, 2.5 g/L peptone, 17 g/L agar, 1 mL of 5 g/L cholesterol in EtOH, 1 mL of 1 M $CaCl_2$, 1 mL of 1 M $MgSO_4$ and 25 mL of 1 M potassium phosphate buffer (pH 6.0), using *E. coli* OP50 as a food

source, as described previously.[92] The *C. elegans* survival assay was carried out following the standard procedure with some modifications.[93] Briefly, synchronised worms (L4 stage) were suspended in a medium containing 95% M9 buffer (1 L of water with 3.0 g of KH_2PO_4, 6.0 g of Na_2HPO_4, 5.0 g of NaCl and 1 mL of 1 M $MgSO_4$), 5% LB broth and 10 μg/mL of cholesterol. The experiment was carried out in 96-well plates with the final volume of 100 μL per well. 25 μL of this suspension of nematodes (25–35 nematodes) were transferred to the wells of a 96-well microtiter plate, where 50 μL of the medium was previously added. Next, 25 μL of the solvent control (1% DMSO) or 25 μL of the concentrated tested compound solution was added to the test wells. Final concentrations of the compounds were 50.00, 25.00, 12.50, 6.25, 3.13 and 1.57 μg/mL. Subsequently, the plates were incubated at 25 °C for 2 days. The fraction of the dead worms was determined after 48 h by counting the number of dead worms and the total number of worms in each well, using a stereomicroscope. The compounds were tested in triplicate and each assay was repeated two times (n = 6). As a negative control experiment, nematodes were exposed to the medium containing 1% DMSO.

3.7.2. Zebrafish (*D. rerio*) embryotoxicity and teratogenicity assay

Zebrafish embryotoxicity assay was performed according to general rules of the OECD Guidelines for the testing of chemicals.[94] Wild-type zebrafish strain was kept under controlled environmental conditions (water temperature 28 °C, 14 h under the light and 10 h in the dark) and fed regularly three times a day with commercially dry flake food supplemented with *Artemia nauplii* (TetraMin™ flakes; Tetra Melle, Germany). Zebrafish embryos were produced by female and male adults mating in the ratio of 1:2. Obtained embryos were collected, washed from detritus, and carefully handled. Only fertilised embryos were selected and distributed into 24-well plates containing 10 embryos per well. Each well contained 1 mL of water for embryos (0.2 g/L of Instant Ocean® Salt in distilled water). For assessing lethal and developmental toxicity, embryos at the 6 and 20 h post fertilisation (hpf) stages[95] were treated with selected compounds at concentrations of 0.10–100.00 μg/mL and incubated at 28 °C (maximum DMSO concentration in the negative control was 1%). Experiments were performed in triplicate, using 30 embryos for each concentration.

For five days, the appearance of different morpho-physiological parameters in embryo development was monitored.[96, 97] Dead embryos were counted and discarded every 24 h. On the fifth day, the embryos were anesthetised by the addition of 0.1% (w/v) tricaine solution, observed under a stereomicroscope (SMZ-143-N2GG, Motic, Germany), photographed and killed by freezing at −20 °C for ≥ 24 h. All experiments involving zebrafish were performed in compliance with the European directive 2010/63/EU and the ethical guidelines of the Guide for Care and Use of Laboratory Animals of the Institute of Molecular Genetics and Genetic Engineering (IMGGE), University of Belgrade, Serbia.

3.8. Statistical analysis

The results are presented as mean ± standard deviation (SD). Statistical analysis was done by comparing means using *t*-test (Two-Sample Assuming Equal Variances) and one-way ANalysis Of VAriance (ANOVA, Single Factor), with Fisher's Least Significant Difference (LSD) post-hoc test. The level of statistical significance is expressed as a *p*-value (probability value), and $p \leq 0.05$ was considered statistically significant. Statistical analysis tests were performed in Microsoft Excel Spreadsheet Software by Data Analysis Tools add-in.

4. Results and discussion

Part of the research presented in this thesis is also included in an article published in the MDPI *Molecules* journal: "Synthesis, anticancer potential and comprehensive toxicity studies of novel brominated derivatives of bacterial biopigment prodigiosin from *Serratia marcescens* ATCC 27117" from the authors Jelena Lazić, Sanja Škaro Bogojević, Sandra Vojnović, Ivana Aleksić, Dušan Milivojević, Martin Kretzschmar, Tanja Gulder, Miloš Petković and Jasmina Nikodinović-Runić (link: https://www.mdpi.com/1420-3049/27/12/3729).

Since the discovery of PG, numerous synthetic routes and approaches have been established for PG and its analogues. In the first total synthesis referred by Rapoport and Willson,[15] PG was successfully obtained by a 7-step protocol, but with an overall yield of 0.1%. Many pathways for total PG synthesis are known today and have been refined over time with the development of the know-how of heterocyclic chemistry. Other total synthesis sequences for various PG related compounds (Fig. 2) are presented elsewhere.[27, 66] The common ground in the total syntheses approaches is that they are costly and time-consuming (some involving 25 reaction steps) and the overall yields are usually low, which is why biotechnology and mutasynthesis have recently taken precedent.[13, 29, 87]

4.1. Optimisation of nutritional and physicochemical factors for prodigiosin production in *S. marcescens* ATCC 27117

PG production in a variety of *S. marcescens* spp. ranges from 5 mg/L[98] to 49.5 g/L[99] by wild-type locally isolated strains. Our initial experiments were designed to optimise the PG production in the selected *S. marcescens* ATCC 27117 strain. Five media, commonly reported for PG production were assessed (Table 4, Fig. 10a). Cultivation of this strain in NB medium supported the highest PG concentration after 24 h (13.6 ± 0.5 mg/L), followed by SCF (11.2 ± 0.2 mg/L), FB (10.8 ± 0.1 mg/L), TSB (10.7 ± 0.2 mg/L) and finally LB medium (3.6 ± 0.1 mg/L) (Fig. 10a and 10b). ANOVA test showed there was a significant difference between these media, and post-hoc Fisher's LSD test indicated that PG production in NB was significantly

higher, and production in LB significantly lower than the production in SCF, FB and TSB. The differences in PG production between SCF, FB and TSB were statistically nonsignificant after 24 h cultivation.

Interestingly, extending the cultivation time to 48 h resulted in a similar biopigment production only in the FB medium (11.1 ± 0.1 mg/L, Fig. 10a and 10b), which had the highest peptone content, while in all other media a decrease in the PG concentration was noticed: NB (10.4 ± 0.3 mg/L), TSB (6.8 ± 0.1 mg/L), SCF (5.8 ± 0.2 mg/L), LB (0.8 ± 0.1 mg/L) (Fig. 10a and 10b). ANOVA and post-hoc Fisher's LSD tests showed a significant difference between PG production in all these media after 48 h cultivation.

The overall decrease in PG production over 5 days was analysed using a *t*-test. When compared to 24 h, cultivations beyond 72 h showed a statistically significant decrease of PG production ($p = 0.037$ at 96 h and $p = 0.007$ at 120 h).

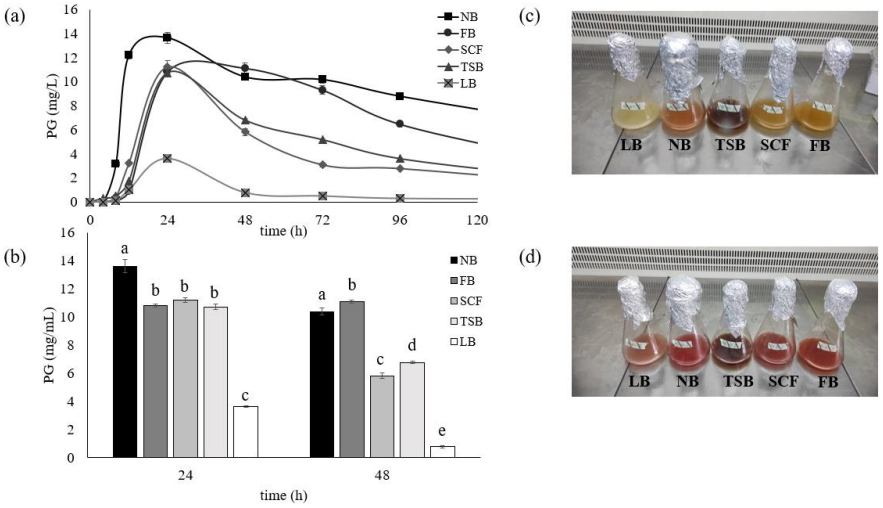

Figure 10. The influence of nutritional factors from different media on PG production in *S. marcescens* ATCC 27117: (a)[g] concentration of PG over 5 days; (b) comparison of mean PG concentrations after 24 and 48 h; means with different letters are significantly different (ANOVA test and post-hoc Fisher's LSD test, $p \leq 0.05$ was considered statistically significant); (c) LB (Luria-Bertani), NB (Nutrient Broth), TSB (Tryptic Soy Broth), SCF (Seed Culture Fluid), FB (Fermentation Broth) flasks upon inoculation, (d) flasks after 24 h cultivation.

[g] This figure is part of the manuscript accepted in the MDPI Molecules journal, see **Chapter 4. Results and discussion** for more details on the manuscript.

Previously, peptone was found to be an excellent nitrogen source and was combined with various carbon sources, such as starch for PG production in *S. marcescens* C3[85], with glycine and sucrose for *S. marcescens* P-125[20] and with glycerol for *S. marcescens* 2170.[30, 100, 101] Another study showed that glycerol plays an important role in a two-step feeding strategy, when *S. marcescens* mutant strain B6 was first fed with glucose, as the initial carbon source, and then with glycerol, as an additional carbon source to induce PG production.[102]

In our optimisation experiment, prolonged cultivation time resulted in an overall PG decrease in each medium, due to depletion of nutrients and possible degradation of PG (Fig. 10a and 10b). Previously, a negative correlation was established between PG production and ATP cellular levels during high-rate, low-cell-density growth, suggesting that PG may function as a molecular mediator of cellular energy spilling, a mechanism for ridding the cell of excess energy (not stored in adenine nucleotides), *e.g.*, by creating futile cycles of ions across the cell membrane.[103]

The effects of physicochemical factors, such as temperature, pH, and agitation rate, on PG production were also examined, using the NB medium (Fig. 11a-c, respectively). From the assessed temperatures, ANOVA test and post-hoc Fisher's LSD test showed statistically significant difference ($p < 0.001$) for both 25 and 30 °C at 180 rpm after 24 h (Fig. 11a). This is in a correlation with several previous studies, where the range of temperatures between 25–30 °C was found to be optimal for *Serratia* spp. cultivation, while temperatures higher than 30 °C have been known to interrupt the PG biosynthesis, most likely due to the biosynthetic enzyme inactivation.[61] Temperature of 28 °C was selected for the scaled-up PG production.

The influence of pH was assessed at 30 °C at 180 rpm, and the statistically significant ($p < 0.001$) highest production rate of PG was noticed at pH 7.0 after 24 h (Fig. 11b), which agrees with the previously established results showing that slightly acidic to neutral pH conditions (5.5–7.0) have been appropriate for PG production in *Serratia* spp.[26]

The highest tested agitation rate of 200 rpm afforded the highest PG production after 24 h (Fig. 11c). ANOVA test and post-hoc Fisher's LSD test showed there was no statistical significance in PG production at 200 rpm in comparison to 180, 150 and

125 rpm, but a significant difference (p = 0.003) was noticed when the highest tested agitation rate was compared to 100 rpm. This result suggested that agitation rates higher than 200 rpm may prove beneficial for PG production, so the agitation rate of 500 rpm was selected for the scaled-up PG production.

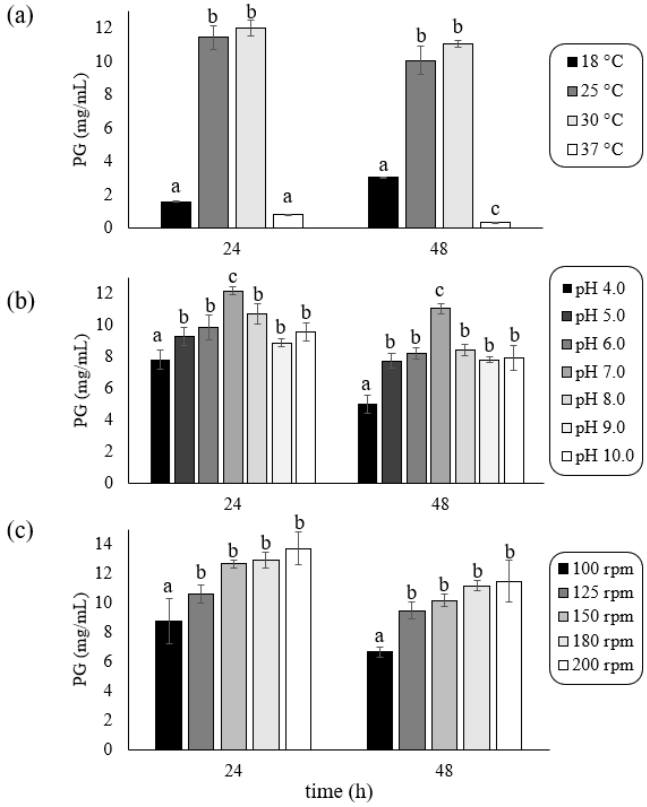

Figure 11. The influence of: (a) temperature; (b) pH; (d) agitation rate, on PG production in *S. marcescens* ATCC 27117 in flasks after 24 and 48 h. Means with different letters are significantly different (ANOVA test and post-hoc Fisher's LSD test, $p \leq 0.05$ was considered statistically significant).

Prolonging the cultivation from 24 to 48 h resulted in a nonsignificant decrease in PG production in all experiments (Fig. 11a-c), which was shown using a *t*-test. The same trend of nonsignificant decrease in PG production was noticed in cultivations prolonged from 48 to 72 h (data not shown).

4.2. Using meat waste stream substrate for prodigiosin production in *S. marcescens* ATCC 27117

Besides pollution and hazard aspects, in many cases meat, poultry and fish processing wastes have a potential for recycling raw materials or for conversion into useful products of higher value. Therefore, second-grade canned meat waste (ME) was initially analysed for its elemental content, and it was shown that carbon content was the highest (at 50.730%), followed by nitrogen (11.510%), hydrogen (7.788%) and sulphur (1.185%) (Table 7). These elements take up 71.213%, and the remaining 28.787% are oxygen and trace elements. In microbes, carbon requirements are usually higher than nitrogen requirements and the balance of these elements (C/N ratio) determines how microorganisms use an organic material.[85]

Table 7. Elemental analysis of second-grade canned meat waste (ME).

Content	**C**	**N**	**H**	**S**
(%)	50.730 ± 0.015	11.510 ± 0.003	7.788 ± 0.018	1.185 ± 0.001

In the case of ME, the C/N ratio was 4.41 and this ratio is slightly higher than the literature values for PG production in some other *Serratia* strains. Previously, the C/N ratio of 2.86 was found optimal for PG production in *S. marcescens* BS 303, affording 540 ± 40 mg/L of PG, but with the addition of Mg^{2+}-, Mn^{2+}-, Fe^{2+}-salts.[104] Using a C/N ratio of 2.5, with the addition of NaCl, a cultivation of a soil microorganism *S. marcescens* N10612 resulted in 1.3 g/L of prodigiosin isoforms (PIPs), containing 33% of PG.[105] However, the nutrients used in the described examples originated from commercially acquired sources (*e.g.* glycerol and casein peptone[104], yeast extract and sucrose[105]), thus elevating the cost of PG production.

Using a waste-stream substrate such as ME as a nutrient for PG production is considered a more economical option, since it is a single substrate representing a source of both carbon and nitrogen. Therefore, our next step was to determine how much of carbon and nitrogen could be substituted with ME in the cultivation medium to maintain a solid PG production. FB was selected as a model for medium composition (Table 4) and was also used as a control medium in this optimisation

experiment. The peptone component of FB was partially or fully replaced with ME (Table 5).

The highest PG production of 56.3 ± 0.2 mg/L rate was observed in medium ME-1 after 24 h, when only ME was used at 18 g/L, followed by 41.5 ± 0.6 mg/L of PG in medium ME-3 (also after 24 h) containing 18 g/L of ME and salts (Table 5 and Fig. 12a). PG production of 56.3 ± 0.2 mg/L in ME-1 after 24 h was 5.5-fold higher than PG production of 10.2 ± 0.3 mg/L observed in FB in this experiment (Fig. 12a). ANOVA test and post-hoc Fisher's LSD test showed a significant difference between PG production between all the tested waste-based media after 24 h.

Prolonging the cultivation from 24 to 48 h resulted in a nonsignificant decrease in PG production in all media (Fig. 12), which was shown using a *t*-test.

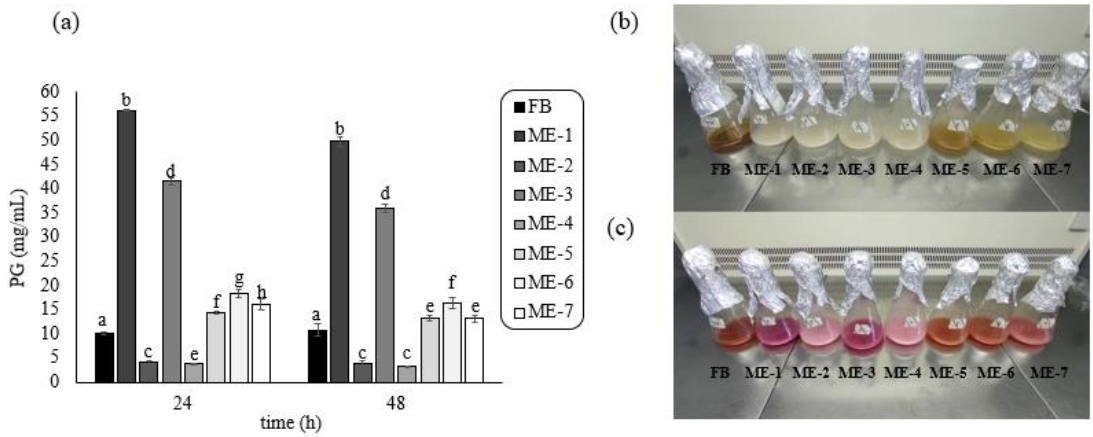

Figure 12. The influence of second-grade canned meat waste (ME) content on PG production in *S. marcescens* ATCC 27117: (a) concentration of PG after 24 and 48 h; means with different letters are significantly different (ANOVA test and post-hoc Fisher's LSD test, $p \leq 0.05$ was considered statistically significant); (b) FB (Fermentation Broth), ME-1 (18 g/L ME), ME-2 (15 g/L ME, 0.3% (v/v) glycerol), ME-3 (18 g/L ME, 3.0 g/L NaCl, 2.0 g/L KCl, 2.0 g/L $MgSO_4$), ME-4 (15 g/L ME, 0.3% (v/v) glycerol, 3.0 g/L NaCl, 2.0 g/L KCl, 2.0 g/L $MgSO_4$), ME-5 (3.6 g/L ME, 12 g/L peptone, 0.24% (v/v) glycerol, 3.0 g/L NaCl, 2.0 g/L KCl, 2.0 g/L $MgSO_4$), ME-6 (9.0 g/L ME, 7.5 g/L peptone, 0.15% (v/v) glycerol, 3.0 g/L NaCl, 2.0 g/L KCl, 2.0 g/L $MgSO_4$), ME-7 (12 g/L ME, 3.0 g/L peptone, 0.3% (v/v) glycerol, 3.0 g/L NaCl, 2.0 g/L KCl, 2.0 g/L $MgSO_4$) flasks upon inoculation; (c) flasks after 24 h cultivation.

Interestingly, all media containing glycerol (ME-2, ME-4 to ME-7, FB) exhibited a PG production rate of < 20 mg/L, even in the presence of ME, suggesting that higher carbon content may be hindering PG production in this particular *Serratia* strain.

4.3. Adsorption of prodigiosin and extraction from a solid carrier

It was shown that Tween-80 was crucial for disrupting the cell membrane permeability and encapsulating PG molecules into nano-micelles. Upon removal of cell debris, the encapsulated biopigment was used for dying cotton fibre.[86] To test the described effects of Tween-80 on the cell membrane of the selected *Serratia* strain, this non-ionic surfactant was added to the production medium (FB). It was visually observed that PG was localised in the cultivation medium in the presence of Tween-80 (Fig. 13a), while in the absence of Tween-80, PG remained inside the cells (Fig. 13b).

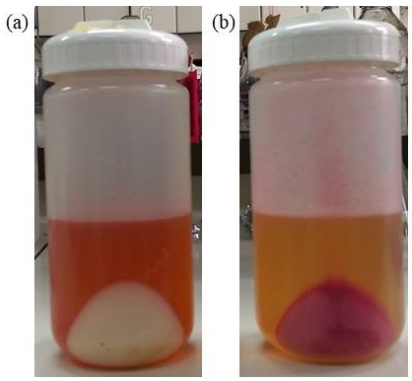

Figure 13. *S. marcescens* ATCC 27117 cultivated in FB (Fermentation Broth): (a) with Tween-80; (b) without Tween-80, after centrifugation.

Once outside the cells, PG from *Pseudomonas putida* KT2440 could also be adsorbed onto an external surface, such as the PUR foam.[29, 87] When this concept was investigated for *S. marcescens* cultivated in FB with Tween-80, it was noticed that the coloration of PUR-FC was only mildly pink after 72 h, indicative of a low PG production rate (Fig. 14).

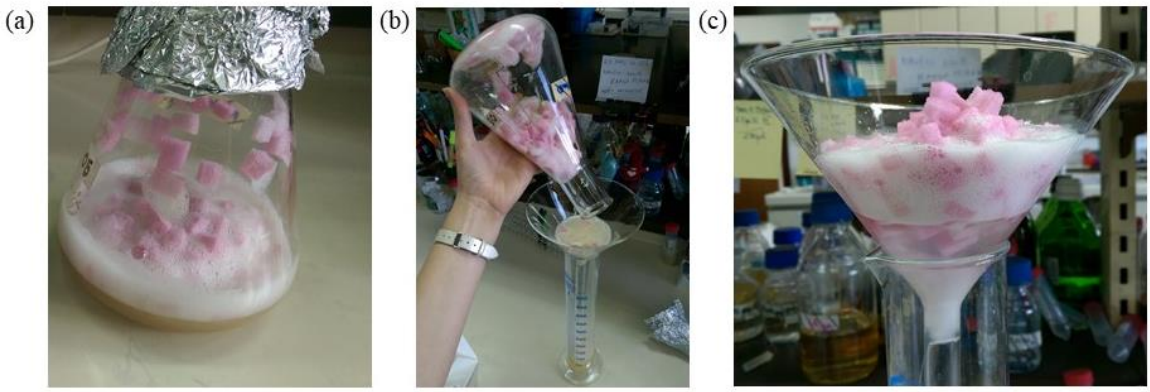

Figure 14. (a) Pink polyurethane foam cubes (PUR-FC) with adsorbed PG; (b) separation of PUR-FC from the FB (Fermentation Broth) medium; (c) rinsing PUR-FC.

Nevertheless, various organic solvents (Fig. 15a) were added over PUR-FC cubes to assess their extraction potential of PG. Each solvent was evaporated to dryness and the mass of the crude extract was weighed.

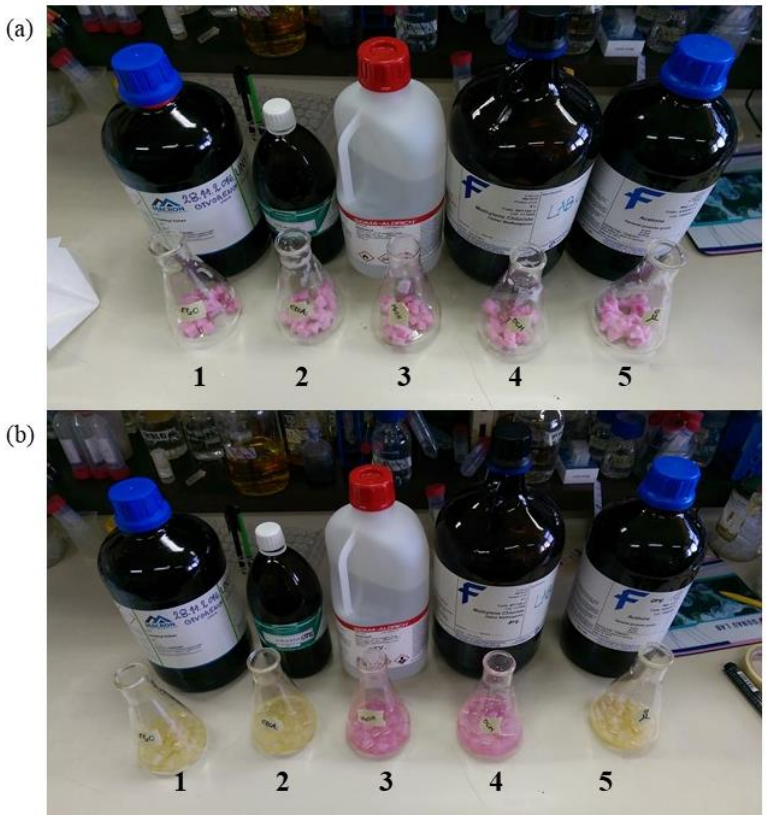

Figure 15. PG adsorbed on the polyurethane (PUR) foam: (a) before; (b) after the addition of organic solvents: 1) Et_2O, 2) EtOAc, 3) MeOH, 4) DCM, 5) acetone.

In cases of Et_2O, EtOAc and acetone, the colour of the dissolved pigment turned from pink to yellow (Fig. 15b). It was reported that the colour of dry and solidified PG is red, whereas dissolved PG can be present in two forms, depending on the solvent and pH: with an absorption maximum at 535 nm (red, pH < 8.0) and 460–470 nm (orange, pH 9.0 to yellow, pH > 9.0).[86, 106] However, this approach of adsorption of PG onto PUR-FC was abandoned for several reasons. First and foremost, the biopigment quantity established after solvent removal was very low (< 5 mg/L). Furthermore, adding a detergent like Tween-80, into the cultivation medium might hinder further purification and derivatisation steps. For those reasons, FB without Tween-80 was used for further large-scale cultivations.

4.4. Optimising the fermentation process

To obtain enough of biopigment for derivatisation reactions, cultivation of *S. marcescens* ATCC 27117 was carried out in the bioreactor, under the optimised cultivation conditions at pH 7.0 and 28 °C, with 500 rpm agitation rate. Fermentations were monitored in NB, FB and ME-1 (Table 8 and Fig. 16). Estimated maximum PG concentrations in the selected three media have been statistically analysed using ANOVA test and post-hoc Fisher's LSD test, and statistically significant difference was established between all three assessed media ($p < 0.001$).

Table 8. Fermentations of *S. marcescens* ATCC 27117 in NB, FB and ME-1.

Fermentation medium	Total fermentation time (h)	Max. PG production (h)	Estimated max. PG conc. (mg/L)	Isolated PG yield (mg/L)
NB	24	20	7.8 ± 0.1	6.9 ± 0.5
FB	48	36	13.4 ± 0.3	13.3 ± 1.1
ME-1	14	12	86.9 ± 3.7	83.1 ± 3.0

The method of choice for the estimation of the production of PG was the spectrophotometric measurement at 535 nm using the extinction coefficient ε_{535} of 0.159 L/(mg×cm) and a conversion to the PG concentration using the Lambert-Beer law.[88] However, due to different extinction coefficients used for these calculations and the purity of compounds, PG concentration can be overestimated even by 270%.[107]

Nevertheless, spectrophotometric monitoring of PG production remains an established method, and the challenging task of PG production assessment can only be determined by a measurement of the biopigment's mass upon extraction and purification.

Fermentation in NB showed the statistically significant ($p < 0.001$) lowest PG production, with the maximum of 7.8 ± 0.1 mg/L observed at 20 h (Table 8 and Fig. 16a), with the most lucent red colour at the end of the fermentation (Fig. 17a). This calculated concentration from the fermentation in NB was almost 2-fold lower than 13.6 ± 0.5 mg/L, which was achieved in NB in the optimisation experiment performed in flasks after 24 h (Fig. 10a and 10b), but leaves room for further optimisation.

The PG concentration of 13.4 ± 0.3 mg/L was observed in FB at 36 h (Table 8 and Fig. 16b) with a darker red colour at the end of the fermentation (Fig. 17b), which was slightly higher (yet with statistical significance $p < 0.001$) than in the NB fermentation. The maximum PG concentration during fermentation in FB is comparable to the optimisation experiment performed in flasks where 11.1 ± 0.1 mg/L of PG was observed after 48 h (Fig. 10a and 10b).

The statistically most successful fermentation ($p < 0.001$) was accomplished in ME-1, with the maximum PG production of 86.9 ± 3.7 mg/L, which was observed already after 12 h (Fig. 16c) and intensively red colour at the end of the fermentation (Fig. 17c). During the fermentation in ME-1, PG production rate was 1.5-fold higher at 12 h than in the flask optimisation experiment, where 56.3 ± 0.2 mg/L was observed after 24 h (Fig. 12a), which suggests that a prolonged fermentation in ME-1 would only result in PG loss.

The results suggest that the waste-based ME-1 medium not only provides optimal nutrients for *S. marcescen*s ATCC 27117 and leads to the highest PG production, but it also promotes the fastest achievement of the PG production maximum (at 12 h) compared to the commonly used peptone-based media (NB and FB at 20 and 36 h, respectively). This medium exhibits a high potential for utilisation in biotechnological production of PG and possibly other valuable biomolecules.

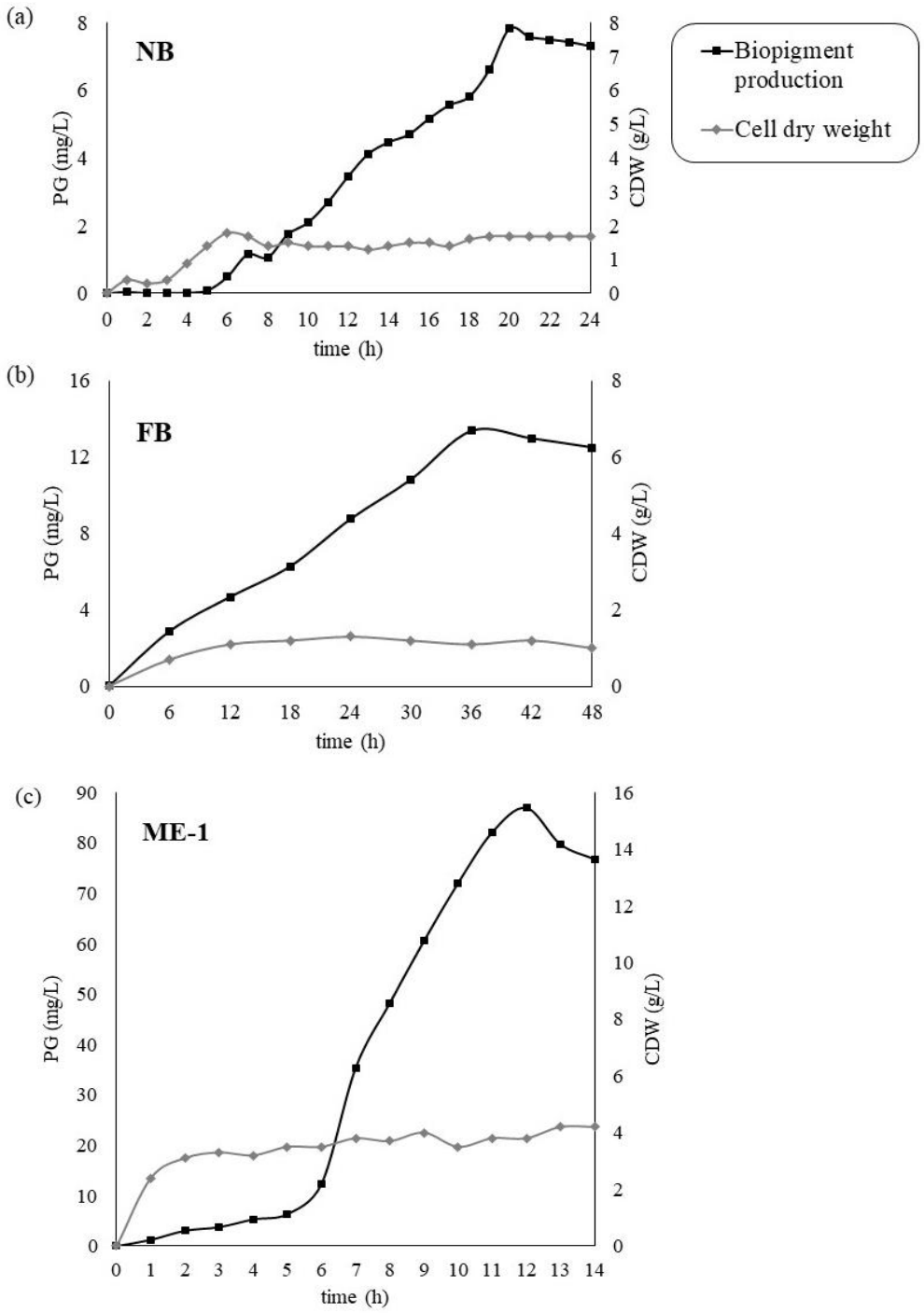

Figure 16. Fermentations of *S. marcescens* ATCC 27117, PG production (primary *y*-axis) and cell dry weight (CDW, secondary *y*-axis) were monitored: (a)[h] in NB (Nutrient Broth) for 24 h (aliquots at 1 h); (b) in FB (Fermentation Broth) for 48 h (aliquots at 6h); (c) in ME-1 (processed meat waste-based medium) for 14 h (aliquots at 1 h).

[h] This figure is part of the manuscript accepted in the MDPI Molecules journal, see **Chapter 4. Results and discussion** for more details on the manuscript.

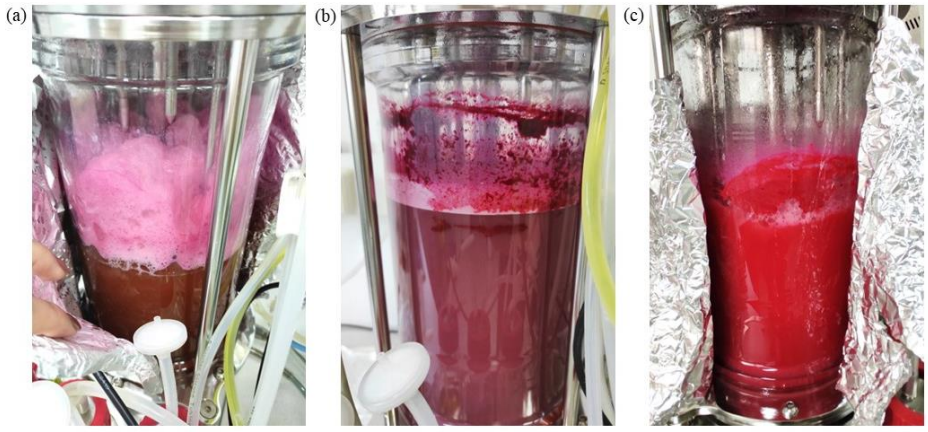

Figure 17. Fermenters with *S. marcescens* ATCC 27117 at the end of fermentation in the selected media: (a) NB (Nutrient Broth) after 24 h; (b) FB (Fermentation Broth) after 48 h; (c) ME-1 (processed meat waste-based medium) after 14 h.

Previously, analogous to the meat waste substrate examined in this work, using waste stream products as substrates for bacterial PG production in *S. marcescens* has been successfully performed, by mixing tannery fleshing (TF) solid waste and wheat bran (7/3) in a solid state fermentation, with the addition of various salts (33.9 g/L $Na_2HPO_4 \cdot 7H_2O$, 15.0 g/L KH_2PO_4, 2.5 g/L NaCl, 5.0 g/L NH_4Cl), affording 70.4 mg PG per kg of TF.[34] Starting from fish processing waste, shrimp head powder (SHP), a novel medium was designed, with 1.5% C/N source (SHP/casein = 9/1), 0.02% K_2SO_4 and 0.025% $Ca_3(PO_4)_2$, affording 6.3 g/L of PG from *S. marcescens* CC17.[60] Similarly, bioprocessing of marine chitinous wastes (MCWs) for the cost-effective preparation of PG from *S. marcescens* TNU01 was established using demineralised shrimp shell powders (deSSP) in a novel culture broth with 1.6% C/N source (deSSP/casein = 7/3), 0.02% K_2SO_4 and 0.05% K_2HPO_4 with the yield of 6.2 g/L.[61] By optimising the *S. marcescens* TNU01 culture medium using a low-cost carbon source cassava wastewater supplemented with 0.25% casein, 0.05% $MgSO_4$ and 0.1% K_2HPO_4 in a 14 L bioreactor, a 6.1 g/L yield of PG was achieved.[99, 108] These examples show that the addition of minerals and salts into the waste-stream based production medium increases PG production, so further optimisation steps for PG production in *S. marcescens* ATCC 27117 could be made in this direction. Finally, the fed-batch fermentations were found to be optimal for PG, as well as some other biopigments production[30, 85, 109], but they were not examined in this study.

4.5. Extraction, purification, and characterisation of the crude extract major components

Upon each fermentation, the culture was centrifuged, the cells were separated from the supernatant, and the extractions from the bacterial cells and from the culture supernatant proceeded as described in Sections 3.4.6.2. and 3.4.6.3, respectively. Crude extract masses from the fermentations were 0.689 ± 0.040 g/L in NB, 1.206 ± 0.020 g/L in FB, and 0.957 ± 0.023 g/L in ME-1. ANOVA test and post-hoc Fisher's LSD test established statistical significance ($p < 0.001$) between all media.

Each crude extract was purified using gravitation column chromatography, as described in Section 3.4.7. (Fig. 18).

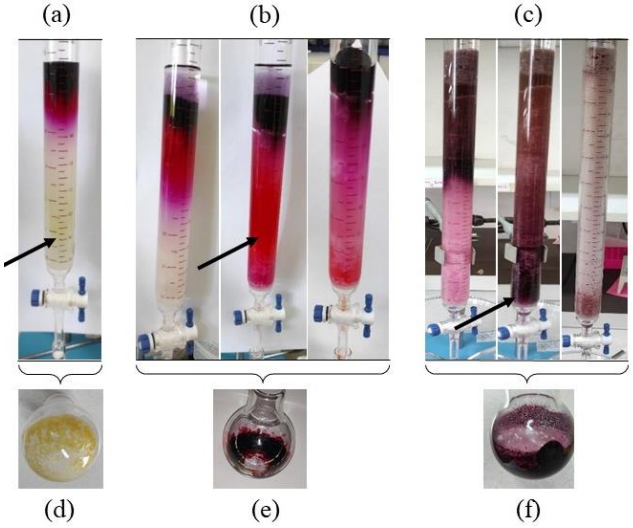

Figure 18. Chromatography of the crude extract from a cultivation in FB (Fermentation Broth) using: (a) *n*-hexane/Et_2O 2/1; (b) EtOAc; (c) MeOH; affording (d) fraction A; (e) fraction B; (f) fraction C.

4.5.1. Isopalmitic acid

The crude extracts were first eluted with *n*-hexane/Et_2O in 2/1 (v/v) (Fig. 18a), affording fraction A as a yellow solid (Fig. 18d), which was confirmed by ^{1}H- and ^{13}C-NMR (Fig. 19) to be 14-methylpentadecanoic fatty acid, previously found in *Serratia* spp.[110], commonly known as the isopalmitic acid (16:0) bearing a methyl group on the next-to-terminal C-atom. From NB, FB, and ME-1 fermentations, 173 ± 8 mg/L, 244 ± 11 mg/L, and 862 ± 14 mg/L of isopalmitic acid ($C_{16}H_{32}O_2$) was

obtained, respectively. ANOVA test and post-hoc Fisher's LSD test established statistical significance ($p < 0.001$) between all media. ^{1}H-NMR (500 MHz, $CDCl_3$): δ 2.35 (t, J = 7.5 Hz, 2H), 2.01 (m, 1H), 1.62 (m, 2H), 1.27 (m, 22H), 1.14 (m, 1H), 0.88 (m, 3H), 0.64 (m, 1H). ^{13}C-NMR (126 MHz, $CDCl_3$) δ 180.3, 34.1, 32.0, 29.7, 29.7, 29.7, 29.6, 29.5, 29.4, 29.3, 29.1, 24.7, 22.7, 15.8, 14.1, 10.9.

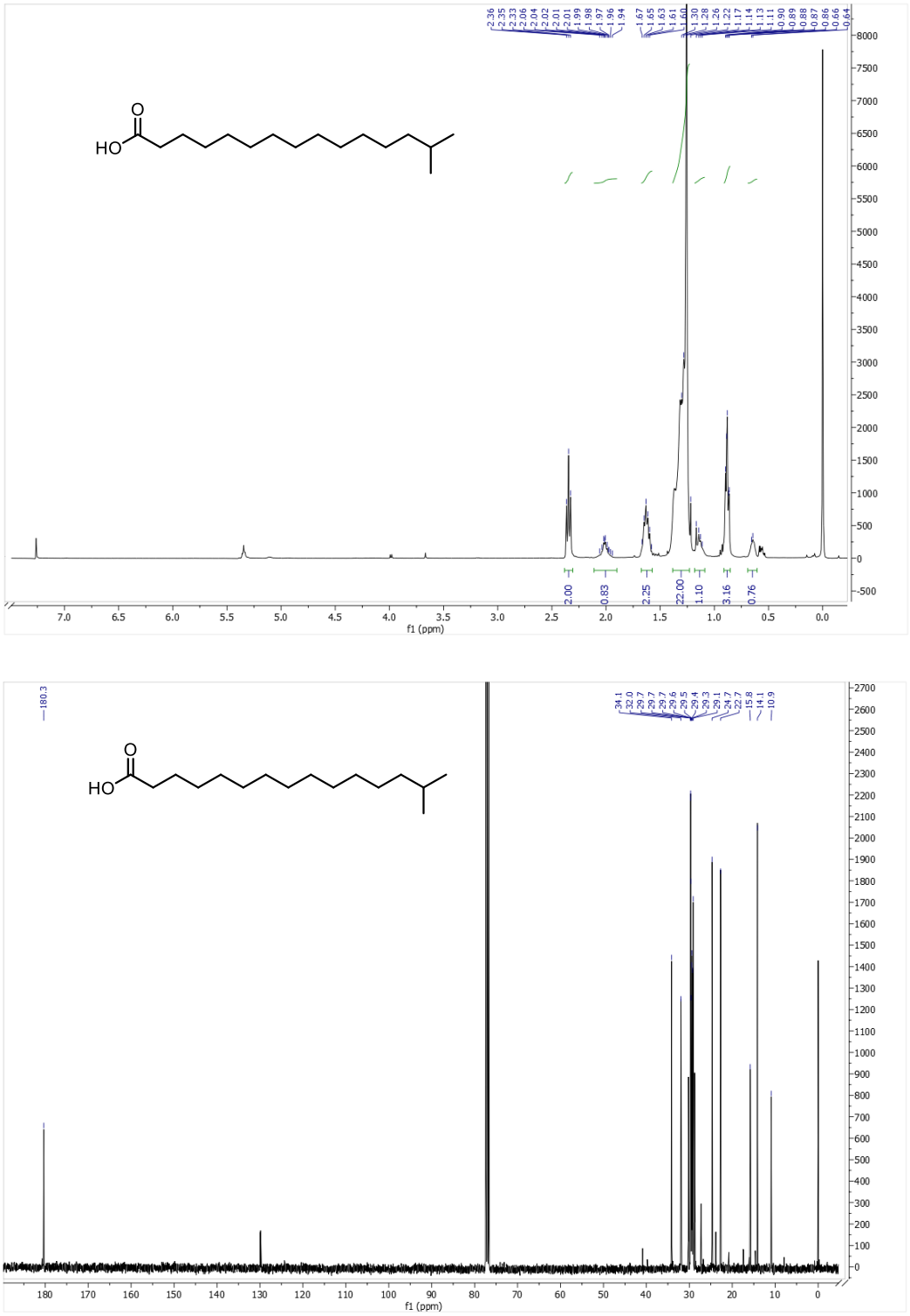

Figure 19. ^{1}H- and ^{13}C-NMR spectra of the isolated isopalmitic acid.

4.5.2. Prodigiosin

Next, the crude extract was eluted using EtOAc (Fig. 18b), which afforded fraction B as a prominently red compound (18e), which was confirmed as PG, and was afforded in concentrations of 6.9 ± 0.5 mg/L, 13.3 ± 1.1 mg/L, and 83.1 ± 3.0 mg/L from NB, FB, and ME-1 fermentations, respectively, suggesting high efficiency of the extraction and purification procedures. ANOVA test and post-hoc Fisher's LSD test established statistical significance ($p < 0.001$) between all media.

PG ($C_{20}H_{25}N_3O$) was obtained as a dark red film. UV-Vis: λ_{max} (EtOAc, nm) 535, 501sh. The chemical structure of purified PG was confirmed by ^{1}H- and ^{13}C-NMR spectroscopy (Fig. 20) which was found to be comparable to literature values.[111] ^{1}H-NMR (500 MHz, methanol-d_4) δ 7.23 (s, H-6'), 7.18 (d, J = 2.6 Hz, H-2), 7.05 – 7.03 (m, H-3'' and H-4), 6.45 (s, H-3'), 6.39 (dd, J = 3.7, 2.6 Hz, H-3), 4.04 (s, 3H, –OMe), 2.45 – 2.41 (m, 2H, H-7''), 2.36 (s, 3H, H-6''), 1.61 – 1.57 (m, 2H, H-8''), 1.39 – 1.35 (m, 4H, H- 9'' and H-10''), 0.94 – 0.91 (m, 3H, H-11''). ^{13}C-NMR (126 MHz, methanol-*d4*) δ 168.5 (C-5''), 151.1 (C-2''), 149.1 (C-3''), 127.6 (C-4''), 127.2 (C-2'), 123.9 (C-5), 123.3 (C-2), 117.7 (C-5'), 117.2 (C-6'), 115.0 (C-4), 113.1 (C-4'), 113.0 (C-3), 94.9 (C-3'), 59.8 (–OMe), 32.8 (C-9''), 31.3 (C-7''), 30.8 (C-8''), 23.6 (C-10''), 14.5 (C-6''), 12.0 (C-11'') ppm. The molecular formula of the purified pigment was determined by HR-LC-ESI-MS at *m/z* calculated for $C_{20}H_{25}N_3O^{+}$ $[M+H]^{+}$ 324.1998 (100.0%), found 324.2098 (100.0%).

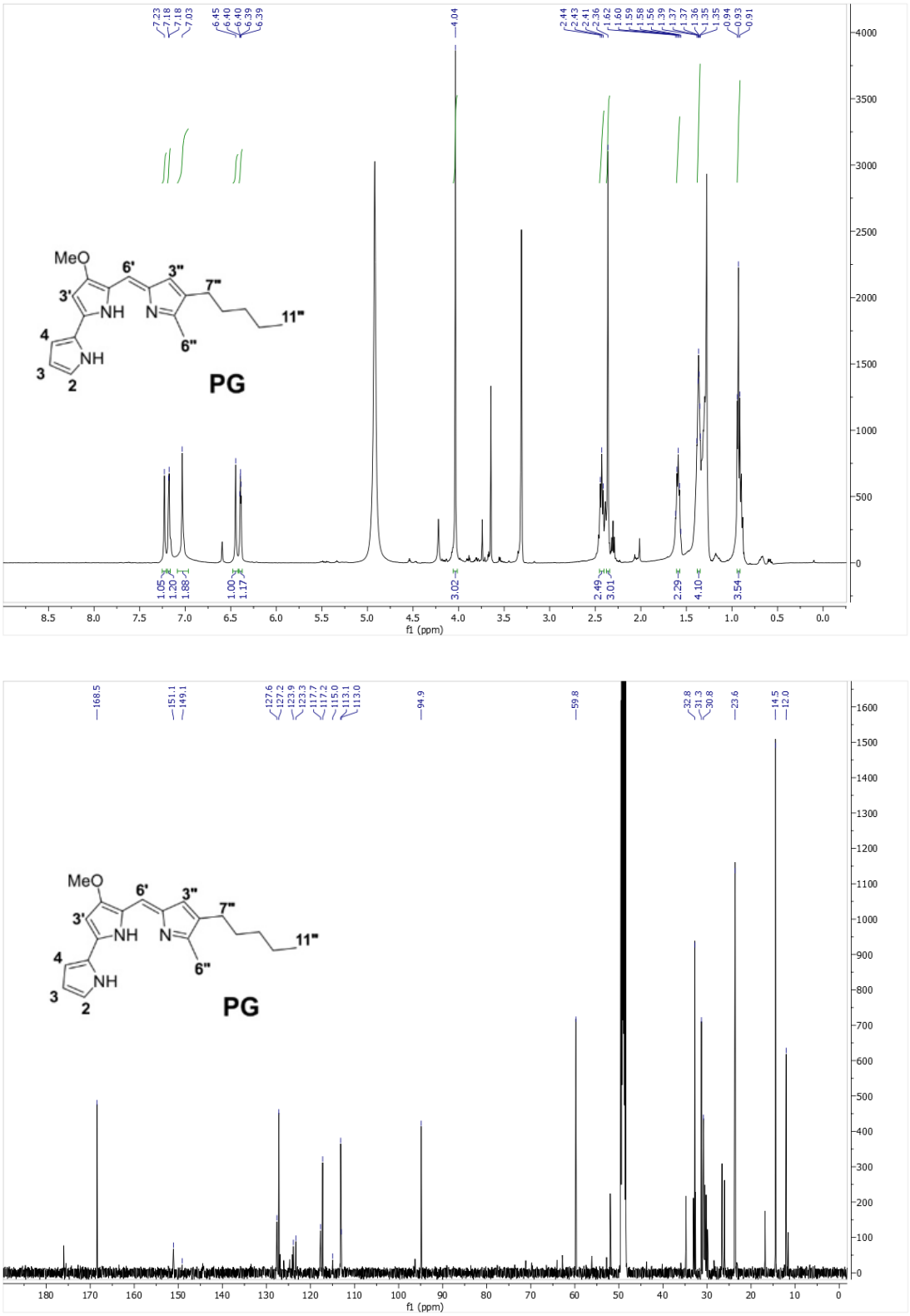

Figure 20.[i] ^{1}H- and ^{13}C-NMR spectra of bacterial prodigiosin (PG).

[i] This figure is part of the manuscript accepted in the MDPI Molecules journal, see **Chapter 4. Results and discussion** for more details on the manuscript.

Finally, the column was successfully washed with MeOH (Fig. 18c) to afford fraction C as a purple amorphous film (Fig. 18f) which was not analysed further.

As this work has shown that the ratio between the crude extract yield and pure PG yield is almost 100-fold in the conventional cultivation media (1.0% yield from NB, 1.1% from FB), the 8.7% yield from waste stream-based substrate ME-1 is a significant improvement of the biotechnological processes, as well as the extraction and purification procedures. The high prices of this natural product (Table 3) are most likely due to the complicated isolation procedures, especially if high purity of PG is required.

Using processed meat waste lowered the cultivation medium cost, shortened the fermentation time, and improved the PG yield 8.7-fold. Other food industry wastes could also be assessed as cheap and accessible substrates for *S. marcescens* ATCC 27117 cultivations which could improve PG production even further.

4.6. Enzymatic halogenation reactions

The enzyme *Am*VHPO I wt was assessed for the biocatalytic bromination of the bacterial PG on a 1 mg scale (Sch. 7). After 3 days, the reaction was quenched as described in Section 3.5.1. and analysed on HPLC-MS (Fig. 21a).

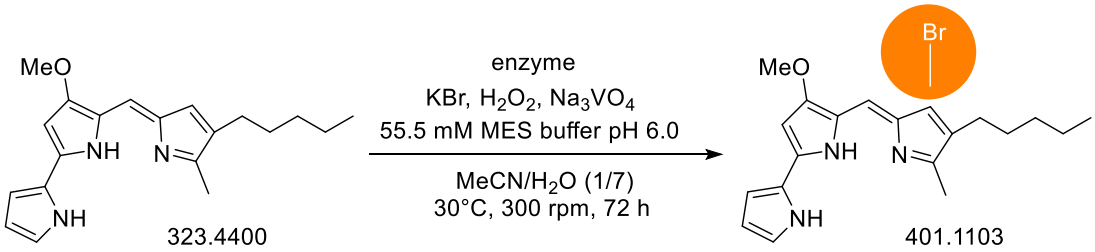

Scheme 7. Biocatalytic bromination reaction conditions using *Am*VHPO I wt. The same conditions were used when *Am*VHPO I Arg425Ser and *Am*VHPO I Arg425Lys mutants were used.

When the wild-type *Am*VHPO I enzyme was used, the most abundant peak in the HPLC-MS chromatogram was the starting compound PG (retention time, RT = 8.62 min, Fig. 21b), but the expected $[M+H]^+$ signal for PG-Br was also observed (RT = 10.34 min, Fig. 21c), with *m/z* 402.23 and 404.25, with signal intensities 1:1, characteristic for the monobrominated compounds.

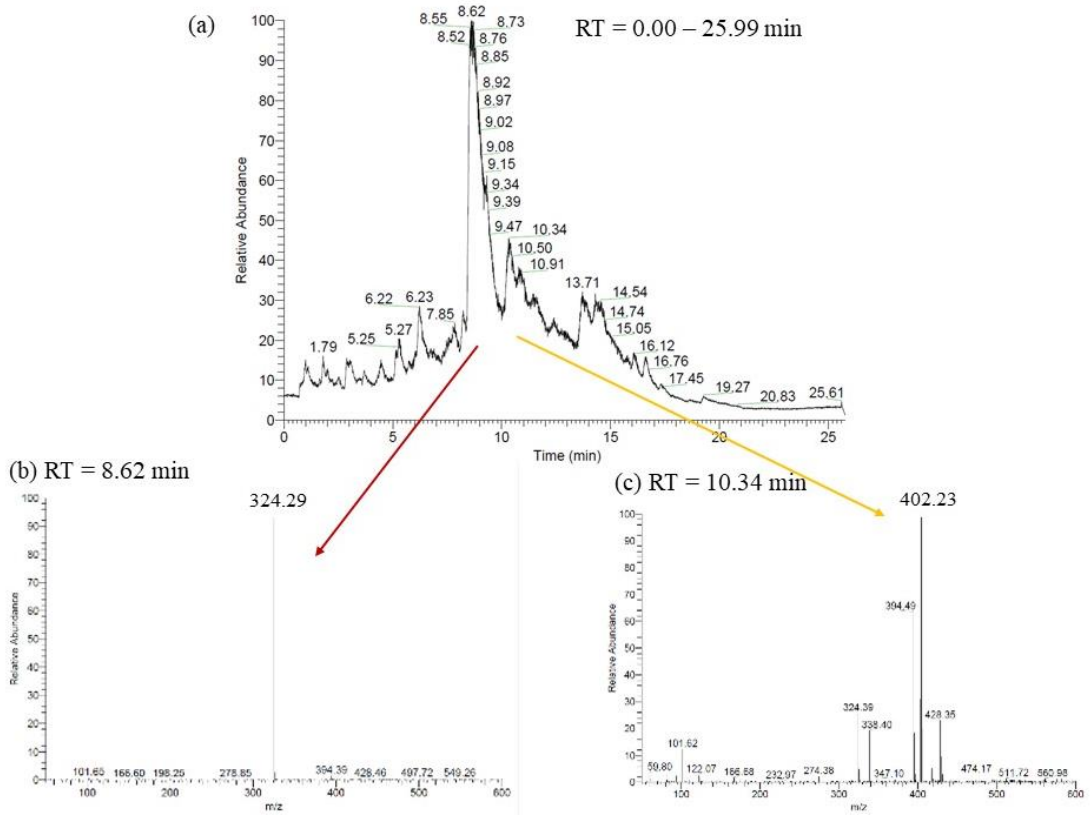

Figure 21. Biocatalytic bromination of PG with *Am*VHPO I wt; reaction mixture analysis: (a) HPLC chromatogram; (b) *m/z* 324.29 at RT = 8.62 min; (c) *m/z* 402.23 and 404.25 (1:1) at RT = 10.34 min.

Similar findings were observed when the mutant enzyme *Am*VHPO I Arg425Ser was used for the enzymatic bromination under the same reaction conditions on a 1 mg scale (Sch. 7): HPLC-MS (Fig. 22a) showed the starting compound PG was recovered as the major mixture component (RT = 8.54 min, Fig. 22b) and only traces of monobrominated PG were detected in the chromatogram (RT = 10.32 min, Fig. 22c).

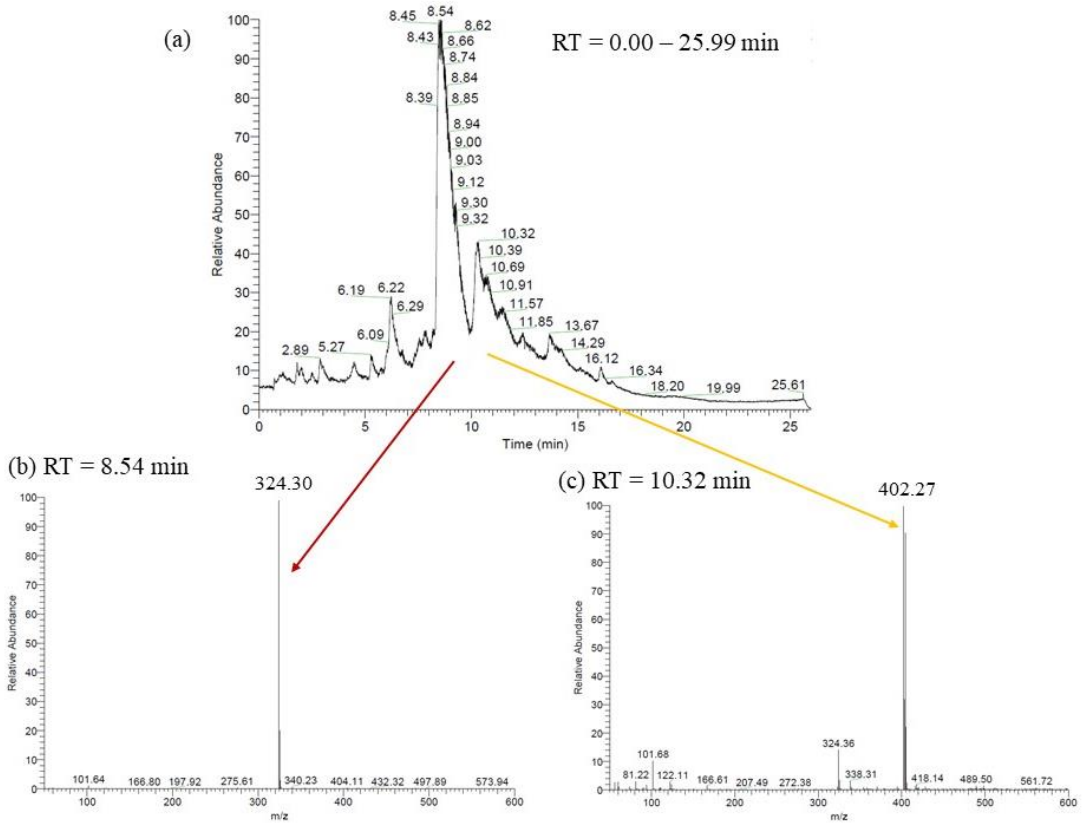

Figure 22. Biocatalytic bromination of PG with *Am*VHPO I Arg425Ser mutant:
(a) HPLC chromatogram; (b) *m/z* 324.30 at RT = 8.54 min;
(c) *m/z* 402.27 and 404.26 (1:1) at RT = 10.32 min.

When the mutant *Am*VHPO I Arg425Lys was used for enzymatic bromination under the established reaction conditions on a 1 mg scale (Sch. 7), HPLC-MS analysis (Fig. 23a) indicated that the starting compound PG was recovered as the major mixture component (RT = 8.66 min, Fig. 23b) and only traces of monobrominated PG were detected in the chromatogram (RT = 10.35 min, Fig. 23c).

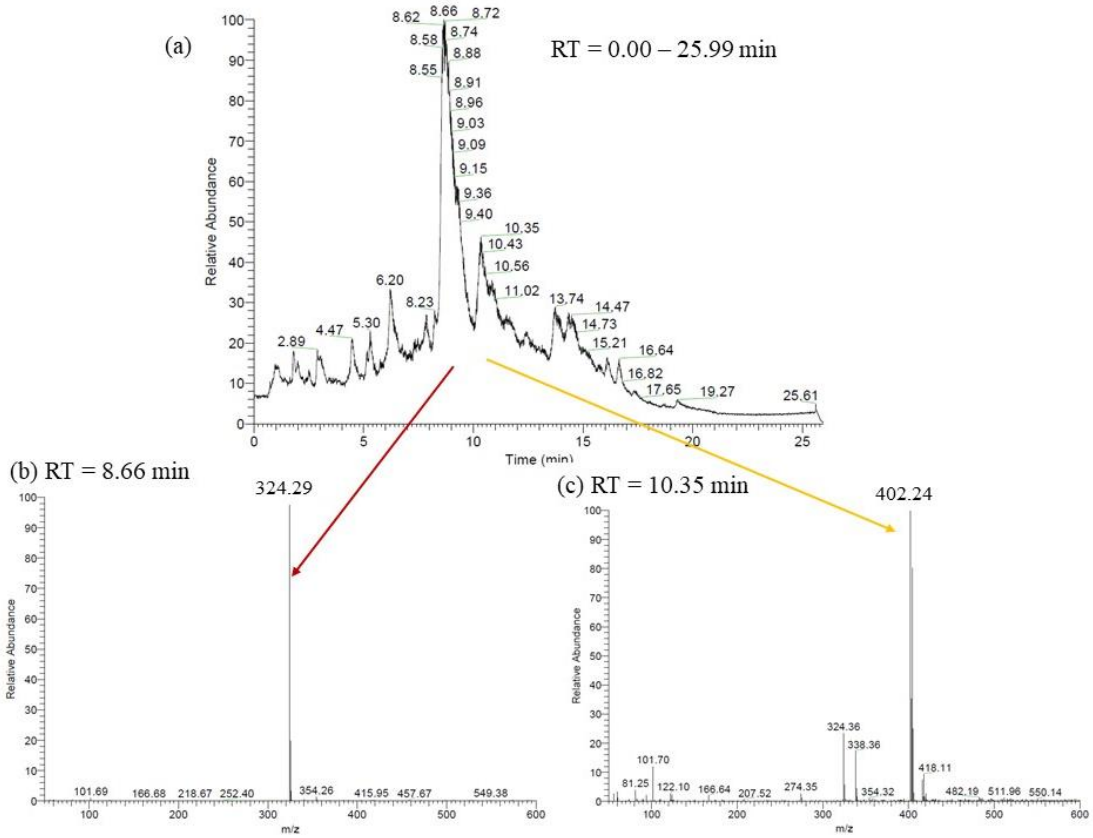

Figure 23. Biocatalytic bromination of PG with *Am*VHPO I Arg425Lys mutant: (a) HPLC chromatogram; (b) *m/z* 324.29 at RT = 8.66 min; (c) *m/z* 402.24 and 404.24 (1:1) at RT = 10.35 min.

The enzyme *Am*VHPO I Arg425Ser mutant was assessed for the biocatalytic chlorination of the bacterial PG on a 1 mg scale (Sch. 8), since this enzyme has shown both enzymatic bromination and chlorination activities (unpublished data, results not shown). After 3 days, the reaction was quenched as described in Section 3.5.1. and analysed on HPLC-MS (Fig. 24a).

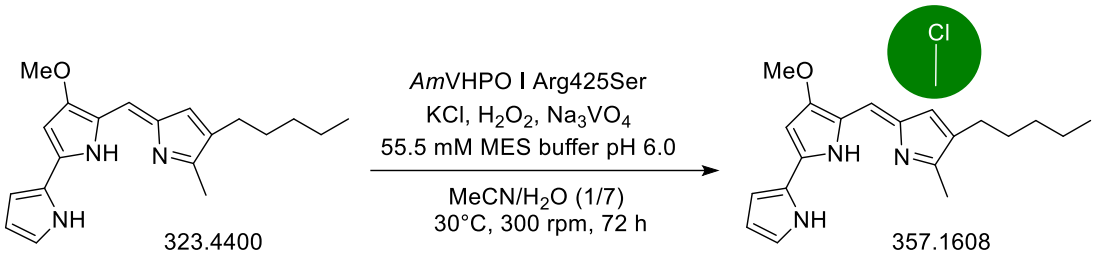

Scheme 8. Biocatalytic chlorination reaction conditions using *Am*VHPO I Arg425Ser mutant.

The most abundant peak in the chromatogram was the starting compound PG (RT = 8.37 min, Fig. 24b), but the expected $[M+H]^+$ signal for PG-Cl was observed (RT = 10.77 min, Fig. 24c), with *m/z* 358.26 and 360.24, with signal intensities 1:0.33, characteristic for the monochlorinated compounds.

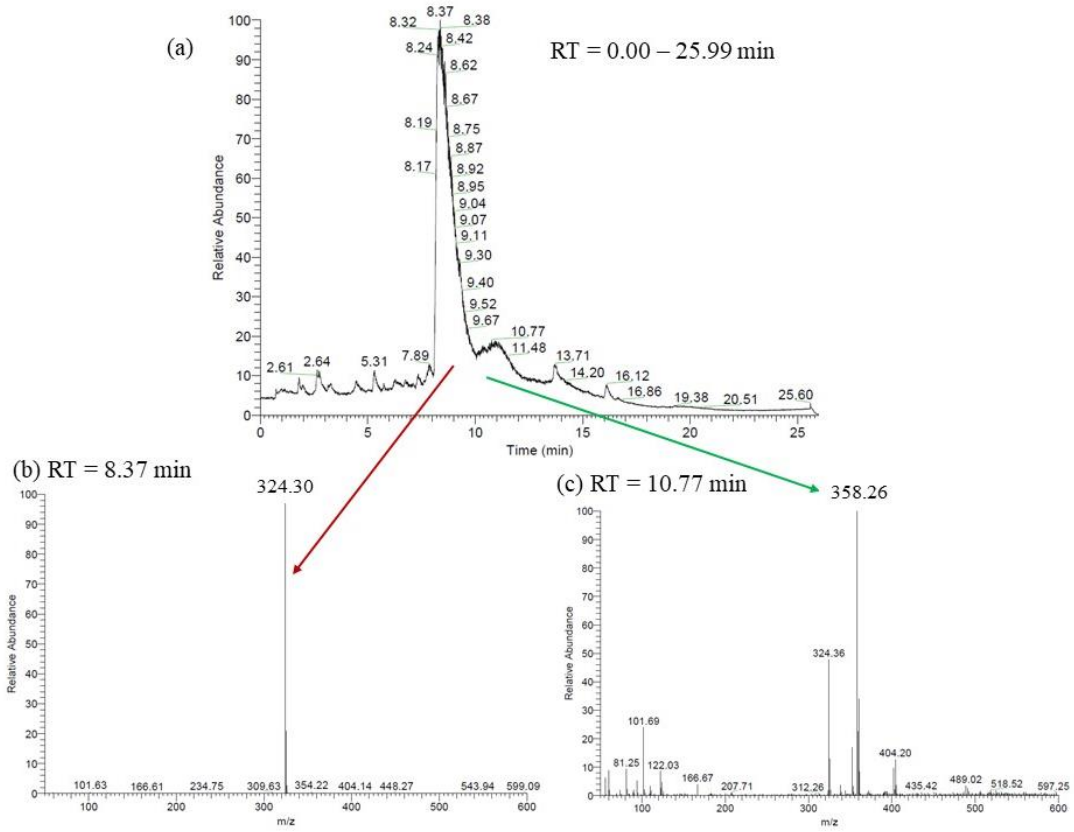

Figure 24. Biocatalytic chlorination of PG with *Am*VHPO I Arg425Ser mutant: (a) HPLC chromatogram; (b) *m/z* 324.30 at RT = 8.37 min; (c) *m/z* 358.26 and 360.24 (1:1) at RT = 10.77 min.

The reactions presented in Schemes 7 and 8 were test reactions to assess if PG is a suitable substrate for the enzymes used in this study; the halogenated product yields were not calculated, nor were the products isolated. These results suggest that an optimisation of the reaction conditions is necessary, in order to obtain the halogenated PG as the major product of biocatalysis. However, enzyme production and purification steps on a large scale are highly resource demanding. Also, these reactions need to be performed in a mixture of a dilute aqueous buffer and an organic solvent, which makes them further economically unfavourable.[81]

In contrast, chemical reagents are commercially available, and, unlike enzymes, they need no purification or preparation prior to use. Besides that, chemical halogenation reactions under mild conditions can be seen as efforts towards green chemistry principles, so they were investigated next.

4.7. Oxidative prodigiosin bromination

After the process of fermentative production and chromatographic purification of PG, derivatisation to obtain novel Br-derivatives was performed using hydrogen peroxide (H_2O_2) and dimethyl sulfoxide (DMSO) as green oxidants (Sch. 9). Bromination reaction of PG using H_2O_2[80] as the oxidising agent yielded a mixture of monobrominated products PG-Br, while DMSO as the oxidant[75] proceeded smoothly to give the dibrominated compound PG-Br_2. Reaction yields were 81% of the monobrominated PG isomers and 63% of the pure dibrominated PG.

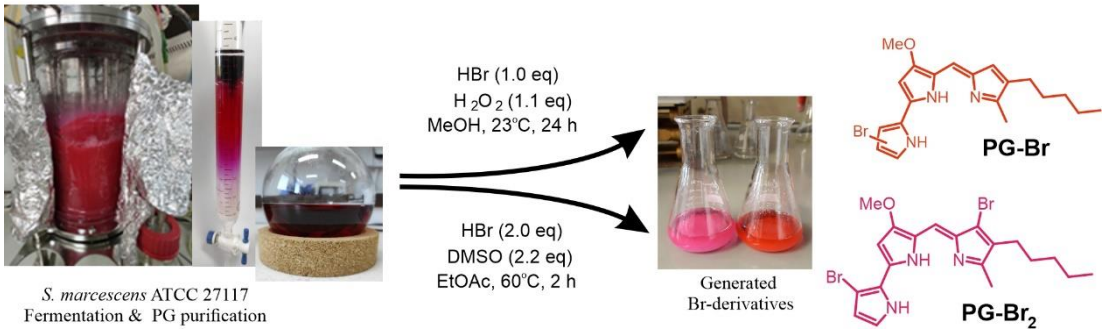

Scheme 9.[j] PG production, purification, and derivatisation, affording two novel brominated derivatives: PG-Br and PG-Br_2.

4.7.1. Monobrominated prodigiosin (PG-Br)

Following a literature procedure[80], a reaction with bacterial PG showed monobrominated product formation (Sch. 10).

[j] This figure is part of the manuscript accepted in the MDPI Molecules journal, see **Chapter 4. Results and discussion** for more details on the manuscript.

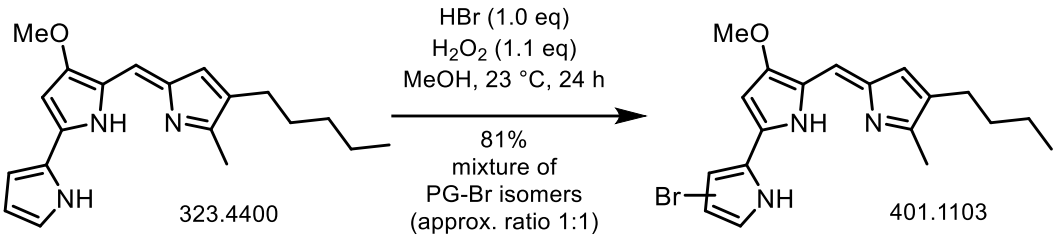

Scheme 10. Reaction conditions affording monobrominated PG (PG-Br).

The crude reaction mixture of monobromination of PG was monitored by HPLC-MS (Fig. 25a) and the most abundant peak in the chromatogram had the expected $[M+H]^+$ signal for PG-Br, with *m/z* 402.25 and 404.25, with signal intensities 1:1, characteristic for monobrominated compounds (RT = 10.19 min, Fig. 25b), while the *m*/*z* of PG was not found. Upon reaction completion, PG-Br was worked-up and purified as described in the Section 3.5.2.1.

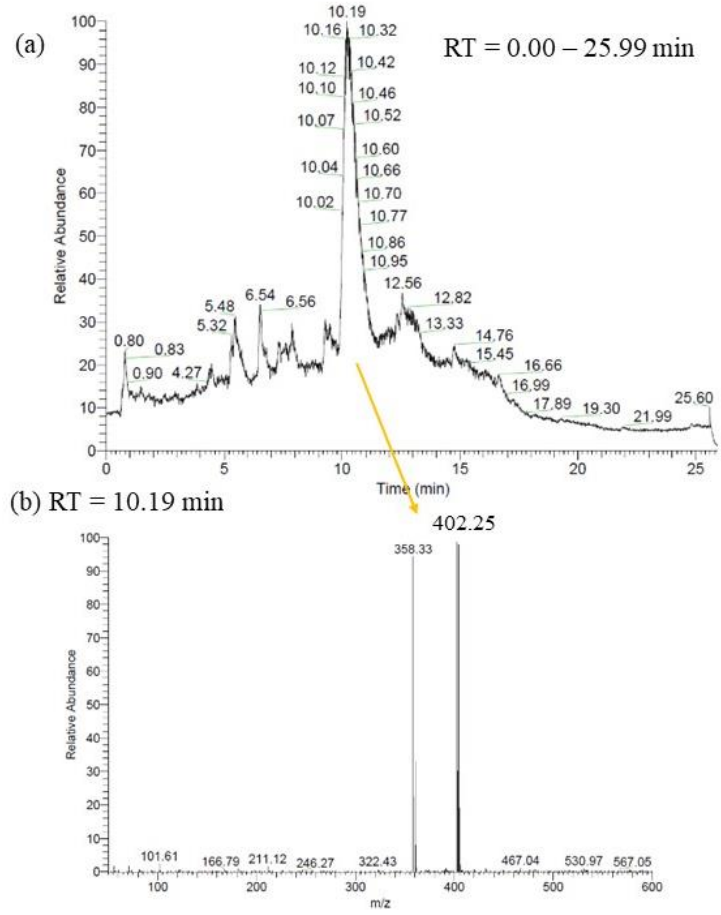

Figure 25. Chemical monobromination reaction of PG: (a) HPLC chromatogram for monobromination; (b) *m*/*z* 402.25 and 404.25 (1:1) at RT = 10.19 min.

As mentioned previously, PG has 6 aromatic protons in the aromatic region (8.00 – 6.00 ppm), at positions 2, 3, 4, 3', 6', 3'' (Fig. 20). If monobromination takes place, it is expected to observe signals from 5 aromatic protons. However, the analysis of the ^{1}H-NMR spectrum of the isolated PG-Br suggested that a mixture of two monobrominated products was obtained (Fig. 26).

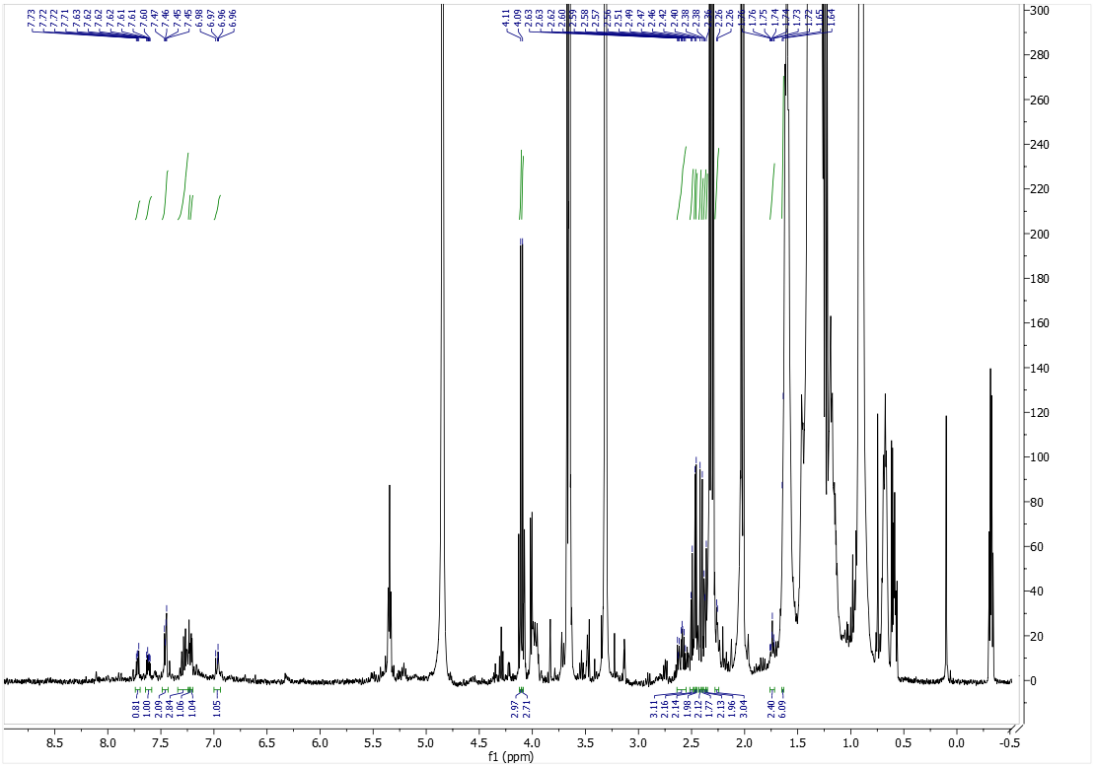

Figure 26.[k] ^{1}H-NMR spectrum of PG-Br isomers (approximate ratio 1:1).

Instead of 5, a total of 10 protons can be integrated within the aromatic region (Fig. 27a). Furthermore, there are two singlet signals at 4.11 and 4.09 ppm, which correspond to the methoxy (–OMe) group on the B ring of PG (Fig. 27b). The position of –Br in each isomer could not be determined and can only be hypothesised, but based on the integrals, it was concluded that both isomers were acquired in approximately equal ratios.

[k] This figure is part of the manuscript accepted in the MDPI Molecules journal, see **Chapter 4. Results and discussion** for more details on the manuscript.

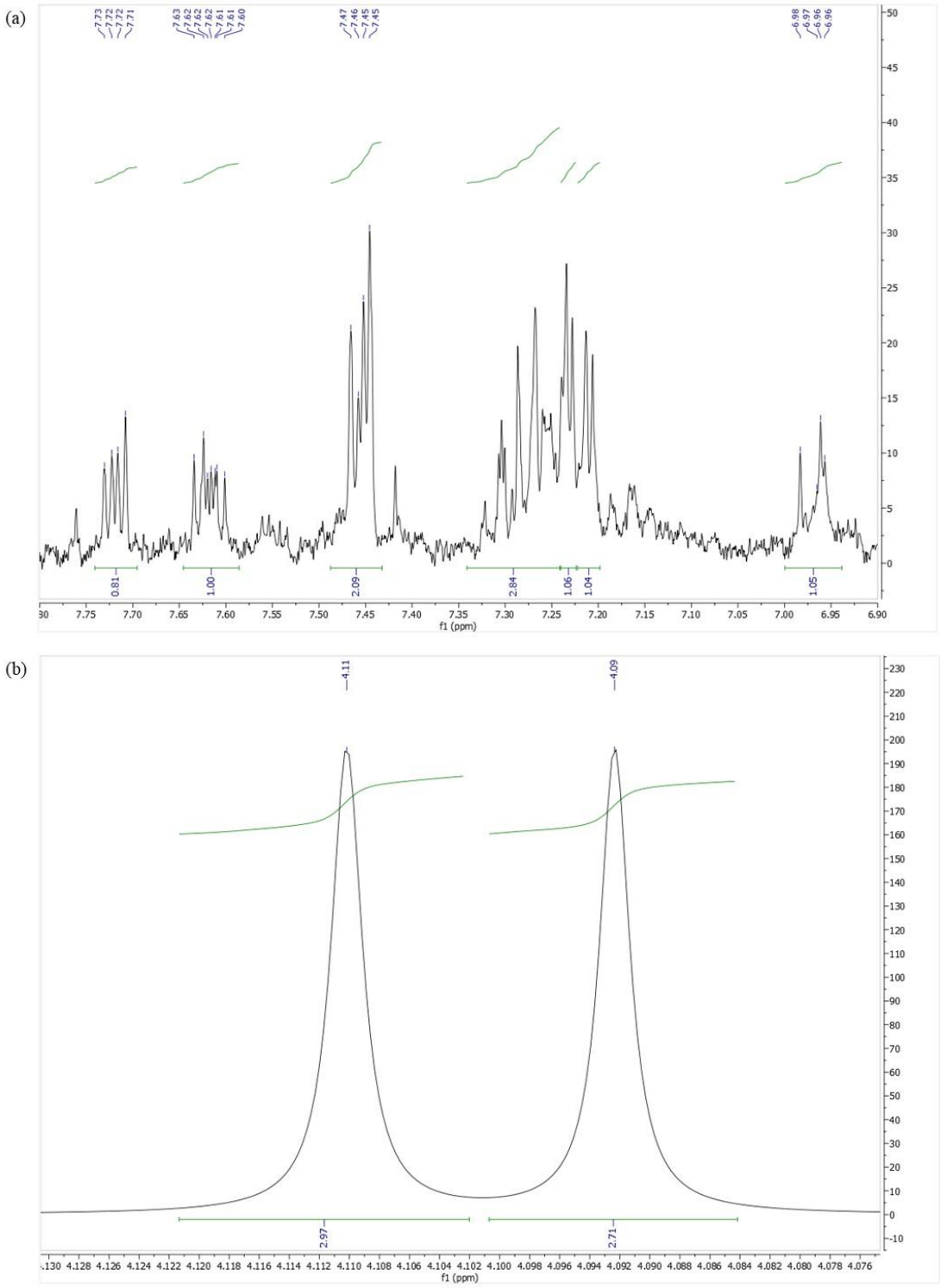

Figure 27. ^{1}H-NMR spectrum of PG-Br isomers showing the regions where the duplicated signals can be distinguished: (a) 10 aromatic protons in the aromatic region (8.00 – 6.00 ppm); (b) 2 signals from different methoxy groups (4.13 – 4.07 ppm).

PG-Br was obtained as an orange-brown oil (8.12 mg, 0.025 mmol, 81%). UV-Vis: λ_{max} (EtOAc, nm) 540, 470. ^{1}H-NMR (500 MHz, methanol-d_4) δ 7.73 – 7.71 (m, 1H), 7.64 – 7.59 (m, 1H), 7.47 – 7.45 (m, 2H), 7.33 – 7.25 (m, 3H), 7.23 – 7.22 (m, 1H), 7.22 – 7.21 (m, 1H), 7.00 – 6.95 (m, 1H), 4.11 (s, 3H), 4.09 (s, 3H), 2.64 – 2.55 (m, 3H), 2.51 – 2.49 (m, 2H), 2.48 – 2.46 (m, 2H), 2.47 – 2.45 (m, 2H), 2.43 – 2.41 (m, 2H), 2.41 – 2.39 (m, 2H), 2.39 – 2.37 (m, 2H), 2.37 – 2.35 (s, 2H), 2.28 – 2.24 (m, 3H), 1.76 – 1.72 (m, 2H), 1.65 – 1.63 (m, 6H). The signals in the ^{13}C-NMR spectrum were not legible due to overlapping of signals from different isomers, as well as the residual solvent signals. HR-LC-ESI-MS: *m/z* calculated for $C_{20}H_{25}BrN_3O^+$ $[M+H]^+$ 402.1176 (100.0%), 404.1155 (97.3%); found 402.1157 (100.0%), 404.1141 (99.4%). Since both these isomers have the same molecular weight (MW), the HR-LC-ESI-MS reported only one mass, even though a mixture of isomers is more likely.

4.7.2. Dibrominated prodigiosin (PG-Br$_2$)

Following a literature procedure[75], a reaction with bacterial PG showed dibrominated product formation (Sch. 11).

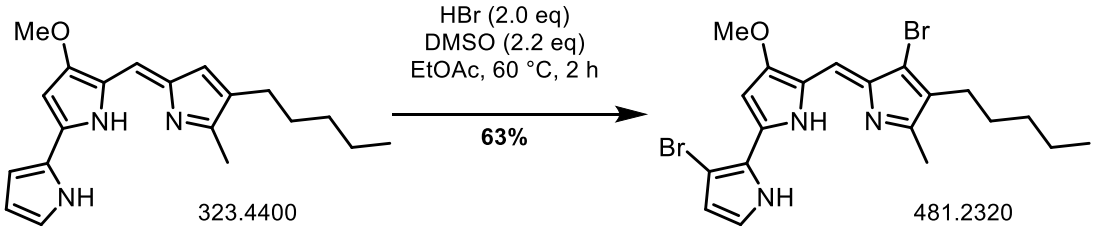

Scheme 11. Reaction conditions affording dibrominated PG (PG-Br$_2$).

The crude reaction mixture of dibromination of PG was monitored by HPLC-MS (Fig. 28a) and the most abundant peak in the chromatogram had the expected $[M+H]^+$ signal for PG-Br$_2$, with *m/z* 480.21, 482.20, 484.20, with signal intensities 1:2:1, characteristic for dibrominated compounds (RT = 13.27 min, Fig. 28b), while the *m/z* of PG was not found. Upon reaction completion, PG-Br$_2$ was worked-up and purified as described in the Section 3.5.2.2.

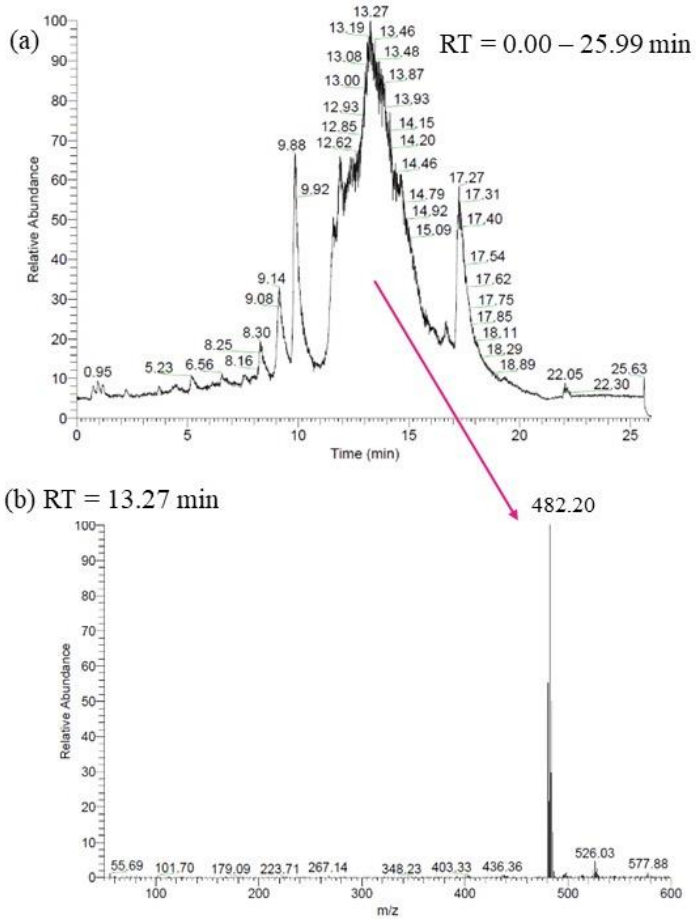

Figure 28. Chemical dibromination reaction of PG: (a) HPLC chromatogram for debromination; (b) *m/z* 480.21, 482.20, 484.20 (1:2:1) at RT = 13.27 min.

PG-Br_2, was obtained as a purple film (8.5 mg, 0,018 mmol, 63%). UV-Vis: λ_{max} (EtOAc, nm) 544, 480. ^{1}H- and ^{13}C-NMR spectra were recorded (Fig. 29) and carefully analysed. ^{1}H-NMR (500 MHz, $CDCl_3$) δ 7.24 (s, H-6'), 7.18 (d, *J* = 4.0 Hz, H-2), 6.55 (s, H-3'), 6.44 (d, *J* = 4.0 Hz, H-3), 4.09 (s, 3H, –OMe), 2.53 – 2.50 (m, 2H, H-7''), 2.40 (s, 3H, H-6''), 1.65 – 1.62 (m, 2H, H-8''), 1.40 – 1.37 (m, 4H, H-9'' and H-10''), 0.95 – 0.87 (m, 3H, H-11''). ^{13}C-NMR (126 MHz, $CDCl_3$) δ 168.6 (C-5''), 148.8 (C-2''), 127.7 (C-4''), 124.9 (C-2'), 123.4 (C-5), 121.1 (C-3''), 118.6 (C-6'), 118.2 (C-5'), 118.1 (C-2), 115.7 (C-4'), 110.0 (C-3), 104.8 (C-4), 94.9 (C-3'), 59.9 (–OMe), 32.8 (C-9''), 31.3 (C-7''), 30.8 (C-8''), 23.6 (C-10''), 14.4 (C-6''), 12.1 (C-11'') ppm. HR-LC-ESI-MS: *m/z* calculated for $C_{20}H_{24}BrN_3O^+$ $[M+H]^+$ 480.0281 (51.4%), 482.0260 (100.0%), 484.0240 (48.6%); found 480.0256 (50.2%), 482.0239 (100.0%), 484.0223 (49.7%).

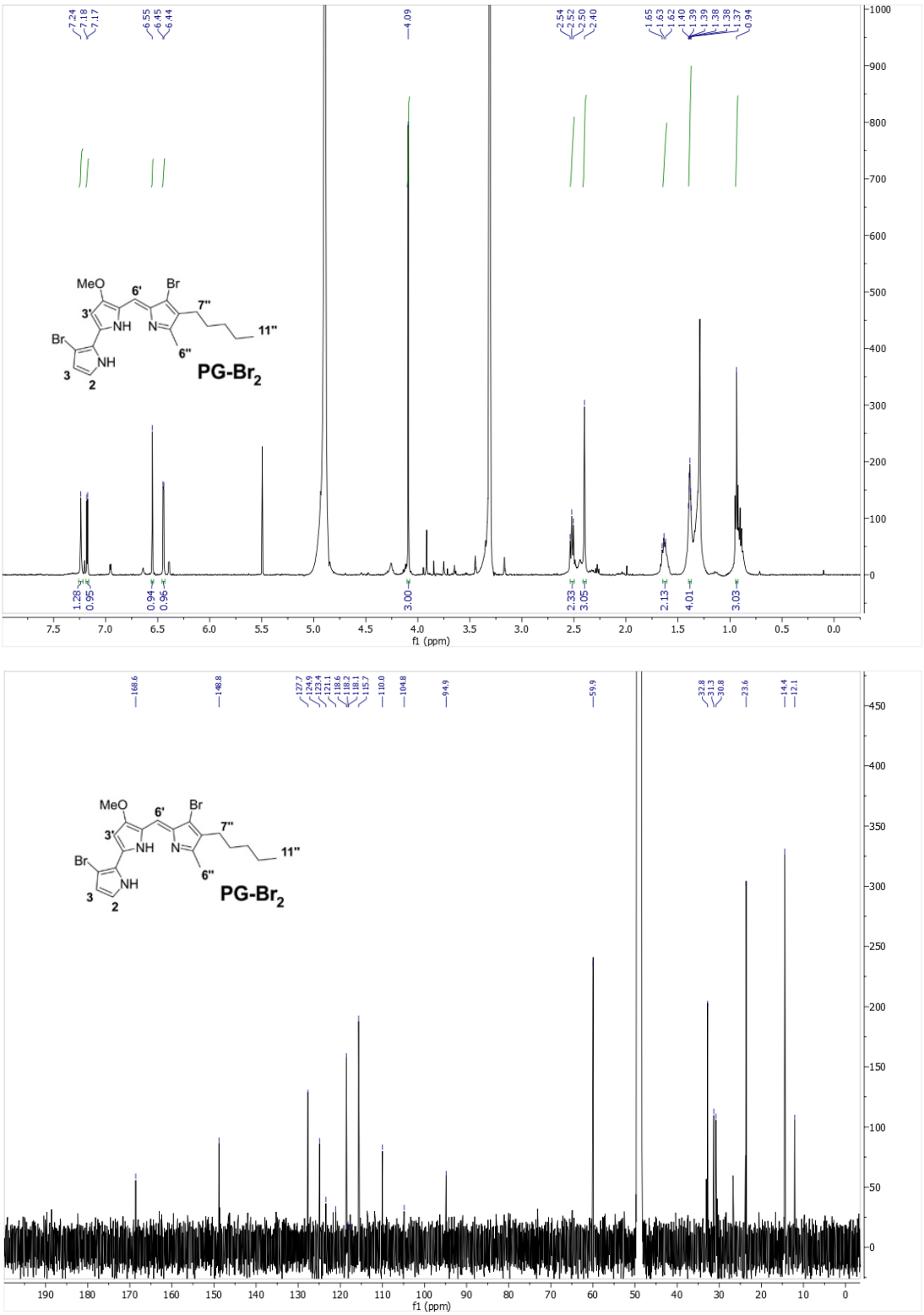

Figure 29.[l] ^{1}H- and ^{13}C-NMR spectra of PG-Br_2.

[l] This figure is part of the manuscript accepted in the MDPI Molecules journal, see **Chapter 4. Results and discussion** for more details on the manuscript.

A careful comparison of the aromatic regions of the ^{1}H-NMR spectra of PG (Fig. 30a) and the compound PG-Br_2 (Fig. 30b) showed that the H-3" and H-4 signals are absent in the spectrum of the dibrominated derivative. Additional evidence for the positions of bromine atoms was the change in the H-3 and H-2 multiplicities. In the spectrum of PG (Fig. 30a), H-3 signal appears in the form of a doublet of doublets, due to coupling with the H-2 and H-4 protons, while in the spectrum of the PG-Br_2 (Fig. 30b), this signal is in the form of a doublet due to coupling with the H-2 proton only. Similarly, H-2 signal in the PG spectrum appears as a multiplet, whereas in the dibrominated derivative it is in the form of a doublet, due to coupling with the vicinal H-3. Based on the positions of Br-atoms in PG-Br_2, it can be assumed that monobrominated isomers have the halogen either at position 4 or at the position 3''.

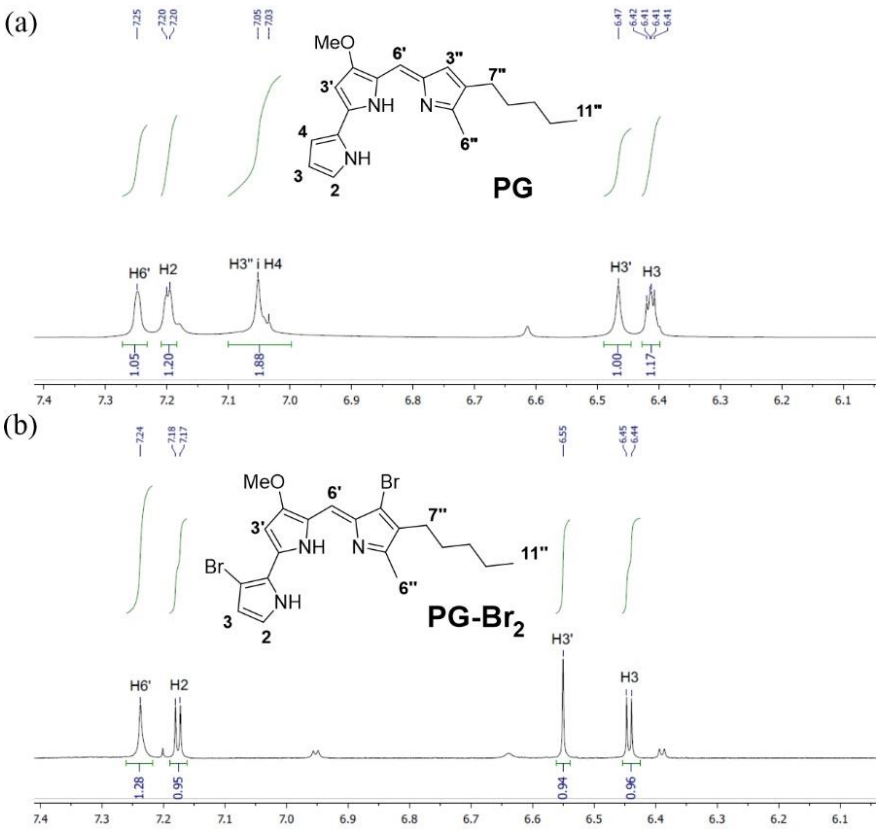

Figure 30.[m] ^{1}H-NMR spectra of the aromatic region (7.40 – 6.00 ppm) of: (a) PG; (b) PG-Br_2.

[m] This figure is part of the manuscript accepted in the MDPI Molecules journal, see **Chapter 4. Results and discussion** for more details on the manuscript.

4.8. Antimicrobial activity of prodigiosin and its Br-derivatives

This study revealed that PG and its Br-derivatives did not have any antibacterial or antifungal effects on the tested strains, even at the highest tested concentration of 200 µg/mL (Table 9).

Table 9. Minimum inhibitory concentration (MIC, µg/mL) of PG and its novel Br-derivatives.

	Bacterial strains			
Compounds	*S. aureus* ATCC 25923	*L. mono-cytogenes* NCTC 11994	*P. aeruginosa* PAO1 NCTC 10332	*E. coli* NCTC 2001
PG	>200	>200	>200	>200
PG-Br	>200	>200	>200	>200
PG-Br$_2$	>200	>200	>200	>200
	Fungal strains			
Compounds	*C. albicans* ATCC 10231	*C. glabrata* ATCC 2001	*C. krusei* ATCC 6258	*C. parapsilosis* ATCC 22019
PG	>200	>200	>200	>200
PG-Br	>200	>200	>200	>200
PG-Br$_2$	>200	>200	>200	>200

A common trait for many secondary metabolites, including PG, is not having a clearly defined physiological role within the producing strain. Possible functions of PG include an eco-physiological response to microbial competition in the natural environment[36] and UV protection[35]. Since all tested bacterial and fungal strains are clinical human pathogens, the results can be interpreted *via* a hypothesis that PG does not have a high affinity against clinical pathogens in general because they are not found in the same environment and thus do not represent their natural competitors. As most *Serratia* spp. are commonly isolated from soil, water, plants and insects[99], it is more likely that PG and its derivatives would prove beneficial against plant pathogens and other environmental microorganisms.

In a recent study, PG isolated from a commercially available strain *Serratia marcescens* ATCC 274 has exhibited antibacterial activity in a Kirby-Bauer standardised disc-diffusion assay on Mueller-Hinton agar against three Gram-positive (MRSA, the methicillin-resistant *Staphylococcus aureus* ATCC 33591, *Staphylococcus aureus* NCTC 8325-4 and *Enterococcus faecalis* V583) and one Gram-negative (*Escherichia coli* OP50) bacteria at 250 and 500 µg/mL, while the

growth of both *Pseudomonas aeruginosa* PA14 and *Salmonella enterica* serovar Typhimurium SL1344 was not negatively affected by PG at these concentrations. However, in the same study, MIC of PG in a microdilution experiment was 20-fold higher at 10 mg/mL against *S. aureus* NCTC 8325–4, *E. faecalis* V583 and *E. coli* OP50, whereas >10 mg/mL was necessary to inhibit the visible growth of MRSA, further suggesting that PG may not be efficient against clinical pathogenic strains.[36] Another example of weak antibacterial activity of PG isolated from *S. marcescens* found in an oil refinery effluent sample, against the clinical *E. faecalis* S1 strain was shown by Clements *et al*.[112] where PG of 80% purity exhibited a MIC of < 750 µg/mL. Resistance to PG was noticed in pathogenic clinical isolates *E. coli* (UFPEDA 224), *P. aeruginosa* (UFPEDA 39) and *Acinetobacter* (UFPEDA 993), which was demonstrated by the lack of zones in the disc-diffusion assay.[113]

Antifungal properties of PG have been assessed previously, but mostly against plant pathogens.[107, 114] Culture extract from *S. marcescens* Bm1 was found to have antifungal activity against various phytopathogens *Pythium myriotylum*, *Rhizoctonia solani*, *Sclerotium rolfsii*, *Phytophthora infestans*, *Fusarium oxysporum*, with 31-71% growth inhibition.[115] A crude extract of PG from *Serratia marcescens* CFFSUR-B2 was found active against ascomycete fungus *Mycosphaerella fijiensis* at 996 µg/mL and was able to inhibit ascospore germ tube growth, but not ascospore germination.[116]

Other prodigiosins (Fig. 3) have exhibited antibacterial and antifungal activities.[14] Undecylprodigiosin (UP) from *Streptomyces* sp. JS520 showed antibacterial activity against *Bacillus subtilis* ATCC 6633 and *Micrococcus luteus* ATCC 379 at the concentration of 50 µg/mL as well as antifungal activity against *Candida albicans* ATCC 10259 at 150 µg/mL.[23] Cycloprodigiosin (cPG) from *Zooshikella rubidus* S1-1 had 9.0-10.5 mm inhibition zones against *Bacillus subtilis* KCTC 1914, *Salmonella typhimurium* KCTC 1926, *Staphylococcus aureus* KCTC 1916 and *Escherichia coli* KCTC 1924, while 9.0 mm inhibition zone against *Candida albicans* KCTC 1940.[117] Streptorubin B from *Streptomyces* sp. MC11024 exhibited mild antibacterial activity against MRSA N315 strain at ≥ 32 µg/mL.[118] Cyclic prodigiosins have generally shown more pronounced antibacterial activity than the linear ones.[117]

4.9. Anticancer potential of prodigiosin and its Br-derivatives

PG has predominantly been explored as an anticancer compound, with promising potential in treating cancers of various cell types invading various organs, such as the brain, lungs, liver, breasts, skin, colon and other.[53] PG has been screened in the 60-cell-line panel of the National Cancer Institute (NCI) and assessed for cytotoxic properties, with the average LC_{50} of 0.68 μg/mL.[119] It was found to inhibit proliferation, migration and invasion of a variety of cancer cell lines, including nasopharyngeal[120], breast[43] and lung.[41] Therefore, PG and two novel PG-Br and PG-Br_2 derivatives were used in cell viability assays on healthy MRC-5 and HaCaT cell lines, as well as a panel of A549, A375, MDA-MB-231 and HCT116 cancer cell lines (Table 10).

Table 10. Antiproliferative activity of PG, PG-Br and PG-Br_2 (IC_{50}, μg/mL) after 48 h treatment. Statistical analysis was done using a *t*-test, $p \leq 0.05$ was considered statistically significant.

Cell line	PG	PG-Br	PG-Br_2
MRC-5	1.20 ± 0.04	5.50 ± 0.02	10.00 ± 0.09
HaCaT	2.10 ± 0.05	10.00 ± 0.08	18.00 ± 0.08
A549	1.30 ± 0.02	8.00 ± 0.06	16.00 ± 0.08
A375	1.25 ± 0.04	6.00 ± 0.05	12.00 ± 0.04
MDA-MB-231	0.62 ± 0.01	6.25 ± 0.04	17.00 ± 0.05
HCT116	0.70 ± 0.02	5.00 ± 0.05	10.00 ± 0.08

Pure PG exhibited excellent activity against all four carcinoma cell lines, with IC_{50} values between 0.62 and 1.30 μg/mL. Previously, the anticancer activity range of PG against A549 was found from as low as 0.03 μg/mL[121] to 3.23 μg/mL[122], so our finding of 1.30 μg/mL is in agreement with the literature data. The melanoma cell line A375 was sensitive to PG at 0.70 μg/mL[123], which was similar to our finding of 1.25 μg/mL. Breast cancer MDA-MB-231 was found to be extremely sensitive to PG in the range from 0.02 μg/mL[43] up to 0.68 μg/mL[44], in line with our result of 0.62 μg/mL. The IC_{50} value reported previously for HCT116 colon cancer was

0.04 µg/mL after 72 h treatment[52], which is 17.5-fold lower in comparison to our findings of 0.70 µg/mL, but after a shorter treatment of 48 h (Table 10).

The overall effect of PG on cancerous cells was compared to the overall effects that PG-Br and PG-Br_2 exhibited on cancerous cells using a *t*-test, and a statistical difference was noticed ($p < 0.001$). PG-Br and PG-Br_2 had higher IC_{50} values, suggesting statistically significant weaker anticancer potential than the parent PG.

However, PG was also highly toxic against tested healthy cells (MRC-5 and HaCaT). The effect of PG on healthy cells was compared to the effect of its novel Br-derivatives on healthy cells using a *t*-test, and a statistical difference was not noticed ($p > 0.05$), suggesting similar level of cytotoxicity of PG and its novel Br-derivatives. This could be one of the reasons that the natural PG has not reached the clinical practice, indicating the need for derivatives with improved selectivity.

Bromination is expected to affect the hydrophobicity of molecules, as well as facilitate transport across membranes and binding to hydrophobic pockets, especially since bromine substituents were proven more hydrophobic than methoxy-moieties *in vitro* and *in silico*[65], thus shorter and longer exposure times were used to examine cytotoxicity in MRC-5 and HCT116 cells (Table 11).

Table 11. Effects of exposure time on cytotoxicity and anticancer activity (IC_{50}, µg/mL) of PG, PG-Br and PG-Br_2 using MRC-5 and HCT116 cell lines. Results were analysed using ANOVA test and post-hoc Fisher's LSD test, $p \leq 0.05$ was considered statistically significant.

Exposure time (h)	**IC_{50} (µg/mL)**		
	PG	**PG-Br**	**PG-Br_2**
Cell line MRC-5			
24	1.80 ± 0.04	7.60 ± 0.08	15.00 ± 0.05
48	1.20 ± 0.04	5.50 ± 0.02	10.00 ± 0.09
72	0.70 ± 0.02	5.98 ± 0.09	10.00 ± 0.08
Cell line HCT116			
24	5.00 ± 0.06	35.00 ± 0.09	50.00 ± 0.09
48	0.70 ± 0.02	5.00 ± 0.05	10.00 ± 0.08
72	0.80 ± 0.02	3.20 ± 0.06	10.00 ± 0.05

Prolonged exposure of MRC-5 cells to PG resulted in statistically nonsignificant lower IC_{50} values over time (2.5-fold lower IC_{50} values after 72 h in comparison to 24 h exposure) (Table 11). For the Br-derivatives, a statistically nonsignificant difference of 1.5-fold was observed between 24 h and 48 h, and the longer treatment of up to 72 h had no further effect (Table 11).

In contrast, when HCT116 cells were exposed to PG and Br-derivatives, the IC_{50} values of Br-derivatives were higher after 24 h, and significantly lower ($p < 0.001$) after the prolonged exposure of 72 h, whereas the difference in IC_{50} values between 48 and 72 h was not significant. An 11-fold lower IC_{50} value upon 72 h in comparison to 24 h exposure was observed for PG-Br (Table 11), suggesting specific dynamics of its uptake and activity.

When healthy HFF (human foreskin fibroblasts) cells were treated with 0.36 µg/mL PG, growth inhibition was 76.16% and the IC_{50} was 0.15 µg/mL after 72 h of treatment[52], exhibiting a higher cytotoxicity than in our results.

When the effect of cPG on breast cancer cell lines was studied, it was found that healthy cells WI-38-40 (fibroblasts) and HBL-100 (breast epithelial cells) required higher doses of cPG for growth inhibition after 72 h exposure, 0.73 µg/mL and 0.57 µg/mL, respectively, than cancer cells, where IC_{50} varied from 0.15-0.20 µg/mL, but the selectivity of cPG towards cancer cells was not notable,[124] similarly to our results from this study, where PG and its novel Br-derivatives were tested (Table 10 and Table 11) and the selectivity of compounds assessed.

Additional to the MTT assay of shorter and longer exposure times (Table 11), cytotoxicity in MRC-5 and anticancer activity in HCT116 cells was visualised under a microscope and selected images are presented (Fig. 31).

Untreated MRC-5 cells have a distinctive spindle shape, and their nuclei are easily spotted (Fig. 31a). In MRC-5 cells treated with 5 µg/mL PG, the biopigment is aggregated inside the cells, fewer cells are noticed due to detachment from the surface of the monolayer, and they have shrunk and/or changed shape (Fig. 31b). Similar effects were noticed in MRC-5 cells treated with Br-derivatives of PG, but at significantly higher concentrations of 12.5 µg/mL of PG-Br (Fig. 31c) and 25 µg/mL of $PG\text{-}Br_2$ (Fig. 31d).

Untreated HCT116 cells are smaller and more densely arranged with clearly distinguished nuclei (Fig. 31e). The amount of slowly swelling and detaching HCT116 cells is the most prominent after treatment with 5 µg/mL of PG (Fig. 31f). These effects are notable after 12.5 µg/mL of PG-Br (Fig. 31g) and PG-Br_2 (Fig. 31h) treatments. There is evidence of cell aggregation in PG-Br treated cells, again suggesting its specific uptake and activity.

This experiment confirmed milder cytotoxicity of the novel Br-derivatives, but also the low selectivity of all three tested compounds.

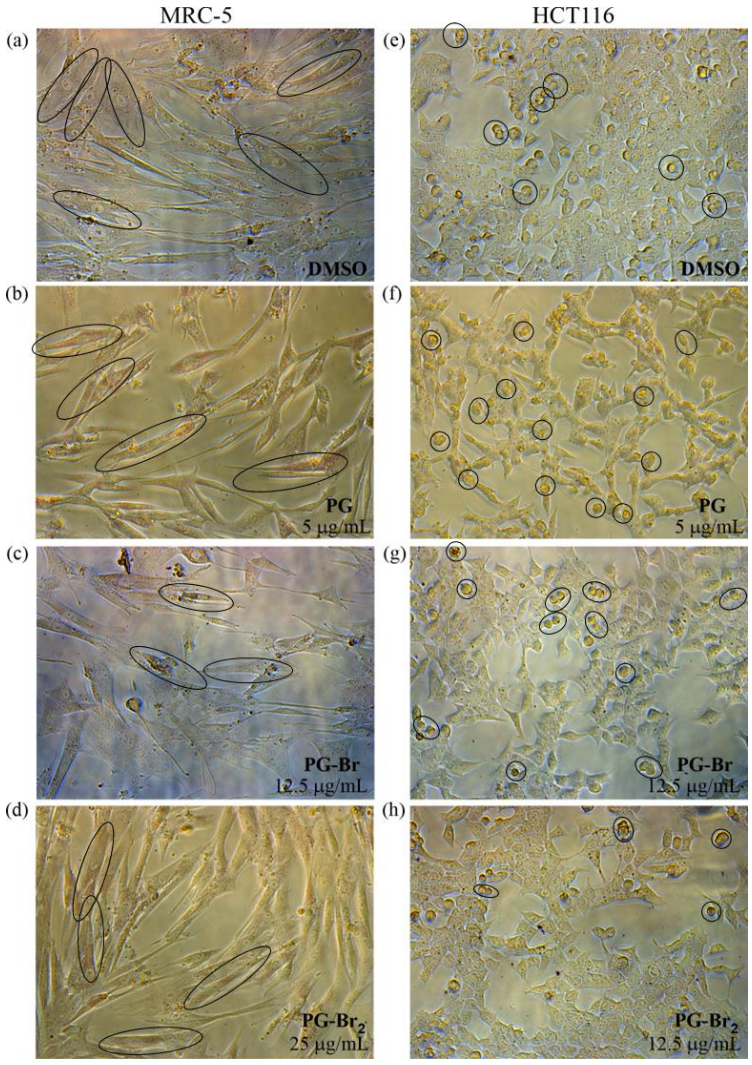

Figure 31.[n] (a-d) MRC-5 cells; (e-h) HCT116 cells, after 24 h treatment with PG and its Br-derivatives were observed under a microscope (20× magnification).

[n] This figure is part of the manuscript accepted in the MDPI Molecules journal, see **Chapter 4. Results and discussion** for more details on the manuscript.

Anticancer mode of action for PG has been investigated in several studies, where a high potential of PG for the induction of apoptosis in different cell types was noticed.[53] We set out next to find out if this mechanism of action is retained in the novel Br-derivatives of PG. Flow cytometry and Annexin V staining were previously used to demonstrate that PG could induce apoptosis of HeLa cells in a dose- and time-associated manner.[125] In this study, fluorescence-activated cell sorting (FACS) flow cytometric analysis of apoptotic markers in MRC-5 cells confirmed the induction of apoptosis triggered by PG and both Br-derivatives (Table 12).

Table 12. Early apoptosis induction in MRC-5 cell line by IC_{50} concentrations of PG, PG-Br and PG-Br_2. Results were analysed using ANOVA test and post-hoc Fisher's LSD test, $p \leq 0.05$ was considered statistically significant.

Annexin V positive cells	**PG**	**PG-Br**	**PG-Br_2**
(%)	20.3 ± 0.5	21.3 ± 0.8	19.6 ± 0.6

Since the emission wavelength of prodigiosin (535 nm) was close to that of propidium iodide (PI), only the levels of early apoptosis were detected using Annexin V and the percentage of necrotic PI positive cells was not evaluated.

Exposure of MRC-5 cells to IC_{50} values of PG and both Br-derivatives resulted in a comparable level of increase of early Annexin V positive cells (Table 12) compared to the nontreated control, but the compounds did not significantly differ among each other, thus suggesting that mono- and dibromination have not impaired the apoptotic potential of PG.

The anticancer potential of Br-derivatives was not significantly improved compared to PG, but these are important preliminary findings are required for further structural optimisations of bacterial PGs. Since two Br-derivatives of PG were obtained for the first time, and having in mind that toxicity and safety assessment of PGs are not readily available in the literature, we proceeded with *in vivo* experiments and tested the parent PG and its novel derivatives on two different model systems.

4.10. Toxicity evaluation of prodigiosin and its Br-derivatives

4.10.1. *C. elegans* model system

The nematode *C. elegans* is a model system which can be used in anticancer drug discovery for toxicity and safety assessment, as well as pharmacogenetics studies, among others.[55] The *C. elegans* genome possesses homologs of about two-thirds of all human disease genes; of its 959 somatic cells, 302 are neurons identifiable by lineage, location, morphology, and neurochemistry in every adult hermaphrodite, and 75 of those are motoneurons, divided by their morphology into 6 excitatory cholinergic and 2 inhibitory GABAergic classes which innervate body wall muscles that provide the thrust during locomotion.[126] *C. elegans* swim using a stereotyped, rhythmic, oscillating body motion, so the motility is a direct readout of the neuromuscular system and an indirect assay of the health of the animal.[127]

PG and its two novel Br-derivatives exhibited a 100% survival rate of *C. elegans* at the highest tested concentration of 50 µg/mL (Table 13). In line with our findings, a report on toxicological assessment of PG obtained from *S. marcescens* in *C. elegans* showed no significant toxic activity[128], which suggested the safe use of PG in eukaryotic system.

Table 13. Influence of PG and its novel Br-derivatives on the survival rate of juvenile *C. elegans*.

Concentration (µg/mL)	**Survival rate (%)**		
	PG	**PG-Br**	**PG-Br_2**
50.00	100 ± 0.00	100 ± 0.00	100 ± 0.00
25.00	100 ± 0.00	100 ± 0.00	100 ± 0.00
12.50	100 ± 0.00	100 ± 0.00	100 ± 0.00
6.25	100 ± 0.00	100 ± 0.00	100 ± 0.00
3.13	100 ± 0.00	100 ± 0.00	100 ± 0.00
1.57	100 ± 0.00	100 ± 0.00	100 ± 0.00

It was, however, observed under the microscope (Fig. 32) that the motility of nematodes treated with PG-Br_2 was impaired at all tested concentrations. Impairment of the neurotransmission of γ-aminobutyric acid (GABA) was shown to induce lower

undulation frequency in *C. elegans* and lower translocation speed during crawling and swimming in both directions.[129] The firing of action potentials in GABAergic synaptic transmission is driven by voltage gated Ca^{2+}- and K^{+}-channels[130], and it is possible that the bulky PG-Br_2 blocks these channels, thus inhibiting action potentials and *C. elegans* body wall muscle contraction and relaxation.

C. elegans motility is a complex behaviour comprised of numerous networks and elucidating the effect that PG-Br_2 exhibits would have to be determined with further experiments. Recently, it was also shown that high-dose irradiation can inhibit motility by accumulating abnormal proteins and organelles, such as mitochondria, which inhibits movement and induces autophagy.[131]

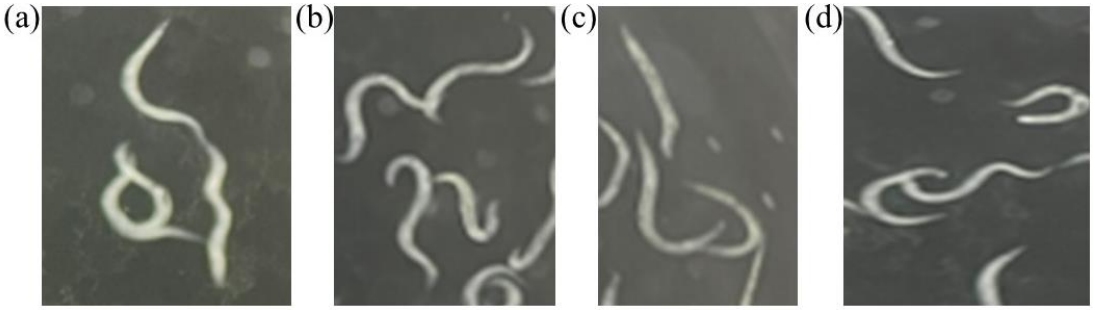

Figure 32.[o] *In vivo* toxicity of PG and Br-derivatives using *C. elegans* model system. Nematodes were treated with 50 µg/mL of: (a) PG; (b) PG-Br; (c) PG-Br_2; (d) DMSO and observed under a microscope (40× magnification).

Furthermore, PG and its five derivatives, [one with an unsaturated hydroxylated chain on the C ring of PG, and four with various cyclic alkyl substituents (C_4, C_5, C_6 and C_{10}) on the C ring], were tested against the *C. elegans* first stage juveniles[38], and the structures of the derivatives determined their activities, with PG exhibiting the highest activity with an EC_{50} value of 0.04 µg/mL. For the synthetic derivatives of PG, no reliable EC_{50} could be determined, as the mortality at the highest tested concentration did not exceed 33%. These findings, similar to ours, suggest that some synthetic PG derivatives may not prove to be toxic towards *C. elegans*.

[o] This figure is part of the manuscript accepted in the MDPI Molecules journal, see **Chapter 4. Results and discussion** for more details on the manuscript.

On the other hand, the nematocidal activity of PG was reported for juvenile *Meloidogyne incognita* J2 species, harmful on black pepper, with an IC_{50} value of 0.2 mg/mL[59], for juveniles of *Radopholus similis* with the LC_{50} value of 83 µg/mL and *Meloidogyne javanica* with the LC_{50} of 79 µg/mL, also exhibiting an antagonistic effect on the nematode egg-hatching ability.[132] Effectiveness of PG against *Heterodera schachtii* J2 was found to be 4.30 µg/mL.[38] Notably, these values are comparable to or higher than cytotoxic IC_{50} values (Table 11), which may hinder direct PG application in the agriculture, but leaves the possibility to use whole-cell bacteria to improve PG stability under agricultural conditions.[14]

4.10.2. *D. rerio* model system

Zebrafish (*Danio rerio*) are commonly used in anticancer drug screens for toxicity assessment (cardiotoxicity, hepatotoxicity…) in eucaryotic systems.[56, 57] Therefore, PG, PG-Br and PG-Br_2 were assessed for their *in vivo* toxicity on the vertebrate zebrafish model (Fig. 33 and Fig. 34) and the results were analysed using ANOVA test and post-hoc Fisher's LSD test, where $p \leq 0.05$ was considered statistically significant. Synthetic derivatives of PG have been tested for their activity on fluorescently labelled leukaemia cells *in vivo* on mutant *casper* zebrafish which lack all pigmentation[133], but the embryotoxicity of PG has not been determined in this model system so far.

Compounds were applied at 6 and 20 h post fertilisation (hpf), for better insights on the embryotoxicity (Fig. 33). Indeed, upon application of 10 µg/mL at 6 hpf, the death rate was 100, 30 and 0% for PG, PG-Br and PG-Br_2, respectively (Fig. 33), which is a statistically significant result ($p < 0.001$). At 10 µg/mL, 60% teratogenicity was noticed only in zebrafish treated with PG-Br.

Applying compounds at 10 µg/mL at the 20 hpf, when embryos were in later stages of the development, resulted in a teratogenicity of 100, 10 and 0% for PG, PG-Br and PG-Br_2, respectively (Fig. 33) which is a statistically significant result ($p < 0.001$), again showing PG as the most toxic. At 10 µg/mL, lethality was only noticed in zebrafish treated with PG-Br. Nevertheless, under both test conditions, PG-Br_2 was found to have the most favourable cytotoxicity profile (Fig. 33).

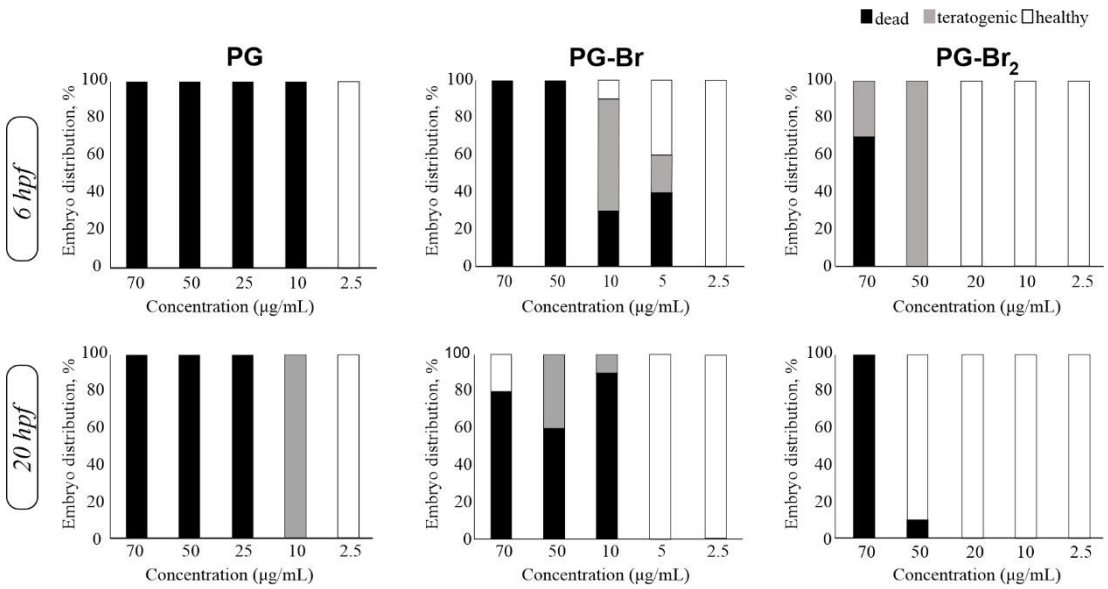

Figure 33.[p] Effects on the development of zebrafish embryos treated with different concentrations of PG, PG-Br and PG-Br_2 at: (a) 6 hpf; (b) 20 hpf, represented as a distribution of dead (black), teratogenic (grey) and healthy (white) embryos. Results were analysed using ANOVA test and post-hoc Fisher's LSD test, $p \leq 0.05$ was considered statistically significant.

When PG concentrations of 2.5 µg/mL were used at 6 hpf, all the embryos survived, but developed into slightly smaller fish with microcephaly (Fig. 34a). At this concentration, neither of the Br-derivatives caused detrimental effects (Fig. 33a). A treatment with a higher concentration of 5 µg/mL PG, both 6 and 20 hpf, caused the embryos to uptake the biopigment and stopped the further development (Fig. 34a and 34b).

When PG-Br at 5 µg/mL was applied at 6 hpf, it affected 60% of embryos (Fig. 33a) with 20% showing teratogenicity (Fig. 34a), while this concentration had no effect when applied at 20 hpf (Fig. 33 and Fig. 34b). At 10 µg/mL, cardiotoxicity was noticed at 6 hpf (Fig. 34a) and hepatotoxicity at 20 hpf (Fig. 34b). However, at high concentrations of 50 µg/mL PG-Br, there was evident uptake of the biopigment inside embryos 6 hpf (Fig. 34a), and teratogenic effects including hepatotoxicity as well as cardiotoxicity were noticed in zebrafish 20 hpf (Fig. 34b).

[p] This figure is part of the manuscript accepted in the MDPI Molecules journal, see **Chapter 4. Results and discussion** for more details on the manuscript.

PG-Br_2 was the least toxic with the 100% embryos survival rate 6 hpf and 20 hpf at concentrations up to 20 µg/mL, without any teratogenic effects (Fig. 33 and Fig. 34). This concentration is 2-fold higher in comparison to IC_{50} values against healthy MRC-5 cells after 48 h and the prolonged exposure of 72 h (Table 11), indicating that further structural optimisations in terms of halogenation may prove beneficial. Nonetheless, at a higher tested concentration of 50–70 µg/mL of PG-Br_2 there is evidence of severe toxicity and lethality at both 6 and 20 hpf (Fig. 33). An abnormal development was noticed upon 50 µg/mL of PG-Br_2 application at 6 hpf (Fig. 34a).

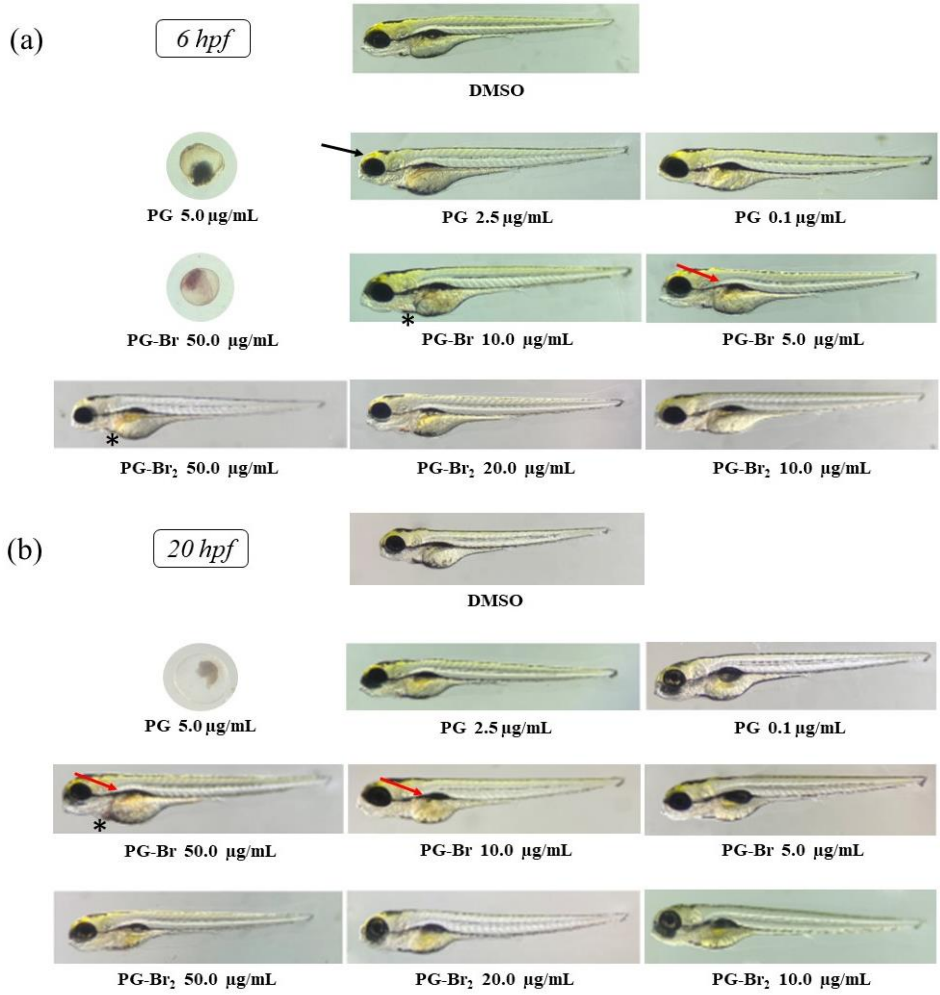

Figure 34.[q] Zebrafish developed from the embryos: (a) 6 hpf; (b) 20 hpf, treated with the tested compounds and compared to the DMSO treated control were observed under a microscope (3.5× magnification). Black arrow (→) points to a smaller head, red arrow (→) points to abnormal liver and asterisk (*) denotes abnormal heart.

[q] This figure is part of the manuscript accepted in the MDPI Molecules journal, see **Chapter 4. Results and discussion** for more details on the manuscript.

5. Conclusions

Moderate yields, unavailability of producing strains, and high cost of extraction and purification still represent the bottleneck in the microbial production of PG. In this study, using meat-based waste stream as a nutrient source in a batch fermentation resulted in the production of PG in a good yield of 83.1 ± 3.0 mg/L from a commercially available bacterial strain *S. marcescens* ATCC 27117. Using food industry waste as a source of both carbon and nitrogen, and incorporating it into the biotechnological process of PG production is the major achievement of this work. Establishing reliable extraction and purification procedures for obtaining highly pure PG from bacterial fermentation are other significant contributions of this work.

PG was used in the enzymatic bromination and chlorination reactions using haloperoxidase enzymes *Am*VHPO I wt and two mutants *Am*VHPO I Arg425Ser and Arg425Lys, but it was not biotransformed, suggesting that an optimisation of the biocatalytic reaction conditions is necessary. On the other side, simple one-step oxidative chemical halogenation reactions under mild conditions have been successfully established. By using late-stage functionalisation strategies and changing the reaction conditions (solvent, temperature, oxidising agent), mono- and dibrominated PGs have been obtained and characterised for the first time. Obtaining natural product analogues through semi-synthesis, using the natural product PG as a starting material, is another achieved milestone. Synthesising halogenated derivatives of PG has not been investigated so far, especially not in the context of the late-stage functionalisation. The developed methodology of installing halogen substituents by electrophilic aromatic substitution (EAS) under environmentally acceptable conditions could be applied to other natural products from the family of prodigiosins (*e.g.*, undecylprodigiosin, streptorubin B…) and even to other structurally different natural products, which could contribute to their structural optimisation.

The physiological role of PG in the producing microorganisms is not fully understood, but it shows numerous biological activities in other organisms. PG and its Br-derivatives did not have any antimicrobial activity neither against four tested bacterial strains (*S. aureus* ATCC 25923, *M. luteus* ATCC 379, *L. monocytogenes* NCTC 11994, *P. aeruginosa* PAO1 NCTC 10332), nor against four fungal strains

(*C. albicans* ATCC 10231, *C. glabrata* ATCC 2001, *C. krusei* ATCC 6258, *C. parapsilosis* ATCC 22019), indicating that the evolution has guided PG bioactivity against environmental and not human clinical pathogens.

The anticancer activity of PG and its Br-derivatives has been studied next, and pure bacterial PG exhibited excellent anticancer activity against four tested carcinoma cell lines (A549, A375, MDA-MB-231, HCT116). However, it was also highly toxic against healthy cells (MRC-5 and HaCaT). This could be one of the reasons that the natural PG has not reached clinical practice (neither as an antimicrobial agent nor as an anticancer agent), suggesting the need for derivatives with lower cytotoxicity and improved selectivity. Both PG-Br and PG-Br_2 showed lower cytotoxicity in comparison to PG, however, the introduction of bromine(s) did not improve selectivity between cancer and healthy cell lines in the initial assessment. Overall, IC_{50} values for both Br-derivatives were still considerably high, and the novel compounds retained anticancer potential. Flow cytometric analysis of apoptotic markers in MRC-5 cells revealed that the potential for the induction of apoptosis was comparable in PG and its novel Br-derivatives, indicating this mode of action was attained in the novel compounds.

Finally, PG and its Br-derivatives were assessed in terms of their *in vivo* toxicity on two model systems (*C. elegans* and *D. rerio*), further adding to the knowledge regarding the safety of these promising drug leads. All compounds did not affect *C. elegans* survival at concentrations up to 50 μg/mL. Still, more favourable toxicity profiles of Br-derivatives in comparison to the parent PG were observed *in vivo* using zebrafish model system, when 10 μg/mL applied at 6 h post fertilisation caused death rates of 100, 30 and 0% by PG, PG-Br and PG-Br_2, respectively. This is another significant finding for further structural optimisations of bacterial PGs.

6. References

1. Cragg, G. M.; Pezzuto, J. M., Natural products as a vital source for the discovery of cancer chemotherapeutic and chemopreventive agents. *Med. Princ. Pract.* **2016,** *25*, 41-59.
2. Huang, M.; Lu, J. J.; Ding, J., Natural products in cancer therapy: past, present and future. *Nat. Prod. Bioprospect.* **2021,** *11*, 5-13.
3. Atanasov, A. G.; Zotchev, S. B.; Dirsch, V. M.; Supuran, C. T., Natural products in drug discovery: advances and opportunities. *Nat. Rev. Drug Discov.* **2021,** *20*, 200-216.
4. Cragg, G. M.; Newman, D. J.; Snader, K. M., Natural products in drug discovery and development. *J. Nat. Prod.* **1997,** *60* (1), 52-60.
5. Newman, D. J.; Cragg, G. M.; Snader, K. M., Natural products as sources of new drugs over the period 1981-2002. *J. Nat. Prod.* **2003,** *66*, 1022-1037.
6. Newman, D. J.; Cragg, G. M., Natural products as sources of new drugs over the last 25 years. *J. Nat. Prod.* **2007,** *70*, 461-477.
7. Newman, D. J.; Cragg, G. M., Natural products as sources of new drugs over the 30 years from 1981 to 2010. *J. Nat. Prod.* **2012,** *75*, 311-335.
8. Newman, D. J.; Cragg, G. M., Natural products as sources of new drugs from 1981 to 2014. *J. Nat. Prod.* **2016,** *79*, 629-661.
9. Newman, D. J.; Cragg, G. M., Natural products as sources of new drugs over the nearly four decades from 01/1981 to 09/2019. *J. Nat. Prod.* **2020,** *83* (3), 770-803.
10. Williamson, N. R.; Fineran, P. C.; Leeper, F. J.; Salmond, G. P. C., The biosynthesis and regulation of bacterial prodiginines. *Nat. Rev. Microbiol.* **2006,** *4*, 887-899.
11. Bennett, J. W.; Bentley, R., Seeing red: The story of prodigiosin. *Adv. Appl. Microbiol.* **2000,** *47*, 1-32.
12. Williamson, N. R.; Fineran, P. C.; Gristwood, T.; Chawrai, S.; Leeper, F. J.; Salmond, G. P. C., Anticancer and immunosuppressive properties of bacterial prodiginines. *Future Microbiol.* **2007,** *2* (6), 605-618.
13. Klein, A. S.; Brass, H. U. C.; Klebl, D. P.; Classen, T.; Loeschcke, A.; Drepper, T.; Sievers, S.; Jaeger, K.-E.; Pietruszka, J. r., Preparation of cyclic prodiginines

by mutasynthesis in *Pseudomonas putida* KT2440. *ChemBioChem* **2018,** *19* (14), 1545.1552.

14. Stankovic, N.; Senerovic, L.; Ilic-Tomic, T.; Vasiljevic, B.; Nikodinovic-Runic, J., Properties and applications of undecylprodigiosin and other bacterial prodigiosins. *Appl. Microbiol. Biotechnol.* **2014,** *98*, 3841-3858.
15. Rapoport, H.; Willson, C. D., The preparation and properties of some methoxypyrroles. *J. Am. Chem. Soc.* **1962,** *84* (4), 630-635.
16. Darshan, N.; Manonmani, H. K., Prodigiosin and its potential applications. *J. Food Sci. Technol.* **2015,** *52* (9), 5393-5407.
17. Rizzo, V.; Morelli, A.; Pinciroli, V.; Sciangula, D.; D-Alessio, R., Equilibrium and kinetics of rotamer interconversion in immunosuppressant prodigiosin derivatives in solution. *J. Pharm. Sci.* **1999,** *88* (1), 72-78.
18. Khayyat, A. N.; Hegazy, W. A. H.; Shaldam, M. A.; Mosbah, R.; Almalki, A. J.; Ibrahim, T. S.; Khayat, M. T.; Khafagy, E.-S.; Soliman, W. E.; Abbas, H. A., Xylitol inhibits growth and blocks virulence in S*erratia marcescens*. *Microorganisms* **2021,** *9* (5), 1083-1096.
19. Araújo, H. W. C. d.; Fukushima, K.; Takaki, G. M. C., Prodigiosin production by *Serratia marcescens* UCP 1549 using renewable-resources as a low cost substrate. *Molecules* **2010,** *15*, 6931-6940.
20. Su, W.-T.; Tsou, T.-Y.; Liu, H.-L., Response surface optimization of microbial prodigiosin production from *Serratia marcescens*. *J. Taiwan Inst. Chem. Eng.* **2011,** *42*, 217-222.
21. Soenens, A.; Imperial, J., Biocontrol capabilities of the genus *Serratia*. *Phytochem. Rev.* **2020,** *19*, 577-587.
22. Danevčič, T.; Borić Vezjak, M.; Tabor, M.; Zorec, M.; Stopar, D., Prodigiosin induces autolysinsin actively grown *Bacillus subtilis* cells. *Front. Microbiol.* **2016,** *7*, Article 27.
23. Stankovic, N.; Radulovic, V.; Petkovic, M.; Vuckovic, I.; Jadranin, M.; Vasiljevic, B.; Nikodinovic-Runic, J., *Streptomyces* sp. JS520 produces exceptionally high quantities of undecylprodigiosin with antibacterial, antioxidative, and UV-protective properties. *Appl. Microbiol. Biotechnol.* **2012,** *96*, 1217-1231.
24. Morrison, D. A., Prodigiosin synthesis in mutants of *Serratia marcesens*. *J. Bacteriol.* **1966,** *91* (4), 1599-1604.

25. Sakai-Kawada, F. E.; Ip, C. G.; Hagiwara, K. A.; Awaya, J. D., Biosynthesis and bioactivity of prodiginine analogs in marine bacteria, *Pseudoalteromonas*: a mini review. *Front. Microbiol.* **2019,** *10*, 1-9.
26. Paul, T.; Bandyopadhyay, T. K.; Mondal, A.; Tiwari, O. N.; Muthuraj, M.; Bhunia, B., A comprehensive review on recent trends in production, purification, and applications of prodigiosin. *Biomass Conv. Bioref.* **2020**, 1-23.
27. Hu, D. X.; Withall, D. M.; Challis, G. L.; Thomson, R. J., Structure, chemical synthesis, and biosynthesis of prodiginine natural products. *Chemical Rev.* **2016,** *116*, 7818-7853.
28. Williamson, N. R.; Simonsen, H. T.; Ahmed, R. A. A.; Goldet, G.; Slater, H.; Woodley, L.; Leeper, F. J.; Salmond, G. P. C., Biosynthesis of the red antibiotic, prodigiosin, in *Serratia*: identification of a novel 2-methyl-3-n-amylpyrrole (MAP) assembly pathway, definition of the terminal condensing enzyme, and implications for undecylprodigiosin biosynthesis in *Streptomyces*. *Mol. Microbiol.* **2005,** *56* (4), 971-989.
29. Klein, A. S.; Domröse, A.; Bongen, P.; Brass, H. U. C.; Classen, T.; Loeschcke, A.; Drepper, T.; Laraia, L.; Sievers, S.; Jaeger, K.-E.; Pietruszka, J. r., New prodigiosin derivatives obtained by mutasynthesis in *Pseudomonas putida*. *ACS Synth. Biol.* **2017,** *6*, 1757-1765.
30. Han, R.; Xiang, R.; Li, J.; Wang, F.; Wang, C., High-level production of microbial prodigiosin: A review. *J. Basic Microbiol.* **2021,** *61* (6), 506-523.
31. Papireddy, K.; Smilkstein, M.; Xu, J.; Shweta, K.; Salem, S. M.; Alhamadsheh, M.; Haynes, S. W.; Challis, G. L.; Reynolds, K. A., Antimalarial activity of natural and synthetic prodiginines. *J. Med. Chem.* **2011,** *54* (15), 5296-5306.
32. Herráez, R.; Quesada, R.; Dahdah, N.; Viñas, M.; Vinuesa, T., Tambjamines and prodiginines: biocidal activity against *Trypanosoma cruzi*. *Pharmaceutics* **2021,** *13* (5), 705-718.
33. Han, S. B.; Park, S. H.; Jeon, Y. J.; Kim, Y. K.; Kim, H. M.; Yang, K. H., Prodigiosin blocks T cell activation by inhibiting interleukin-2Rα expression and delays progression of autoimmune diabetes and collagen-induced arthritis. *J. Pharmacol. Exp. Ther.* **2001,** *299* (2), 415-425.
34. Arivizhivendhan, K. V.; Mahesh, M.; Boopathy, R.; Swarnalatha, S.; Mary, R. R.; Sekaran, G., Antioxidant and antimicrobial activity of bioactive prodigiosin

produces from *Serratia marcescens* using agricultural waste as a substrate. *J. Food Sci. Technol.* **2018,** *55* (7), 2661-2670.

35. Borić, M.; Danevčič, T.; Stopar, D., Prodigiosin from *Vibrio* sp. DSM 14379; a new UV-protective pigment. *Microb. Ecol.* **2011,** *62*, 528-536.
36. Yip, C.-H.; Mahalingam, S.; Wan, K.-L.; Nathan, S., Prodigiosin inhibits bacterial growth and virulence factors as a potential physiological response to interspecies competition. *PLoS ONE* **2021,** *16* (6), e0253445.
37. Suryawanshi, R. K.; Patil, C. D.; Koli, S. H.; Hallsworth, J. E.; Patil, S. V., Antimicrobial activity of prodigiosin is attributable to plasma-membrane damage. *Nat. Prod. Res.* **2016,** *31* (5), 572-577.
38. Habash, S. S.; Brass, H. U. C.; Klein, A. S.; Klebl, D. P.; Weber, T. M.; Classen, T.; Pietruszka, J. r.; Grundler, F. M. W.; Schleker, A. S. S., Novel prodiginine derivatives demonstrate bioactivities on plants, nematodes, and fungi. *Front. Plant Sci.* **2020,** *11*, article 579807.
39. Someya, N.; Nakajimai, M.; Hirayae, K.; Hibi, T.; Akutsu, K., Synergistic antifungal activity of chitinolytic enzymes and prodigiosin produced by biocontrol bacterium, *Serratia marcescens* strain B2 against gray mold Pathogen, *Botrytis cinerea*. *J. Gen. Plant Pathol.* **2001,** *67*, 312-317.
40. Amorim, L. F. A.; Mouro, C.; Riool, M.; Gouveia, I. C., Antimicrobial food packaging based on prodigiosin-incorporated double-layered bacterial cellulose and chitosan composites. *Polymers* **2022,** *14* (2), 315-332.
41. Zhang, J.; Shen, Y.; Liu, J.; Wei, D., Antimetastatic effect of prodigiosin through inhibition of tumor invasion. *Biochem. Pharmacol.* **2005,** *69*, 407-414.
42. Elahian, F.; Moghimi, B.; Dinmohammadi, F.; Ghamghami, M.; Hamidi, M.; Mirzaei, S. A., The anticancer agent prodigiosin is not a multidrug resistance protein substrate. *DNA Cell Biol.* **2013,** *32* (3), 90-97.
43. Wang, Z.; Li, B.; Zhou, L.; Yu, S.; Su, Z.; Song, J.; Sun, Q.; Sha, O.; Wang, X.; Jiang, W.; Willert, K.; Wei, L.; Carson, D. A.; Lu, D., Prodigiosin inhibits Wnt/β-catenin signaling and exerts anticancer activity in breast cancer cells. *PNAS USA* **2016,** *113* (46), 13150-13155.
44. Anwar, M. M.; Shalaby, M.; Embaby, A. M.; Saeed, H.; Agwa, M. M.; Hussein, A., Prodigiosin/PU-H71 as a novel potential combined therapy for triple negative breast cancer (TNBC): preclinical insights. *Sci. Rep.* **2020,** *10*, article 14706.

45. Cheng, S. Y.; Chen, N. F.; Kuo, H. M.; Yang, S. N.; Sung, C. S.; Sung, P. J.; Wen, Z. H.; Chen, W. F., Prodigiosin stimulates endoplasmic reticulum stress and induces autophagic cell death in glioblastoma cells. *Apoptosis* **2018,** *23* (5), 314-328.
46. Llagostera, E.; Soto-Cerrato, V.; Joshi, R.; Montaner, B.; Gimenez-Bonafé, P.; Pérez-Tomàs, R., High cytotoxic sensitivity of the human small cell lung doxorubicin-resistant carcinoma (GLC4/ADR) cell line to prodigiosin through apoptosis activation. *Anticancer drugs* **2005,** *16*, 393-399.
47. Campàs, C.; Dalmau, M.; Montaner, B.; Barragán, M.; Bellosillo, B.; Colomer, D.; Pons, G.; Pérez-Tomás, R.; Gil, J., Prodigiosin induces apoptosis of B and T cells from B-cell chronic lymphocytic leukemia. *Leukemia* **2003,** *17*, 746-750.
48. Yenkejeh, R. A.; Sam, M. R.; Esmaeillou, M., Targeting survivin with prodigiosin isolated from cell wall of *Serratia marcescens* induces apoptosis in hepatocellular carcinoma cells. *Hum. Exp. Toxicol.* **2017,** *36*, 402-411.
49. Dalili, D.; Fouladdel, S.; Rastkari, N.; Samadi, N.; Ahmadkhaniha, R.; Ardavan, A.; Azizi, E., Prodigiosin, the red pigment of *Serratia marcescens*, shows cytotoxic effects and apoptosis induction in HT-29 and T47D cancer cell lines. *Nat. Prod. Res.* **2011,** *26*, 2078-2083.
50. Hosseini, A.; Espona-Fiedler, M.; Soto-Cerrato, V.; Quesada, R.; Pérez-Tomás, R.; Guallar, V., Molecular interactions of prodiginines with the BH3 domain of anti-apoptotic Bcl-2 family members. *PLOS ONE* **2013,** *8* (2), e57562.
51. Soto-Cerrato, V.; Llagostera, E.; Montaner, B.; Scheffer, G. L.; Pérez-Tomás, R., Mitochondria-mediated apoptosis operating irrespective of multidrug resistance in breast cancer cells by the anticancer agent prodigiosin. *Biochem. Pharmacol.* **2004,** *68*, 1345-1352.
52. Hong, B.; Prabhu, V. V.; Zhang, S.; van den Heuvel, A. P. J.; Dicker, D. T.; Kopelovich, L.; El-Deiry, W. S., Prodigiosin rescues deficient p53 signaling and antitumor effects *via* upregulating p73 and disrupting its interaction with mutant p53. *Cancer Res.* **2014,** *74*, 1153-1165.
53. Lin, S.-R.; Chen, Y.-H.; Tseng, F.-J.; Weng, C.-F., The production and bioactivity of prodigiosin: *quo vadis*? *Drug Discov. Today* **2020,** *25* (5), 828-836.
54. Kobet, R. A.; Pan, X.; Zhang, B.; Pak, S. C.; Asch, A. S.; Lee, M.-H., *Caenorhabditis elegans*: A model system for anti-cancer drug discovery and therapeutic target identification. *Biomol. Ther.* **2014,** *22* (5), 371-383.

55. Ye, F. B.; Hamza, A.; Singh, T.; Flibotte, S.; Hieter, P.; O'Neil, N. J., A multimodal genotoxic anticancer drug characterized by pharmacogenetic analysis in *Caenorhabditis elegans*. *Genetics* **2020,** *215*, 609-621.
56. Nathan, J.; Kannan, R. R., Antiangiogenic molecules from marine actinomycetes and the importance of using zebrafish model in cancer research. *Heliyon* **2020,** *6*(12), e05662.
57. Teame, T.; Zhang, Z.; Ran, C.; Zhang, H.; Yang, Y.; Ding, Q.; Xie, M.; Gao, C.; Ye, Y.; Duan, M.; Zhou, Z., The use of zebrafish (Danio rerio) as biomedical models. *Anim Front* **2019,** *9* (3), 68-77.
58. Dairi, K.; Tripathy, S.; Attardo, G.; Lavalleé, J.-F., Two-step synthesis of the bipyrrole precursor of prodigiosins. *Tetrahedron Lett.* **2006,** *47*, 2605-2606.
59. Nguyen, T. H.; Wang, S.-L.; Doan, M. D.; Nguyen, T. H.; Tran, T. H. T.; Tran, T. N.; Doan, C. T.; Ngo, V. A.; Ho, N. D.; Do, V. C.; Nguyen, A. D.; Nguyen, V. B., Utilization of by-product of groundnut oil processing for production of prodigiosin by microbial fermentation and its novel potent anti-nematodes effect. *Agronomy* **2022,** *12* (1), 41-66.
60. Nguyen, V. B.; Wang, S.-L.; Nguyen, A. D.; Phan, T. Q.; Techato, K.; Pradit, S., Bioproduction of prodigiosin from fishery processing waste shrimp heads and evaluation of its potential bioactivities. *Fishes* **2021,** *6* (3), 30-47.
61. Nguyen, T.-H.; Wang, S.-L.; Nguyen, D.-N.; Nguyen, A.-D.; Nguyen, T.-H.; Doan, M.-D.; Ngo, V.-A.; Doan, C.-T.; Kuo, Y.-H.; Nguyen, V.-B., Bioprocessing of marine chitinous wastes for the production of bioactive prodigiosin. *Molecules* **2021,** *26* (11), 3138-3151.
62. Jiang, S.; Zhang, L.; Cui, D.; Yao, Z.; Gao, B.; Lin, J.; Wei, D., The important role of halogen bond in substrate selectivity of enzymatic catalysis. *Sci. Rep.* **2016,** *6*, 34750-34756.
63. Fejzagić, A. V.; Gebauer, J.; Huwa, N.; Classen, T., Halogenating enzymes for active agent synthesis: First steps are done and many have to follow. *Molecules* **2019,** *24* (21), 4008-4041.
64. Kosjek, T.; Heath, E., *Halogenated Heterocycles as Pharmaceuticals*. Springer-Verlag Berlin Heidelberg: **2012**; Vol. 27.
65. Leong, S. W.; Chia, S. L.; Abas, F.; Yuso, K., In-vitro and in-silico evaluations of heterocyclic-containing diarylpentanoids as Bcl-2 inhibitors against LoVo colorectal cancer cells. *Molecules* **2020,** *25* (17), 3877-3892.

66. Fürstner, A., Chemistry and biology of roseophilin and the prodigiosin alkaloids: A survey of the last 2500 years. *Angew. Chem. Int. Ed.* **2003,** *42* (31), 3582-3603.
67. van Pée, K.-H., *Biosynthesis of Halogenated Alkaloids*. Elsevier Inc.: **2012**; Vol. 71.
68. Laus, G., *Biological activities of natural halogen compounds*. Elsevier B.V. : **2001**; Vol. 25 (Part F).
69. Hong, B.; Luo, T.; Lei, X., Late-stage diversification of natural products. *ACS Cent. Sci.* **2020,** *6* (5), 622-635.
70. Wagner, C.; El Omari, M.; König, G. M., Biohalogenation: Nature's way to synthesize halogenated metabolites. *J. Nat. Prod.* **2009,** *72*, 540-553.
71. Lang, A.; Polnick, S.; Nicke, T.; William, P.; Patallo, E. P.; Naismith, J. H.; van Pée, K.-H., Changing the regioselectivity of the Tryptophan 7-halogenase PrnA by site-directed mutagenesis. *Angew. Chem. Int. Ed.* **2011,** *50*, 2951-2953.
72. Vaillancourt, F. H.; Yeh, E.; Vosburg, D. A.; Garneau-Tsodikova, S.; Walsh, C. T., Nature's inventory of halogenation catalysts: oxidative strategies predominate. *Chem. Rev.* **2006,** *106*, 3364-3378.
73. Butler, A.; Sandy, M., Mechanistic considerations of halogenating enzymes. *Nature* **2009,** *460*, 848-854.
74. Weichold, V.; Milbredt, D.; van Pée, K.-H., Specific enzymatic halogenation - from the discovery of halogenated enzymes to their applications in vitro and in vivo. *Angew. Chem. Int. Ed.* **2016,** *55* (22), 6374-6389.
75. Frank, A.; Seel, C. J.; Groll, M.; Gulder, T., Characterization of a cyanobacterial haloperoxidase and evaluation of its biocatalytic halogenation potential. *ChemBioChem* **2016,** *17*, 2028-2032.
76. Jia, Y.; Xu, L.; Yin, B.; Zhou, M.; Song, J., Synthesis and characterization of *meso*-to-*meso* directly linked porphyrin-diazaporphyrin triads. *J. Porphyr. Phthalocyanines* **2018,** *22*, 1-7.
77. Pati, P. B.; Zade, S. S., Selective bromination of 2,5-bis(2-thienyl)pyrroles and solid-state polymerization through the β-carbon of pyrrole. *RSC Adv.* **2014,** *4*, 17022-17027.
78. Yip, C.-H.; Yarkoni, O.; Ajioka, J.; Wan, K.-L.; Nathan, S., Recent advancements in high-level synthesis of the promising clinical drug, prodigiosin. *Appl. Microbiol. Biotechnol.* **2019,** *103* (4), 1667-1680.

79. El-Bialy, H. A.; El-Nour, S. A. A., Physical and chemical stress on *Serratia marcescens* and studies on prodigiosin pigment production. *Ann. Microbiol.* **2015,** *65*, 59-68.
80. Kajorinne, J. K.; Steers, J. C. M.; Merchant, M. E.; MacKinnon, C. D., Green halogenation reactions for (hetero)aromatic ring systems in alcohol, water, or no solvent. *Can. J. Chem.* **2018,** *96* (12), 1087-1091.
81. Podgoršek, A.; Zupan, M.; Iskra, J., Oxidative halogenation with "green" oxidants: oxygen and hydrogen peroxide. *Angew. Chem. Int. Ed.* **2009,** *48*, 8424-8450.
82. Dinesh, C. U.; Kumar, R.; Pandey, B.; Kumar, P., Catalytic halogenation of selected organic compounds mimicking vanadate-dependent marine metalloenzymes. *J. Chem. Soc. Chem. Commun.* **1995,** *0*, 611-612.
83. Song, S.; Sun, X.; Li, X.; Yuan, Y.; Jiao, N., Efficient and practical oxidative bromination and iodination of arenes and heteroarenes with DMSO and hydrogen halide: A mild protocol for late-stage functionalization. *Org. Lett.* **2015,** *17*, 2886-2889.
84. Kandepi, V. V. K. M.; Narender, N., Ecofriendly oxidative nuclear halogenation of aromatic compounds using potassium and ammonium halides. *Synthesis* **2012,** *44*, 15-26.
85. Chen, W.-C.; Yu, W.-J.; Chang, C.-C.; Chang, J.-S.; Huang, S.-H.; Chang, C.-H.; Chen, S.-Y.; Chien, C.-C.; Yao, C.-L.; Chen, W.-M.; Wei, Y.-H., Enhancing production of prodigiosin from *Serratia marcescens* C3 by statistical experimental design and porous carrier addition strategy. *Biochem. Eng. J.* **2013,** *78*, 93-100.
86. Ren, Y.; Gong, J.; Fu, R.; Li, Z.; Yu, Z.; Lou, J.; Wang, F.; Zhang, J., Dyeing and functional properties of polyester fabric dyed with prodigiosins nanomicelles produced by microbial fermentation. *J. Clean. Prod.* **2017,** *148*, 375-385.
87. Domröse, A.; Klein, A. S.; Hage-Hülsmann, J.; Thies, S.; Svensson, V.; Classen, T.; Pietruszka, J. r.; Jaeger, K.-E.; Drepper, T.; Loeschcke, A., Efficient recombinant production of prodigiosin in *Pseudomonas putida*. *Front. Microbiol.* **2015,** *6*, 1-10.
88. Ryazantseva, I. N.; Saakov, V. S.; Andreyeva, I. N.; Ogorodnikova, T. I.; Zuev, Y. F., Response of pigmented *Serratia marcescens* to the illumination. *J. Photochem. Photobiol. B* **2012,** *106*, 18-23.

89. Faraag, A. H.; El-Batal, A. I.; El-Hendawy, H. H., Characterization of prodigiosin produced by *Serratia marcescens* strain isolated from irrigation water in Egypt. *Nat. Sci.* **2017,** *15* (5), 55-68.
90. Arendrup, M. C.; Cuenca-Estrella, M.; Lass-Flörl, C.; Hope, W.; EUCAST-AFST, EUCAST technical note on the EUCAST definitive document EDef 7.2: method for the determination of broth dilution minimum inhibitory concentrations of antifungal agents for yeasts EDef 7.2 (EUCAST-AFST). *Clinical Microbiology and Infection (CMI)* **2012,** *18* (7), E246-E247.
91. Mosmann, T., Rapid colorimetric assay for cellular growth and survival: application to poliferation and cytotoxicity assays. *J. Immunol. Methods* **1983,** *65*, 55-63.
92. Stiernagle, T., Maintenance of *C. elegans*. In *WormBook: The Online Review of C. elegans Biology [Internet]*, Fay, D., Ed. **2006**; pp 1-11.
93. Brackman, G.; Cos, P.; Maes, L.; Nelis, H. J.; Coenye, T., Quorum sensing inhibitors increase the susceptibility of bacterial biofilms to antibiotics *in vitro* and *in vivo*. *Antimicrob. Agents Chemother.* **2011,** *55* (6), 2655-2661.
94. Buschmann, J., *The OECD guidelines for the testing of chemicals and pesticides*. Springer: **2013**; Vol. 947.
95. Kimmel, C. B.; Ballard, W. W.; Kimmel, S. R.; Ullmann, B.; Schilling, T. F., Stages of Embryonic Development of the Zebrafish. *Dev. Dyn.* **1995,** *203* (3), 253-310.
96. Nagel, R., *Dar*T: The embryo test with the zebrafish *Danio rerio* - a general model in ecotoxicology and toxicology. *ALTEX* **2002,** *19*, 38-48.
97. OECD, Test No. 236: Fish Embryo Acute Toxicity (FET) Test. In *OECD Guidelines for the Testing of Chemicals, Section 2: Effects on Biotic Systems*, OECD Publishing: **2013**.
98. Harned, R. L., The production of prodigiosin by submerged growth of Serratia marcescens. *Appl. Microbiol.* **1954,** *2* (6), 365-368.
99. Casullo de Araújo, H. W.; Fukushima, K.; Takaki, G. M. C., Prodigiosin production by *Serratia marcescens* UCP 1549 using renewable-resources as a low cost substrate. *Molecules* **2010,** *15* (10), 6931-6940.
100. Herráez, R.; Mur, A.; Merlos, A.; Viñas, M.; Vinuesa, T., Using prodigiosin against some gram-positive and gram-negative bacteria and *Trypanosoma cruzi*. *J. Venom. Anim. Toxins incl. Trop. Dis.* **2019,** *25*, e20190001.

101. Montaner, B.; Navarro, S.; Piqué, M.; Vilaseca, M.; Martinell, M.; Giralt, E.; Gil, J.; Pérez-Tomás, R., Prodigiosin from the supernatant of *Serratia marcescens* induces apoptosis in haematopoietic cancer cell lines. *Br. J. Pharmacol.* **2000,** *131*, 585-593.
102. Tao, J.-l.; Wang, X.-d.; Shen, Y.-l.; Wei, D.-z., Strategy for the improvement of prodigiosin production by a *Serratia marcescens* mutant through fed-batch fermentation. *World J. Microbiol. Biotechnol.* **2005,** *21* (6), 969-972.
103. Haddix, P. L.; Shanks, R. M. Q., Production of prodigiosin pigment by *Serratia marcescens* is negatively associated with cellular ATP levels during high-rate, low-cell-density growth. *Can. J. Microbiol.* **2020,** *66* (3), 243-255.
104. Chávez-Castilla, L. R.; Aguila, O., An integrated process for the *in situ* recovery of prodigiosin usingmicellar ATPS from a culture of *Serratia marcescens*. *J. Chem. Technol. Biotechnol.* **2016,** *91*, 2896-2903.
105. Zang, C.-Z.; Yeh, C.-W.; Chang, W.-F.; Lin, C.-C.; Kan, S.-C.; Shieh, C.-J.; Liu, Y.-C., Identification and enhanced production of prodigiosin isoform pigment from *Serratia marcescens* N10612. *J. Taiwan Inst. Chem. Eng.* **2014,** *45*, 1133-1139.
106. Andreyeva, I. N.; Ogorodnikova, T. I., Pigmentation of *Serratia marcescens* and spectral properties of prodigiosin. *Microbiol.* **2015,** *84* (1), 28-33.
107. Choi, S. Y.; Lim, S.; Yoon, K.-h.; Lee, J. I.; Mitchell, R. J., Biotechnological activities and applications of bacterial pigments violacein and prodigiosin. *J. Biol. Eng.* **2021,** *15*, 10-25.
108. Tran, L. T.; Techato, K.; Nguyen, V. B.; Wang, S.-L.; Nguyen, A. D.; Phan, T. Q.; Doan, M. D.; Phoungthong, K., Utilization of cassava wastewater for low-cost production of prodigiosin via *Serratia marcescens* TNU01 fermentation and its novel potent α-glucosidase inhibitory effect. *Molecules* **2021,** *26* (20), 6270-6286.
109. Chen, G.; Shi, K.; Song, D.; Quan, L.; Wu, Z., The pigment characteristics and productivity shifting in high cell density culture of Monascus anka mycelia. *BMC Biotechnology* **2015,** *15* (1), 72.
110. Bergan, T.; Grimont, P. A. D.; Grimont, F., Fatty acids of *Serratia* determined by gas chromatography. *Curr. Microbiol.* **1983,** *8*, 7-11.

111. Song, M.-J.; Bae, J.; Lee, D.-S.; Kim, C.-H.; Kim, J.-S.; Kim, S.-W.; Hong, S.-I., Purification and characterization of prodigiosin produced by integrated bioreactor from *Serratia* sp. KH-95. *J. Biosci. Bioeng.* **2006,** *101* (2), 157-161.
112. Clements, T.; Rautenbach, M.; Ndlovu, T.; Khan, S.; Khan, W., A metabolomics and molecular networking approach to elucidate the structures of secondary metabolites produced by *Serratia marcescens* strains. *Front. Chem.* **2021,** *9*, Article 633870.
113. Lapenda, J. C.; Silva, P. A.; Vicalvi, M. C.; Sena, K. X. F. R.; Nascimento, S. C., Antimicrobial activity of prodigiosin isolated from *Serratia marcescens* UFPEDA 398. *World J. Microbiol. Biotechnol.* **2015,** *31*, 399-406.
114. Wang, S.-L.; Nguyen, V. B.; Doan, C. T.; Tran, T. N.; Nguyen, M. T.; Nguyen, A. D., Production and potential applications of bioconversion of chitin and protein-containing fishery byproducts into prodigiosin: A review. *Molecules* **2020,** *25* (12), 2744-2766.
115. Jimtha, C. J.; Jishma, P.; Sreelekha, S.; Chithra, S.; Radhakrishnan, E. K., Antifungal properties of prodigiosin producing rhizospheric *Serratia* sp. *Rhizosphere* **2017,** *3* (1), 105-108.
116. Gutiérrez-Romén, M. I.; Holguín-Meléndez, F.; Dunn, M. F.; Guillén-Navarro, K.; Huerta-Palacios, G., Antifungal activity of *Serratia marcescens* CFFSUR-B2 purified chitinolytic enzymes and prodigiosin against *Mycosphaerella fijiensis*, causal agent of black Sigatoka in banana (*Musa* spp.). *BioControl* **2015,** *60*, 565-572.
117. Lee, J. S.; Kim, Y.-S.; Park, S.; Kim, J.; Kang, S.-J.; Lee, M.-H.; Ryu, S.; Choi, J. M.; Oh, T.-K.; Yoon, J.-H., Exceptional production of both prodigiosin and cycloprodigiosin as major metabolic constituents by a novel marine bacterium, *Zooshikella rubidus* S1-1. *Appl. Environ. Microbiol.* **2011,** *77* (14), 4967-4973.
118. Suzuki, N.; Ohtaguro, N.; Yoshida, Y.; Hirai, M.; Matsuo, H.; Yamada, Y.; Imamura, N.; Tsuchiya, T., A compound inhibits biofilm formation of *Staphylococcus aureus* from *Streptomyces*. *Biol. Pharm. Bull.* **2015,** *38* (6), 889-592.
119. Manderville, R. A., Synthesis, proton-affinity and anti-cancer properties of the prodigiosin-group natural products. *Curr. Med. Chem. - Anti-Cancer Agents* **2001,** *1*, 195-218.

120. Liu, Y.; Zhou, H.; Ma, X.; Lin, C.; Lu, L.; Liu, D.; Ma, D.; Gao, X.; Qian, X. Y., Prodigiosin inhibits proliferation, migration, and invasion of nasopharyngeal cancer cells. *Cell. Physiol. Biochem.* **2018,** *48*, 1556-1562.
121. Baldino, C. M.; Parr, J.; Wilson, C. J.; Ng, S.-C.; Yohannesa, D.; Wasserman, H. H., Indoloprodigiosins from the C-10 bipyrrolic precursor: New antiproliferative prodigiosin analogs. *Bioorg. Med. Chem. Lett.* **2006,** *16*, 701-704.
122. Chiu, W.-J.; Lin, S.-R.; Chen, Y.-H.; Tsai, M.-J.; Leong, M. K.; Weng, C.-F., Prodigiosin-emerged PI3K/Beclin-1-independent pathway elicits autophagic cell death in doxorubicin-sensitive and -resistant lung cancer. *J. Clin. Med.* **2018,** *7* (10), 321-335.
123. Abrahantes-Pérez, M. C.; Reyes-González, J.; Véliz Ríos, G.; Bequet-Romero, M.; Gómez Riera, R.; C, C. G.; Huerta, V.; González, L. J.; Canino, C.; Suarez, J. G.; Váldez, J.; Reyes, B.; Váldes, R. M.; Martínez, E., Cytotoxic proteins combined with prodigiosin obtained from *Serratia marcescens* have both broad and selective cytotoxic activity on tumor cells. *J. Chemother.* **2006,** *18* (2), 172-181.
124. Yamamoto, D.; Kiyozuka, Y.; Uemura, Y.; Yamamoto, C.; Takemoto, H.; Hirata, H.; Tanaka, K.; Hioki, K.; Tsubura, A., Cycloprodigiosin hydrochloride, a H^+/Cl^- symporter, induces apoptosis in human breast cancer cell lines. *J. Cancer Res. Clin. Oncol.* **2000,** *126*, 191-197.
125. Lin, P.-B.; Shen, J.; Ou, P.-Y.; Liu, L.-Y.; Chen, Z.-Y.; Chu, F.-J.; Wang, J.; Jin, X.-B., Prodigiosin isolated from *Serratia marcescens* in the *Periplaneta americana* gut and its apoptosis-inducing activity in HeLa cells. *Oncol. Rep.* **2019,** *41*, 3377-3385.
126. Gjorgjieva, J.; Biron, D.; Haspel, G., Neurobiology of *Caenorhabditis elegans* locomotion: Where do we stand? *BioScience* **2014,** *64* (6), 476-486.
127. Buckingham, S. D.; Partridge, F. A. S., David B., Automated, high-throughput, motility analysis in *Caenorhabditis elegans* and parasitic nematodes: Applications in the search for new anthelmintics. *Int. J. Parasitol. Drugs Drug Resist.* **2014,** *4* (3), 226-232.
128. Seah, S.-W.; Nathan, S.; Wan, K.-L. In *Toxicity evaluation of prodigiosin from Serratia marcescens in a Caenorhabditis elegans model*, AIP Conference Proceedings, (AIP), A. I. o. P., Ed. **2016**; p 020015.

129. Deng, L.; Denham, J. E.; Arya, C. Y., Omer; Cohen, N.; Haspel, G., Inhibition underlies fast undulatory locomotion in *Caenorhabditis elegans*. *eNeuro* **2020,** *8* (2), 1-23.
130. Gao, S.; Zhena, M., Action potentials drive body wall muscle contractions in *Caenorhabditis elegans*. *PNAS USA* **2011,** *108* (6), 2557-2562.
131. Yamasaki, A.; Suzuki, M.; Funayama, T.; Moriwaki, T.; Sakashita, T.; Kobayashi, Y.; Zhang-Akiyama, Q.-M., High-dose irradiation inhibits motility and induces autophagy in *Caenorhabditis elegans*. *Int. J. Mol. Sci.* **2021,** *22* (18), 9810-9826.
132. Rahul, S.; Chandrashekhar, P.; Hemant, B.; Chandrakant, N.; Laxmikant, S.; Satish, P., Nematicidal activity of microbial pigment from *Serratia marcescens*. *Nat. Prod. Res.* **2014,** *28* (17), 1399-1404.
133. Smithen, D. A.; Forrester, A. M.; Corkery, D. P.; Dellaire, G.; Colpitts, J.; McFarland, S. A.; Berman, J. N.; Thompson, A., Investigations regarding the utility of prodigiosenes to treat leukemia. *Org. Biomol. Chem.* **2013,** *11* (1), 62-68.

Appendix: Scientific contributions

During my PhD studies at the University of Nova Gorica – Graduate School, I have had 4 (four) scientific contributions:

1. I have submitted an abstract **"Bromination of natural products prodigiosin and undecylprodigiosin"** which was accepted for a flash poster presentation No. 092 at the *online* event 18th Hellenic Symposium on Medicinal Chemistry (HSMC), on 25-27 February 2021. The authors are Jelena Lazić, Sanja Škaro Bogojević, Qingqi Zhao, Tanja Gulder and Jasmina Nikodinović-Runić.

2. I have submitted an abstract **"Synthesis, characterization, and anticancer properties of novel brominated derivatives of the bacterial pigment prodigiosin"** which was accepted for a poster presentation No. P061 at the *online* event Frontiers in Medicinal Chemistry 2022 (MedChem2022), on 14-16 March 2022. The authors are Jelena Lazić, Sanja Škaro Bogojević, Sandra Vojnović, Tanja Gulder and Jasmina Nikodinović-Runić.

3. An article **"Synthesis, anticancer potential and comprehensive toxicity studies of novel brominated derivatives of bacterial biopigment prodigiosin from *Serratia marcescens* ATCC 27117"** was submitted to MDPI Molecules on 9th May 2022, revised on 31st May 2022, accepted on 6th June 2022, and published on 9th June 2022. The authors are Jelena Lazić, Sanja Škaro Bogojević, Sandra Vojnović, Ivana Aleksić, Dušan Milivojević, Martin Kretzschmar, Tanja Gulder, Miloš Petković and Jasmina Nikodinović-Runić.

   Molecules **2022**, *27*(12), 3729; https://doi.org/10.3390/molecules27123729

4. I have submitted an abstract **"From food waste to valuable bio-pigments prodigiosin and pyocyanin"** which was accepted for a poster presentation at the *online* event European Federation of Biotechnology 2022 (EFB2022), on 4-5 October 2022. The authors are Jelena Lazić, Lena Pantelić, Sandra Vojnović, Sanja Škaro Bogojević, Jasmina Nikodinović-Runić.